Islamic University of Gaza
Deanery of Graduate Studies
Faculty of Engineering
Department of Electrical Engineering

تحسين هوائي أحادي القطبية و هوائي مستوي بشكل مقلوب F للشبكات اللاسلكية على جسم الإنسان مع ميزات التنوع

Enhancement of PIFA Top Loaded Monopole Antenna for WBAN with Diversity Features

Submitted by
Ammar T. A. EL-Tatar

Supervisors
Dr. Mohamad Ouda

Dr. Talal Skaik

A Thesis Submitted in Partial Fulfillment of Requirements for the Degree of Master in Electrical Engineering-Communication Systems.
1434هـ -2013 م

Abstract

Wireless body area network (WBAN) has become a major field of interest for researchers due to the increasing applications in personal communications systems, where devices can be carried in the user's pockets or attached to the user's body.

In any wireless device, the performance of radio communications depends on the design of an efficient antenna. Diversity antenna has been used to overcome fading and interference that affect the reliability and quality of service of wireless links.

The objective of this thesis is to enhance a diversity antenna suitable for use within WBAN terminals at the Industrial, Scientific and Medical (ISM) band at 2.45 GHz. To satisfy the environment of WBAN where different natures of the received signals are present, a planar inverted-F antenna (PIFA) and a top loaded monopole antenna are used. Professional software design High Frequency Structural Simulator (HFSS) is used to design and to study the effects of each parameter in the antenna performance.

Parasitic elements have been used to enhance the impedance bandwidth of the top loaded monopole antenna and folded slots in the PIFA ground have been used to reduce the mutual coupling between the two antennas and to enhance the impedance bandwidth of PIFA. The antenna performance in the presence of the human body was also investigated

Dedication

This thesis is dedicated to

My Parents

My Wife

And

My lovely Son and Daughters

Acknowledgement

First and the foremost, I would like to thank Almighty Allah for bestowing His blessings upon me and giving me the strength to carry out and complete this work.

I am extremely grateful to my supervisors Dr. Mohamad Ouda and Dr. Talal Skaik for their valuable advice, guidance, beneficial discussions and encouragement throughout my research. Apart from their valuable academic advice and guidelines, they have been extremely kind, friendly, and helpful.

I am also very grateful to my thesis committee members, Dr. Fadi Al-Nahal and Dr. Mustafa Abu Al-Nasr for their care, cooperation and constructive advices.

Special thanks to my colleagues and friends especially Eng. Abed esalam Al-Astal, Eng. Ahmed Abu Absa and Eng. Hazem Abu Karish for their encouragements and various help that they provided throughout my graduate studies. I would like to give my special thanks to my parents, brothers, sisters and my wife for their support, patience and love. Without their encouragement, motivation and understanding, it would have been impossible for me to complete this work.

Contents

List of Figures

Lists of Tables

Chapter 1

Introduction

1.1 Introduction

Body Area Network (BAN) is a wireless network that has nodes situated on or near the human body. The concept of BAN was first used for medical diagnostics in which various sensors, like temperature sensor, Electrocardiogram (ECG), blood pressure monitoring kit, blood sugar device etc., are put on the body of a patient and they interact with a base unit on or off the body. The term BAN is nowadays used in a broader spectrum to include all types of body-centric communications [1].

Body-centric wireless networks (BCWN) would inherit and adhere to attributes defined for wireless personal and body area networks (WPAN/WBAN) by the IEEE 802.15 standardization group depending on the applications it is intended for (e.g., on-body, off-body or in-body communications). Figure 1.1 shows example of on-body and off-body communications [2].

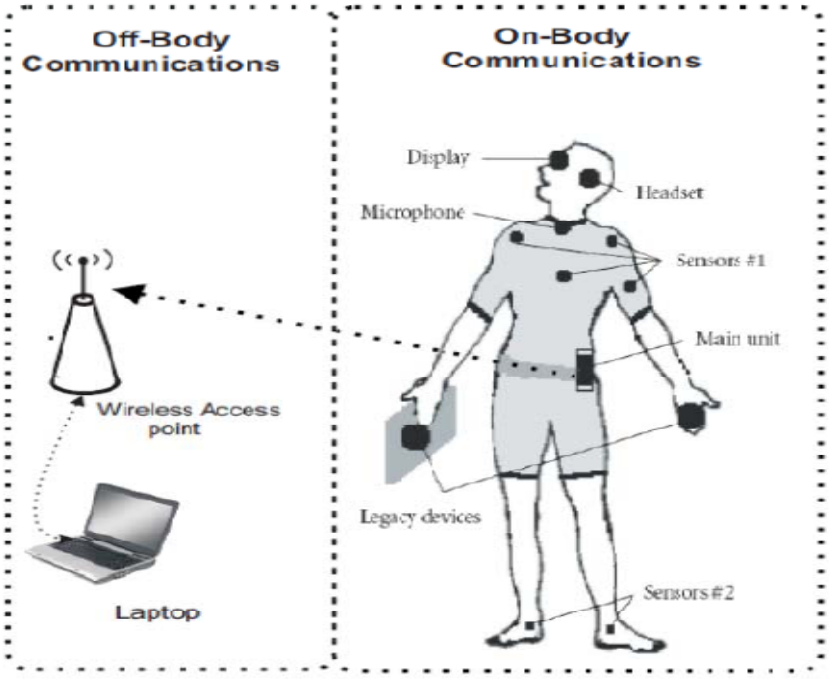

Figure 1.1 BCWN and its possible components showing on-body and off-body communications [2].

• **On-body communications:** describe the link between body mounted devices communicating wirelessly.
• **Off-body communications:** defines the radio links between body-worn devices and base units or mobile devices located in the surrounding environments.
• **In-body communications:** is concerned with relaying and exchanging information between wireless implants and on-body nodes.

Wireless body area network (WBAN) is a term used to describe a network of wearable devices with wireless communication capabilities as shown in Figure 1.2 [3]. Initial applications of WBANs have appeared in the healthcare domain for continuous monitoring of patients suffering from chronic diseases, other applications include sports, military, or security.

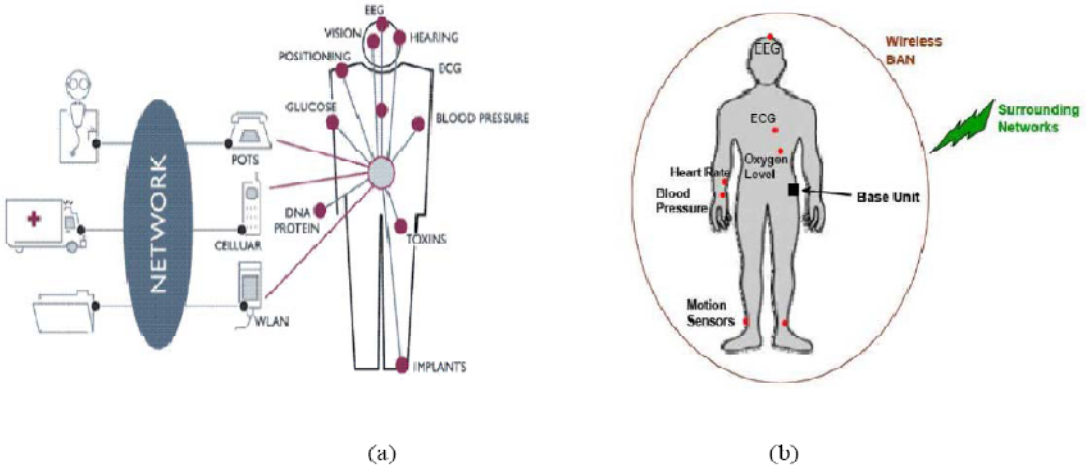

(a) (b)

Figure 1.2 (a) BCWNs for health monitoring, (b) Wireless BAN in Healthcare Applications [2].

As portable devices like cellular phones, pagers and MP3 players become popular; people start to carry such devices around their bodies. In 1996, Zimmerman [4] studied how such electronic devices operate on and near the human body. He used the term wireless personal area network (PAN). He characterized the human body and used it as a communication channel for intra-body communications.

Later around 2001, the term PAN has been modified to body area network (BAN) to represent all the applications and communications on, in and near the body [5]. Efforts have been made to develop standards for the BAN and an IEEE task group, IEEE 802.15.6 (IEEE 802.15.BAN), has been established for this purpose in November 2007. This task group is the sixth task group of the IEEE 802.15 working group. The IEEE 802.15 is an IEEE standard for Wireless Personal Area Networks (WPAN) and has, so far, seven task groups and one interest group for Terahertz. The task group 802.15.6 or 802.15.BAN and task group 802.15.7 are still in the process of developing new standards for BAN and Visible Light Communication (VLC), respectively. IEEE 802.15.1, first published in June 2002, is a standard for WPAN based on Bluetooth, whereas, 802.15.2 provides recommendations for the coexistence of the WPANs and Wireless Local Area Networks (WLAN). The details of other task groups of IEEE 802.15 are given on its website [6].

1.2 Motivation

A WBAN-based wireless medical sensor network system when implemented in medical centers has significant advantages over the traditional wired-based patient data collection schemes by providing better rehabilitation and improved patient's quality of life. In addition, a WBAN system has the potential to reduce the healthcare cost as well as the workload of medical professions, resulting in a higher efficiency [7].

One of the targeted applications of WBAN is in medical environments where a large number of patients are continuously being monitored in real time; Wireless monitoring of physiological signals of a large number of patients is one of the current needs in order to deploy a complete wireless sensor network in healthcare system. Such an application presents some challenges in both software and hardware designs. Some of them are as follows: reliable communication by eliminating collisions of two sensor signals and interference from other external wireless devices, low-cost, low power consumption, small size, and suitable data rate.

There are already a number of monitoring systems developed or being used in medical centers. The available medical monitoring systems are generally bulky and thus

uncomfortable to be carried by patients. Most of the current effort has mainly been focused on the devices that are monitoring one or few physiological signals only. When multiple sensors are involved, wires are used to connect the sensors to a wearable wireless transmitter. Wired systems restrict patients' mobility and comfort level, especially during sleep studies. Future implementation of medical monitoring necessitates the use of small, low-power sensor nodes with wireless capability [8–10].

For BAN applications, the proper antenna design is a critical stage. The antennas are required to be compact, light weighted, low profile, and should have a suitable feeding structure for proper integration in small-sized body-worn devices. It is worth noting that some of the antenna performance parameters, like gain, radiation pattern, efficiency, matching etc., change significantly compared to the free space operation when the antenna operates on or in close proximity of a lossy medium, such as human body tissue. The antennas can be detuned when mounted on the body. The amount of detuning depends upon the type of antenna and the type of tissue. The use of ground plane to cover the antenna from the body may be helpful in avoiding this problem in some cases, but with antennas having no or small ground plane, the design should be aimed for a high bandwidth of the antenna to minimize the effect of detuning. The radiation pattern of the antenna is another important parameter to be considered [1].

1.3 Objectives

The objectives of this thesis are to investigate, simulate and enhance an antenna for WBAN at the Industrial, Scientific and Medical (ISM) band at 2.45 GHz. In order to improve the performance, a diversity technique is used and an antenna with minimized size is designed for comfortable handling on human body.

At 2.45 GHz frequency, electromagnetic propagation involves two main aspects. Firstly, propagation takes place over the surface of the body by creeping or surface waves. Such propagation may be significantly affected by the motion of the body. Secondly, multipath propagation around the body, which is due to reflections from the surrounding environment and the body parts, will also occur. Propagation through the body is negligible at this and higher frequencies. Fading will occur due to the large relative movement of the body parts, shadowing, polarization mismatch, and scattering due to the body and the surrounding environment. To improve the performance and overcome fading, diversity is a very powerful tool. The principle behind diversity is the use of more than one independent antenna and hence uncorrelated received signals which will fade independently of each other [11].

To satisfy the antenna diversity gain for (WBAN), combination of a planar inverted-F antenna (PIFA) and a top loaded monopole yields distinct patterns fitting the different natures of the received waves so that when the surface/creeping waves are dominant, the top loaded monopole provided the highest signal, and diversity did not bring any added value. However, for scenarios where the surface waves are dominated by or equivalent to the waves reflected by the environment, the monopole and PIFA signals are sufficiently uncorrelated with similar received powers. Consequently, good performances were obtained when a selection diversity scheme was applied [12].

To study the techniques of enhancing the antenna parameters and size miniaturizing of the antenna to exhibit excellent performance, An EM simulation software such as CST and HFSS will be utilized to design the antenna.

Starting from paper in [12] that has been mentioned above, an extensive study will be carried out on its design in order to improve the performance of the antenna and reduce its size.

1.4 Diversity for WBAN

To improve the performance and overcome fading (Fading is the time variation of signal power at the receiver due to changes in the transmission path [13]), diversity has been used as a very powerful tool. The principle behind diversity is the use of two or more uncorrelated branches with independent fading statistics. If two or more channels are separated sufficiently in time, frequency, space, radiation pattern, and/or polarization, the fading on the individual channels is independent due to the different channel conditions [14].

It is unlikely that all the branch signals will be at the same fade level at a certain instant. So that, if the branch signals are combined properly, the deep fades can be minimized thus yielding an overall improvement in SNR. In principle, diversity works at its best if fading at the branches is uncorrelated and the branch signals have the same average power level [15].

Antenna diversity refers to the implementation of diversity system in which two or more antennas are used to achieve the diversity branches. Antenna diversity can be achieved in various ways, as shown in Figure 1.3.

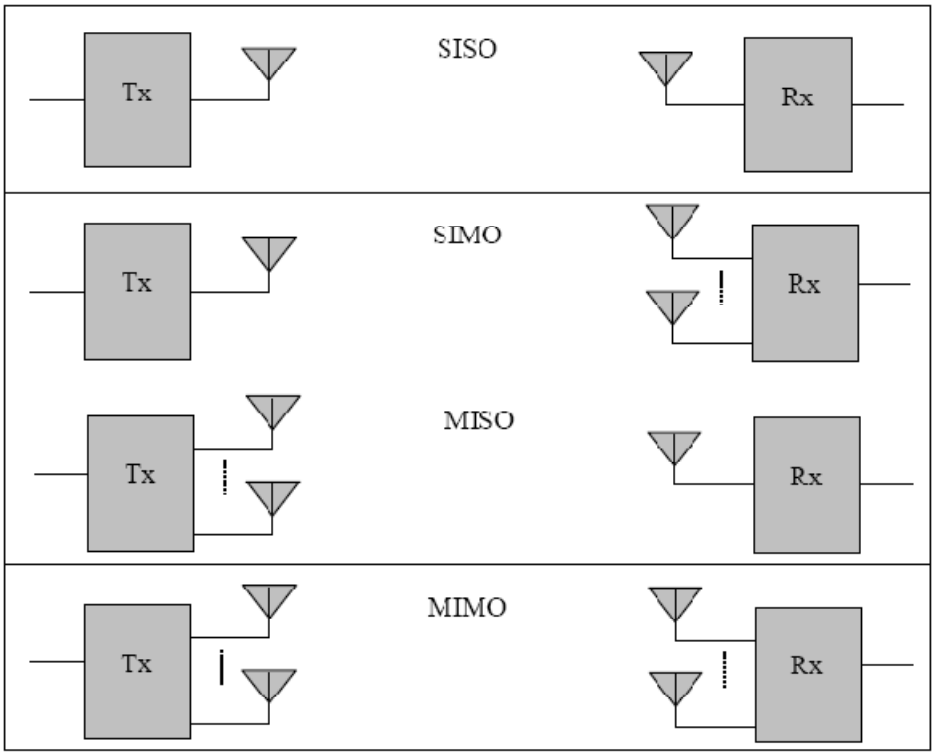

Figure 1.3 Communication system classification based on number of antennas [16].

On-body channel communication generally takes place between a single transmitter-receiver pair. So, the cost of implementing diversity either at the transmitter or at the receiver is the same. There may be some applications where a single transmitter communicates with multiple devices mounted on the body. Even then, the number of receivers are only few. Hence, diversity reception (SIMO) is a much better choice for on-body channels compared to its counterpart; transmit diversity (MISO), due to better performance.

Much work has been done on the use of diversity at the hand-held devices and the base station while very limited amount of work has been done so far to investigate and quantify the diversity performance for WBAN communication channels and specifically for on-body channels [16].

The diversity antenna must be as compact as possible due to the tendency of miniaturization of WBAN devices. One of the limiting factors on the overall size of the diversity antenna is the spacing between the antennas. This is not an issue for polarization diversity but an important aspect of the space diversity and up to some extent, the pattern diversity. Those types of diversity will be explained later in this section. If the spacing between the antennas for diversity branches is reduced, the mutual coupling between the antenna elements is increased. In principle, high mutual coupling can increase the correlation between the branch signals and can decrease the capacity gain and the diversity performance. High mutual coupling can significantly distort the radiation pattern of the antenna elements and can reduce the radiation efficiency of the elements. However, for very closely spaced antennas, low mutual coupling can actually cause de-correlation of the branch signals and thus increase the capacity. In general, the antenna should be designed such that it is compact, have low mutual coupling and low correlation between the elements, and has high radiation efficiency [16].

1.4.1 Diversity Combining Schemes

The diversity combining are classified in four common ways namely, Switched Combining (SWC), Selection Combining (SC), Equal Gain Combining (EGC), and Maximal Ratio Combining (MRC). The combining can be done before or after the detection stage, thus referred to as pre-detection or post-detection combining, respectively [14]. An RF combiner circuit may be used at the RF stage to avoid using a separate receiver for each diversity branch thus minimizing the cost and the size of the diversity receiver [17].

Linear combiners are used, where signals from various branches are weighted individually and then added when an N-branch diversity receiver having N receiving antennas, the combined signal, y(t), achieved from superposition of N branches is [14]:

$$y(t) = \sum_{i=1}^{N} a_i r_i(t) \tag{1.1}$$

where $r_i(t)$ is the received signal at the i^{th} antenna, $y(t)$ is the diversity combined signal at the output of the combiner, and a_i is the scaling factor or the weight of the i^{th} branch signal, block diagram of the diversity combiner is shown in Figure 1.4.

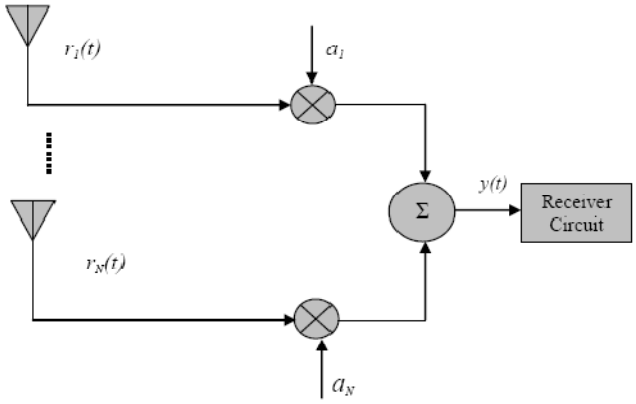

Figure 1.4 Simplified block diagram of a diversity combiner at RF stage [16].

In switched combining, the branch with SNR higher than a pre-defined threshold value is selected as an output of the combiner and connected to the rest of the receiver circuit. This branch signal is used until its SNR goes below the threshold. In practical

systems, it is difficult to measure the SNR, so the branch with highest signal power plus noise power is selected [14].

Selection combining implements the same concept of switching but in a more advanced way. Rather than switch-and-stay-connected to a branch, all the branch signals are scanned instantaneously and the branch with the highest SNR is selected, The selection decision is taken instantaneously rather than based on a threshold value [18].

But MRC and EGC use the combined effect of all the signals. In their techniques, the signals are weighted and then added. Before combining, the branch signals must be co-phased by adjusting the phase of one branch signal according to the relative phase difference between the two branch signals, as shown in Figure 1.5 [14].

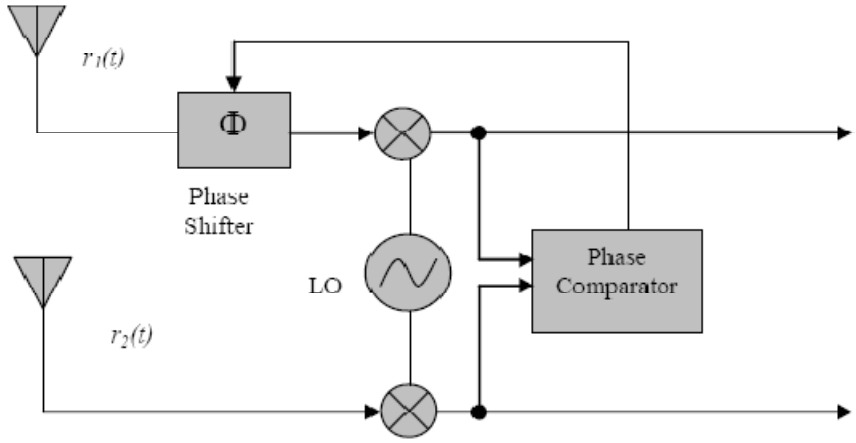

Figure 1.5 Co-phasing circuit for a two-branch diversity receiver [14].

In EGC the weight for all the branches is set to 1, i.e., all the branch signals are simply added together. Assuming that the co-phasing has been done, the weight for EGC is, a_i=1 in eq. (1.1).

While in MRC branch signals are weighted proportional to their signal voltage to noise power ratio such that the output is the sum of their SNR. The weight a_i in eq. (1.1) is thus directly proportional to RMS value of the branch signal and inversely proportional to the average noise power at the i^{th} branch [15, 18], i.e.

$$a_i = \frac{r_{i(RMS)}}{< n_i^2 >} \tag{1.2}$$

where $r_{i(RMS)} = \sqrt{< r_i^2 >}$ is the RMS value of the signal and $< n_i^2 >$ is the average noise power at the i^{th} branch.

To obtain the diversity-combined signal with SC, EGC and MRC for an N branch diversity combiner are given in simplified way in [19] as:

$$SC(t) = \max(r_1(t), r_2(t), ...r_N(t)) \tag{1.3}$$

$$EGC(t) = \frac{(r_1(t) + r_2(t) + ... + r_N(t))}{\sqrt{N}} \tag{1.4}$$

$$MRC(t) = \sqrt{(r_1^2(t) + r_2^2(t) + ... + r_N^2(t))} \tag{1.5}$$

where $r_i(t)$ is the received signal envelope at the i^{th} branch.

Selection combining and switched combining are the simplest and cheapest methods. They do not rely on the phase information of the received signals and are thus easy to implement. The performance is not as good as the EGC and MRC schemes. MRC is the optimum combining technique in terms of the diversity improvement but is complicated and expensive [15].

1.4.2 Correlation of the Branch Signals

Diversity receiver performance greatly depends upon the correlation between the received signals at the diversity branches. Low correlation is desirable as it assures that the branch signals fade differently. A correlation coefficient of 0.7 is considered good for most of the mobile communication scenarios [15].

Correlation coefficient can be used in three different forms, the power correlation coefficient, ρ_p, the envelope correlation coefficient, ρ_e, and the complex signal correlation coefficient, ρ_s. The complex signal correlation coefficient is useful in system design as it contains both the phase and amplitude correlation, whereas the power correlation coefficient gives a good insight of the correlated power in the diversity branches. For a two-branch diversity system, the correlation coefficients can be computed as in [19]:

$$\rho_s = \frac{\sum_{k=1}^{N} v_1(k) v_2{}^*(k)}{\sqrt{\sum_{k=1}^{N} v_1(k) v_1{}^*(k)} \sqrt{\sum_{k=1}^{N} v_2(k) v_2{}^*(k)}} \tag{1.6}$$

$$\rho_p = \frac{\sum_{k=1}^{N} s_1(k) s_2(k)}{\sqrt{\sum_{k=1}^{N} s_1(k) s_1(k)} \sqrt{\sum_{k=1}^{N} s_2(k) s_2(k)}} \tag{1.7}$$

$$\rho_e = \frac{\sum_{k=1}^{N} (r_1(k) - \overline{r_1})(r_2(k) - \overline{r_2})}{\sqrt{\sum_{k=1}^{N} (r_1(k) - \overline{r_1})^2} \sqrt{\sum_{k=1}^{N} (r_2(k) - \overline{r_2})^2}} \tag{1.8}$$

where S_1 and S_2 represent the zero-mean received power signals, V_1 and V_2 represent the zero-mean complex voltage signals, and r_1 and r_2 are the received short-term fading signal envelopes. $\overline{r_i}$ is the mean value of the signal envelope at the i^{th} branch and * represents the complex conjugate [15].

1.4.3 Diversity Gain

Diversity gain (DG) is a scale to measure the improvement due to the use of diversity. It is an improvement in the signal strength, or SNR, or bit error rate (BER), over a single antenna with no diversity, at a certain level of outage probability [15, 20]. It is calculated by a difference in signal levels (or SNR) of the diversity combined signal and the strongest branch signal (taken as a reference) among all the diversity branches at some outage probability, as shown in eqns. (1.9) and (1.10).

$$DG = \frac{p_{div}}{p_{ref}} \tag{1.9}$$

$$DG = p_{dBdiv} - p_{dBref}\,(dB) \tag{1.10}$$

where P_{div} is the power level of the diversity combined signal and P_{ref} is the power level of the reference signal (which is strongest among the branch signals) at a certain probability level. P_{dBdiv} and P_{dBref} are the same values as P_{div} and P_{ref} but expressed in dB. These expressions can also be presented in terms of SNR or BER.

Probability level of 10% and 1% are commonly used. Figure 1.6 shows the Cumulative Distribution Function (CDF) of two branch signals and a diversity combined signal with diversity gain calculated at 1% probability.

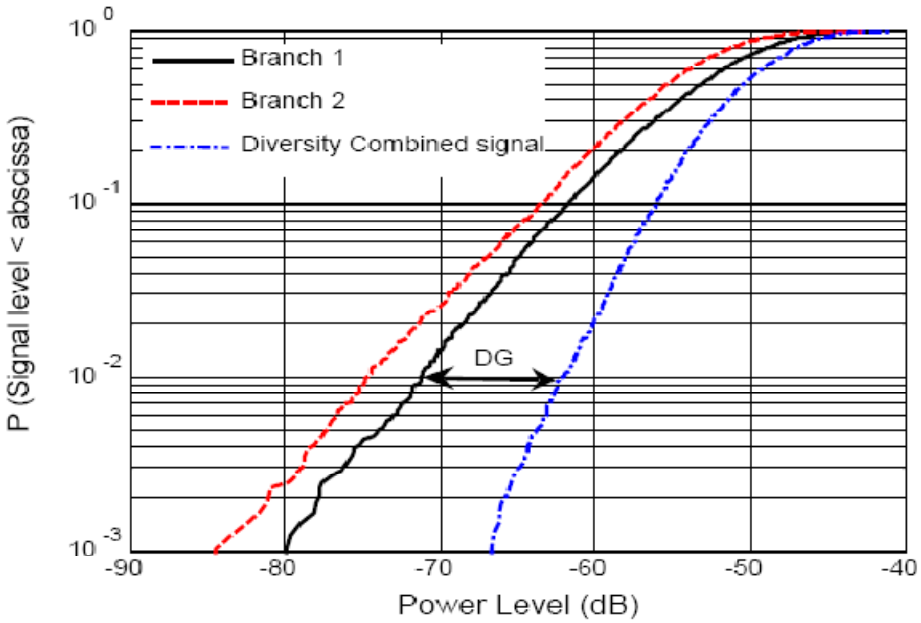

Figure 1.6 Diversity gain calculation [16].

Diversity gain depends upon the correlation among the branch signals. It is the more the branches are uncorrelated, the higher is the diversity gain.

Also the power imbalance among the received branch signals is another factor affecting the diversity gain. If the power difference among the branch signals is more, the diversity combiner will favor the strongest signal for most of the time so no or very small diversity gain will be achieved. If the power imbalance is very high, the performance of EGC becomes worse than that of SC because the branch with very low power level introduces additional noise and very less improvement to the desired signal is achieved, which results in overall decrease in the output SNR [19].

1.4.4 Types of Diversity

Diversity can be classified in various ways, e.g. time diversity, frequency diversity, space (spatial) diversity, polarization diversity, and pattern (angle) diversity [14].

A. Time Diversity

In time diversity, the amplitude samples of the signal are transmitted in different time slots. If the separation between the time slots is sufficient, the sequential amplitude samples of the fading signal will be uncorrelated [14].

B. Frequency Diversity

When different frequencies are used for the diversity branches, another type of diversity, called frequency diversity, can be achieved. The spacing between frequencies must be greater than the coherence bandwidth (The bandwidth or frequency separation over which the spectral components are affected almost the same way [21]). Frequency diversity utilizes much more bandwidth than the other diversity schemes and a separate transmitter-receiver pair is required for each branch [14].

C. Space Diversity

Space diversity scheme uses multiple antennas on transmit and/or receive side to get diversity branches distributed in space. Two or more antennas are separated by certain spacing between them to achieve a space diversity antenna. This technique does not consume extra spectrum and the basic issue is the spacing of the antennas, which determines the amount of mutual coupling between the adjacent branch antennas and the correlation among the branch signals. The spacing between the antennas should be such that the mutual coupling and correlation is minimized and the received signals on the antenna are faded independently. A spacing of $\lambda/2$ is sufficient for most of the applications [14].

The correlation between two branch signals varies with the spacing between the antennas in a space diversity receiver. If the antennas are too close to each other, the patterns of the antennas are distorted due to mutual coupling and the correlation increases [22].

D. Pattern Diversity

When directional antennas are used either at transmitter or at receiver, another type of diversity scheme appear called radiation pattern diversity or angle diversity. The diversity branches are produced by directing the radiation pattern in different angles.

The most desirable situation is where the overlap between the adjacent radiation patterns is minimal and the combination gives an omnidirectional pattern. The signals radiated in different directions undergo different fading and hence are uncorrelated. In most cases, an array with appropriate beam switching is used at either transmitter, or receiver, or both. Pattern diversity is more effective in situation when the angle of arrival has more spread and variation [23].

E. Polarization diversity

In polarization diversity if two signals are transmitted or received with orthogonal polarization, the fading in the signals is uncorrelated [14]. Thus, two antennas with different polarization or a single dual-polarized antenna can be used to constitute a two-branch diversity system. It has an advantage over space diversity that it does not require two antennas separated by some distance, as a single dual-polarized antenna can be used to implement it and thus offers size and cost reduction compared to the space diversity receiver [19].

1.4.5 Diversity for Interference Rejection

Co-channel interference is a main issue for mobile communication systems, especially at the edge of cells with two nearby cells using the same frequency band. It becomes even more significant for Personal Communication Systems (PCS) and body-centric communications when two BAN operate in the near vicinity of each other. The mobility of persons, carrying the body-worn devices, can introduce large amount of interference in other BANs or PCS terminals operating in the same frequency band. In mobile cellular network, co-channel interference can be minimized by keeping the transmitted power within a range where it cannot reach the closer cell using the same frequency while in PCS or BAN applications, it is very hard to keep a safe distance

between the moving terminals to avoid interference. Specifically in BAN, the mobile terminals carrying transmitters and receivers can operate very close to other mobile terminals carrying similar devices. Thus, interference rejection becomes more important in this scenario [16].

Among many interference rejection techniques, receive diversity is a way to reject the interference and maximize the output signal to interference plus noise ratio (SINR). Just like the diversity combining to maximize the SNR, the received branch signals can be combined in an optimum way to increase the output SINR and thus reject the interference. This combining technique is usually referred to as Interference Rejection Combining (IRC) [16]. Various IRC algorithms have been proposed in the [24-26].

1.5 Structure of the Thesis

Chapter 1: Introduction; this chapter is organized in five points: Introduction, motivation, objectives, diversity for WBAN and structure of the thesis.

Chapter 2: Antenna Theory and Literature Review; it contains review for antenna theory, electromagnetic waves, antenna types and antenna parameters, also the types of antennas used for WBAN and the effects of human body on antenna performance are discussed.

Chapter 3: Monopole and PIFA Antennas; it defines common types of the antenna and their advantages and disadvantages. It presents the fundamental principles of monopole and PIFA antennas and their applications.

Chapter 4: Designs and Simulations of PIFA and Top Loaded Monopole Antennas; it contains the methodology and the design concepts for PIFA and monopole. Also investigate the antennas parameters and different methods for enhancing the antenna performance, and displays the results from the simulations as well as showing the effects of human body on the antenna design.

Chapter 5: Conclusions; it includes comments on the results of the simulations and provides a summary of the main contributions and findings of the study and concludes the accomplished work packages. It also introduces suggestions for future research activities.

References

[1] I. Khan, "Diversity and MIMO for body-centric wireless communication channels," PhD thesis, University Of Birmingham, Sept. 2009.

[2] M. M. Khan, "Antenna and Radio Channel Characterization for Low-Power Personal and Body Area Networks," PhD thesis, University of London, February 2012.

[3] W. G. Scanlon, G. A. Conway, and S. L. Cotton, "Antennas and propagation considerations for robust wireless communications in medical body area networks," presented at the IET Seminar Antennas Propag. Body-Centric Wireless Commun., April 2007.

[4] T.G. Zimmerman, "Personal Area networks: near-field intra-body communication," IBM Systems Journal 35 (3 & 4), 1996.

[5] K.V. Dam, S. Pitchers, M. Barnard, "From PAN to BAN: why body area networks? In: Proceedings of the Wireless World Research Forum (WWRF) Second Meeting, " Nokia Research Centre, Helsinki, Finland, May 10–11, 2001.

[6] http://ieee802.org/15/index.html.

[7] M. R. Yuce. "Implementation of wireless body area networks for healthcare systems," Sensors and Actuators: A. Physical, Vol. 162, pp 116–129, July 2010.

[8] C. Park, P.H. Chou, Y. Bai, R. Matthews, A. Hibbs, "An ultra-wearable, wireless, low power ECG monitoring system," Proceedings of IEEE BioCAS, pp.241–244, 2006.

[9] Wireless ECG patch by IMEC. http://www2.imec.be/, 2008.

[10] EEG sensor by Icap. http://www.icaptech.com/, 2008.

[11] A. A. Serra, P. Nepa, G. Manara, and P. S. Hall, "Diversity for body area networks," presented at the URSI Gen. Assembly, 2008.

[12] T. Alves, B. Poussot, and Jean-Marc Laheurte "PIFA–Top-Loaded-Monopole Antenna With Diversity Features for WBAN Applications, " IEEE Antennas and Wireless Propagation Letters, Vol. 10, No. 1, pp. 693–696, July 2011.

[13] R. Prasad, "Universal Wireless Personal Communications", Artech House, London, 1998.

[14] W. C. Jakes, "Microwave Mobile Communications", New York Wiley, 1997.

[15] R. G. Vaughan, J Bach Andersen, "Antenna Diversity in Mobile Communications", IEEE transaction On Vehicular Technology, Vol. VT-36., No. 4, Nov 1987.

[16] I. Khan, “Diversity and MIMO for Body-Centric Wireless Communication Channels”, PhD thesis, University of Birmingham, September 2009.

[17] M. Karaboikis, C. Soras, G. Tsachtsiris and V. Makios, “Three-branch Antenna Diversity Systems on Wireless Devices Using Various Printed Monopoles", 2003 IEEE International Symposium on Electromagnetic Compatibility, Istanbul, May 11-16, 2003.

[18] D. G. Brennan, “Linear Diversity Combining Techniques”, Proceedings of the IEEE, Vol. 91, No. 2, February 2003.

[19] M. D. Turkmani, A. A. Arowojolu, P. A. Jefford, and C. J. Kellett “An Experimental Evaluation of the Performance of Two-Branch Space and Polarization Diversity Schemes at 1800 MHz”, IEEE Transactions on Vehicular Technology, Vol. 44, ,No. 2, May 1995.

[20] Per-Simon Kildal, K. Rosengren, “Electromagnetic Analysis of Effective and Apparent Diversity Gain of Two Parallel Dipoles”, IEEE Antennas and Wireless Propagation Letters, Vol. 2, 2003.

[21] R. Prasad, “Universal Wireless Personal Communications”, Artech House, London, 1998.

[22] C. B. Dietrich, Jr., K. Dietze, J. R. Nealy, and W. L. Stutzman, “Spatial, Polarization, and Pattern Diversity for Wireless Handheld Terminals”, IEEE Transactions on Antennas and Propagation, Vol. 49, No. 9, September 2001.

[23] P. Irazoqui-Pastor, J. T. Bernhard, “Examining the Performance Benefits of Antenna Diversity Systems in Portable Wireless Environments”, IEEE Antenna Applications Symposium, Allerton Park, Sep 15-17, 1999.

[24] J. Karlsson and J. Heinegard, “Interference Rejection Combining for GSM”, in Proc. of 5th IEEE Int. Conf. on Universal Personal Comm., 1996.

[25] D. Bladsjo, A. Furuskar, S. Javerbring, E. Larsson, “Interference Cancellation using Antenna Diversity for EDGE-Enhanced Data Rates in GSM and TDMA/136”, in Proc. of the 50th IEEE Vehicular Tech Conf., Fall 1999.

[26] J. H. Winters, “Optimum combining in Digital Mobile Radio with Co-channel Interference”, IEEE Journal on selected areas in communications, Vol. SAC-2, No. 4, July 1984.

Chapter 2

Antenna Theory and Literature Review

In this chapter an approach to WBAN antennas is made in order to review with the reader what has been done so far on the field. One will start to read a brief presentation concerning to the theory of antennas, allowing the comprehension of its main features, types and parameters. Finally, a study of the WBAN antennas and their advantages and disadvantages regarding the influence of the human body to their parameters are also discussed.

2.1 Introduction to antenna

An antenna can be defined as a usually metallic device which radiates and receives electromagnetic waves (EM waves – see section 2.2), more specifically, radio waves [1]. Another explanation says that an antenna is the transition between a guided EM wave and a free-space EM wave [2], and vice-versa. This process is explained by a general communication between a transmitting antenna and a receiving antenna, as described in Figure 2.1.

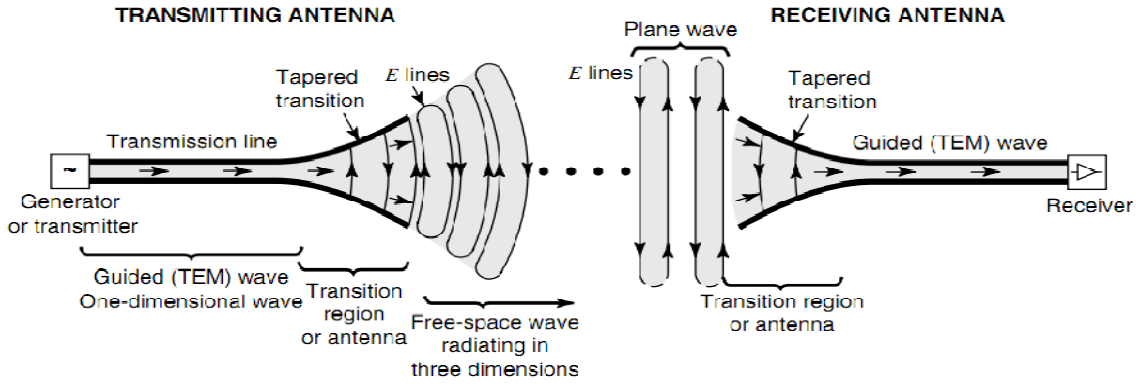

Figure 2.1 The antenna as a transition structure, for a transmitting antenna and for a receiving antenna [3].

As shown above, for both antennas, the transmission line has the form of a coaxial line or a waveguide. The latter, when a transmitting antenna is considered, is connected to a transmitter that generates radio-frequency (RF – see section 2.2) energy that is guided through the uniform part of the line as a plane Transverse Electromagnetic (TEM) wave with little loss, transformed into a signal that is amplified, modulated and applied to the antenna; otherwise, when a receiving antenna is considered, the transmission line is connected to a receiver which collects the alternating currents that resulted from the transformation process of the received radio waves by the antenna [3].

Antenna characteristics concerning to radiation are basically the same regardless of its type. Therefore, if a time-changing current or an acceleration (or deceleration) of charge occurs, the radiation will be created in a certain length of current element. This can be described by [1]:

$$l.\frac{dI}{dt} = l.q_l.\frac{dv}{dt}(A.m/s) \tag{2.1}$$

Where:

l - Length of the current element in meters (m);

$\frac{dI}{dt}$ - Time-changing current in ampere per second (A/s);

q_l - Charge per unit length (coulombs/m). Note that q = I. t = 1.602×10^{-19}

Furthermore, the radiation is always perpendicular to the acceleration and its power is proportional to the square of both parts of the equation (2.1). It is important to refer that the spacing between the two wires of the transition line is just a small part of a wavelength (see section 2.2); therefore, the more the transition curve of the antenna opens out the more the order of a wavelength or more is reached; consequently, the more the wave tends to be radiated and launched into the free-space [3].

Looking at the antenna structure as a whole, the transition region of the antenna is like a radiation resistance (R_r) to the transmission line point of view, which represents the radiation that the antenna emits, analyzing it as a circuit. Figure 2.2 shows the complete circuit of an antenna; where the source is an ideal generator with a tension V_g(or V_s) and with an impedance Z_g (or Z_s); the transmission line is a line with characteristic impedance Z_c (or Z_o), and the antenna itself is represented by a load impedance Z_A [$Z_A=(R_L+ R_r) + jX_A$] connected to the transmission line. The load resistance R_L is used to represent the conduction and dielectric losses associated with the antenna structure while R_r, referred to as the radiation resistance, is used to represent radiation by the antenna. The reactance X_A is used to represent the imaginary part of the impedance associated with radiation by the antenna. Therefore, if ideal conditions are applied, the radiation resistance R_r, which is used to represent radiation by the antenna, will get all the energy that is generated by the transmitter (the source) [1].

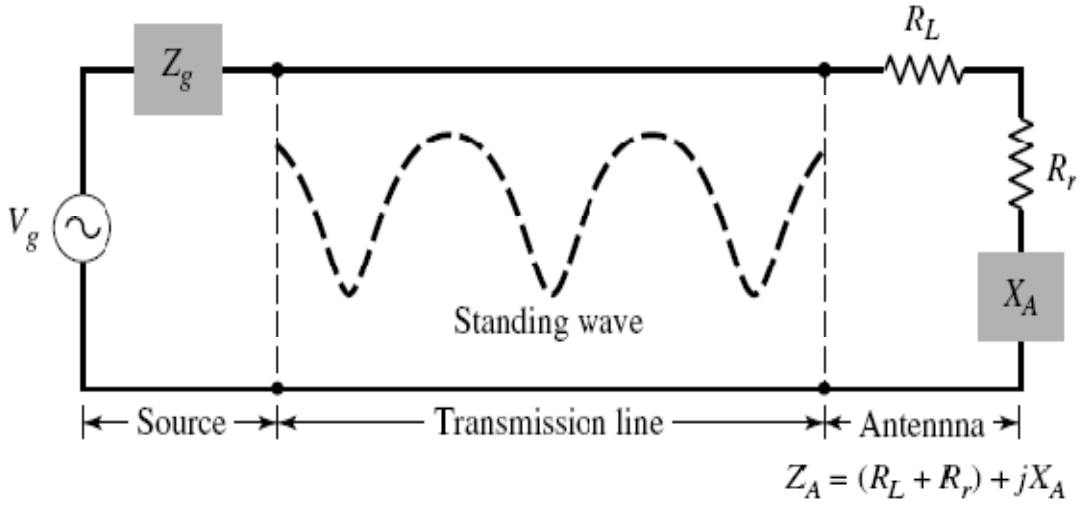

Figure 2.2 Circuit representing antenna as whole structure [1].

2.2 Radio-Frequency

EM waves are a type of electromagnetic radiation which is organized according to the frequency (*f*) of its waves. Frequency counts the number of incidences that a repetition of an event occurs per unit of time. Usually, a frequency is given in Hertz (Hz) which means the number of cycles per second. Each cycle is also mentioned as a period (*T*). Therefore, frequency is the reciprocal of period:

$$f = 1/T \tag{2.2}$$

EM waves cover the whole spectrum; radio waves and optical waves are just two examples of EM waves. We can see light but we cannot see radio waves. The

whole spectrum is divided into many frequency bands. Some radio frequency bands are listed in Table 2.1.

Frequency	Band	Wavelength	Applications
3-30 kHz	VLF	100 – 10 km	Navigation, sonar, fax
30-300 kHz	LF	10 – 1 km	Navigation
0.3-3 MHz	MF	1 – 0.1 km	AM broadcasting
3-30 MHz	HF	100 – 10 m	Tel, fax, CB, ship communications
30-300 MHz	VHF	10 – 1 m	TV, FM broadcasting
0.3-3 GHz	UHF	1 – 0.1 m	TV, mobile, radar
3-30 GHz	SHF	100 – 10 mm	Radar, satellite, mobile, microwave links
30-300 GHz	EHF	10 – 1 mm	Radar, wireless communications
0.3-3 THz	THz	1 – 0.1 mm	THz imaging

Table 2.1 EM spectrum and applications [4].

Although the whole spectrum is infinite, the useful spectrum is limited and some frequency bands, such as the UHF, are already very congested. Normally, significant license fees have to be paid to use the spectrum, although there are some license-free bands: the most well-known ones are the industrial, science and medical (ISM) bands, which we are interested in one of its bands (2.45 GHz) [4].

Another very important parameter is the wavelength (λ), which is the distance between two consecutive points of the same phase, given in meters. Figure 2.3 shows the plot of wavelength and Figure 2.4 the difference between highest and lowest frequencies.

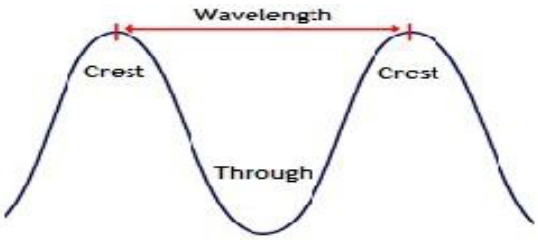

Figure 2.3 Wavelength measurement.

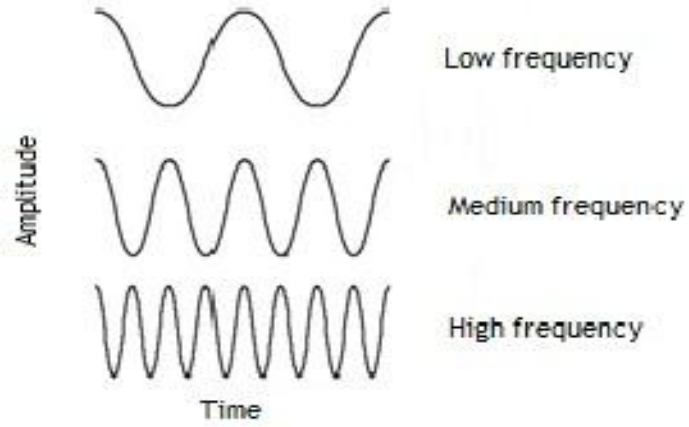

Figure 2.4 Frequency quality.

The *wave velocity, v,* is linked to the frequency, f, and wavelength, λ, by this simple equation:

$$v = \lambda f \tag{2.3}$$

It is well known that the speed of light (an EM wave) is about 3×10^8 m/s in free space. The higher the frequency, the shorter the wavelength is.

2.3 Types of Antennas

There are several types of antennas which were developed since the past times due nowadays. In this section, a brief discussion of the different antennas according to their physical structures will be presented. The following types of antennas are: Wire antennas; aperture antennas; microstrip antennas; array Antennas; reflector antennas; and lens antennas [1].

2.3.1 Wire Antennas

Wire antennas are between the most used antennas. Basically, they are very simple and cheap, with linear or curved forms. Examples include dipoles, monopoles, loops, helices, Yagi–Uda and log-periodic antennas [4]. They are:

- Dipole antennas: Dipoles are one of the simplest but most widely used types of antenna. Hertz used them for his famous experiment. As shown in Figure 2.5 (a), a dipole can be considered a structure evolved from an open-end, two-wire transmission line. A typical structure of a dipole consists of two metal wires which are normally of equal length.
- Monopole antennas: The monopole antenna is half of the dipole antenna as shown in Figure 2.5 (d), there are a lot of similarities between them, but there are also some differences which will be discussed thoroughly in chapter 3.
- Loop antennas: It can be a circular, square, triangle, rectangular or elliptical form. In the past they were used in pagers. While the dipole is considered to be a configuration evolved from an open-end transmission line, the loop can be viewed as a configuration evolved from a short-end transmission line, as shown in Figure 2.5 (b).
- Helical antennas: with a shape defined by helices, similarly to a spring shape. Those antennas are used for space telemetry as shown in Figure 2.5 (c).

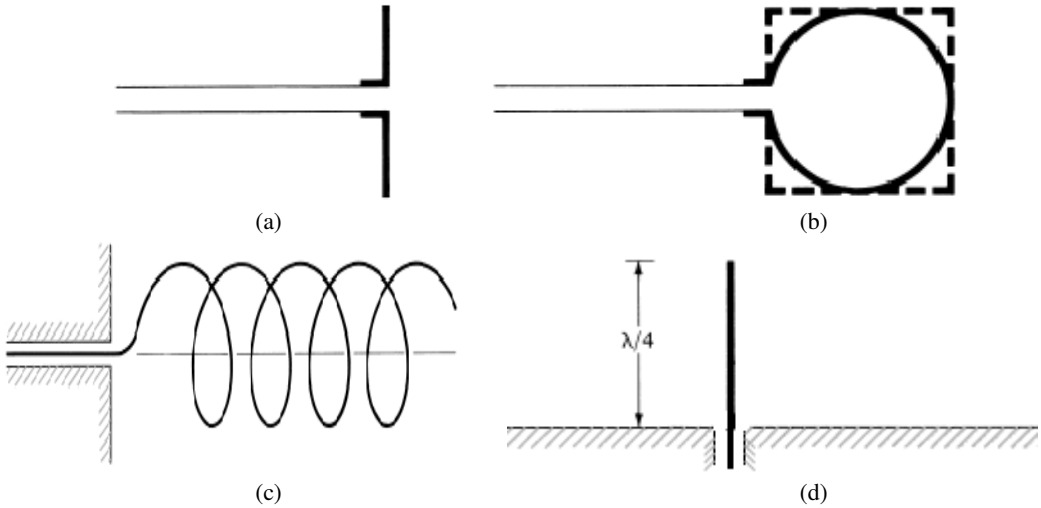

Figure 2.5 Types of wire antennas (a) Dipole (b) Loop (c) Helix (d) Monopole [1].

- Yagi–Uda Antennas: The Yagi–Uda antenna (also known as a Yagi) is another popular type of end-fire antenna widely used in the VHF and UHF bands (30 MHz to 3 GHz) because of its simplicity, low cost and relatively high gain. The most noticeable application is for home TV reception and these can be found on the rooftops of houses. A typical one is shown in Figure 2.6.

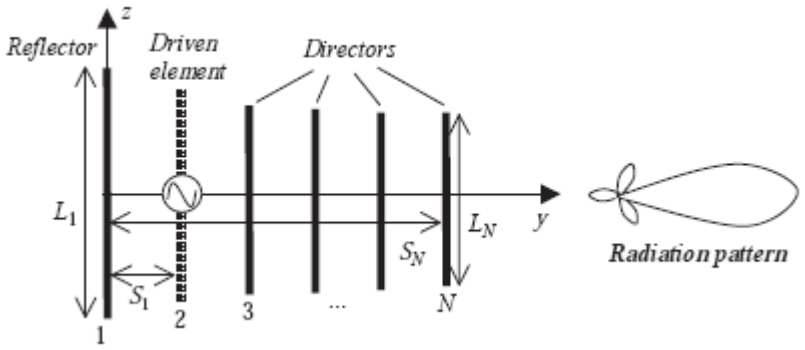

Figure 2.6 Configuration of a Yagi–Uda antenna and its radiation pattern [4].

- Log-Periodic Antennas: A very similar configuration to the Yagi–Uda antenna. It produces a similar end-fire radiation pattern and directivity (typically between 7 and 15 dB more than isotropic radiator) to the Yagi–Uda and, also like the Yagi–Uda, is widely used in the VHF and UHF bands. However, Yagi–Uda antennas have wider bandwidth and each element is connected to the source and can be seen as a feeder [4].

2.3.2 Aperture Antennas

These types of antennas are utilized at high frequencies. Aperture antennas largely depend on their aperture, because this property is directly related to gain. A notable example of an aperture antenna is the horn antenna. Although another well-liked aperture antenna is the slot antenna. Antennas of this type are very useful for aircraft and spacecraft applications, because they can be very conveniently flush-mounted on the skin of the aircraft or spacecraft. Both are described as follows: [1]

- Horn antennas: Horn antennas are the simplest and one of the most widely used forms of microwave antenna – the antenna is nicely integrated with the feed line (waveguide) and the performance can be controlled easily. They are mainly used for standard antenna gain and field measurements, feed elements for reflector antennas and microwave communications.
- Slot antenna: Usually, frequencies up to 24 GHz can be reached. Another interesting property of these antennas is their almost inexistent directivity, allowing omnidirectional radiation.

2.3.3 Microstrip Antennas

Microstrip antennas or microstrip patch antennas are usually very cheap and small, with an easier manufacture. They are printed directly onto a printed circuit board (PCB), and they are made of a metallic patch with a rectangular or circular shape, embedded on a grounded substrate, which will be discussed in detail in chapter 3 [4].
Different feed configurations, including aperture coupled, microstrip line feed and coaxial feed can be used as shown in Figure 2.7.

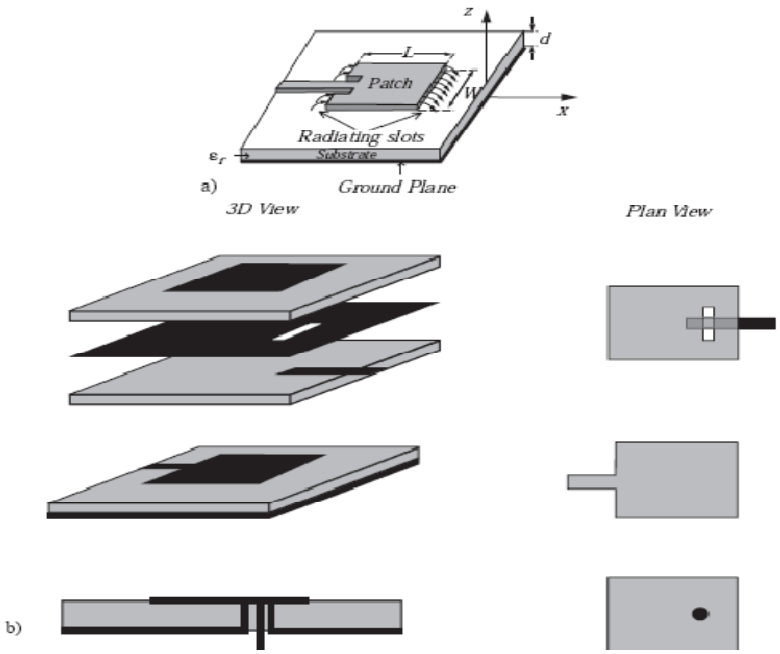

Figure 2.7 Microstrip antennas and their feeds (a) a microstrip antenna with its coordinates, (b) three feeding configurations: coupling feed, microstrip feed and coaxial feed respectively [4].

2.3.4 Array Antennas

Sometimes we need to be able to control the antenna radiation pattern, for example for tracking or anti-jamming/interference applications. A single-element antenna is not good enough to meet such a requirement. In this case, an antenna array could be a good solution.

The arrangement of the array may be such that the radiation from the elements adds up to give a radiation maximum in a particular direction, minimum in others, or otherwise as desired. Typical examples of arrays are shown in Figure 2.8. Usually the term *array* is reserved for an arrangement in which the individual radiators are separate as shown in Figures 2.8(a–c). However the same term is also used to describe an assembly of radiators mounted on a continuous structure, shown in Figure 2.8(d). The major advantages of an array are: the flexibility to form a desired radiation pattern, the high directivity and gain [1,4].

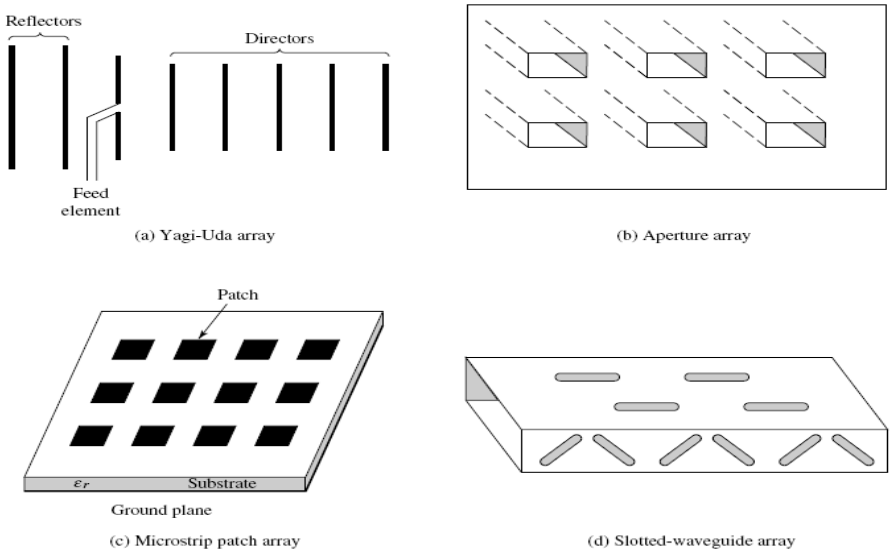

Figure 2.8 Typical wire, aperture, and microstrip array configurations [1].

2.3.5 Reflector Antennas

Reflector antennas, also known as satellite dish antennas, are a specific type of antennas for long distance communications. They are probably the most widely used antennas for high-frequency and high-gain applications in radio astronomy, radar, microwave and millimeter wave communications and satellite tracking and communications [1,4].

2.3.6 Lens Antennas

As reflector antennas, lens antennas can convert a spherical wave into a plane wave to produce high gains. They are suitable for high-frequency > 4 GHz applications. There are of many types but the most important two types are delay lenses, in which the electrical path length is increased by the lens medium (using low-loss dielectrics with a relative permittivity greater than one, such as Lucite or polystyrene), and fast lenses, in which the electrical path length is decreased by the lens medium (using metallic or artificial dielectrics with a relative permittivity smaller than one) [4].

2.4 Antenna Parameters

Antennas are defined by several parameters according to their constitution and shape. In this section, the most important are considered and explained, and an overview of each is essential to describe antenna's performance.

2.4.1 Radiation Pattern

An antenna *radiation pattern* or *antenna pattern* is defined as "a mathematical function or a graphical representation of the radiation properties of the antenna as a function of space coordinates. In most cases, the radiation pattern is determined in the far field region and is represented as a function of the directional coordinates. Radiation properties include power flux density, radiation intensity, field strength, directivity, phase or polarization." [5].

A mathematical illustration of the radiation properties of an antenna as a function of the space coordinates defined by the spherical coordinates θ and ϕ, as shown in Figure 2.9.

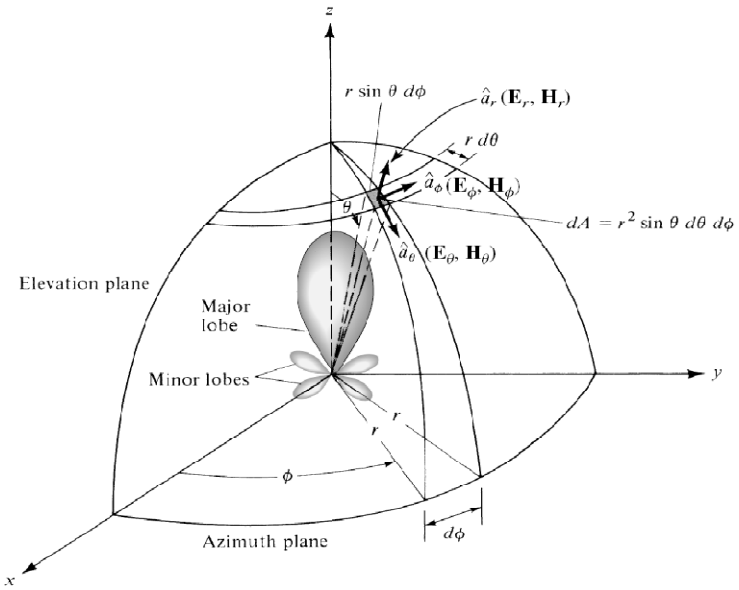

Figure 2.9 Coordinate system for antenna Analysis [5].

A trace of the received electric (magnetic) field at a constant radius is called the amplitude *field pattern*. On the other hand, a graph of the spatial variation of the power density along a constant radius is called an amplitude *power pattern*, Often the *field* and *power* patterns are normalized with respect to their maximum value, yielding *normalized field* and *power patterns*. Also, the power patterns usually plotted on a logarithmic scale or more commonly in decibels (dB) [5].

Various parts of a radiation pattern are referred to as *lobes*, which may be sub-classified into *major* or *main, minor, side*, and *back* lobes as shown in figure 2.10. A *radiation lobe* is a "portion of the radiation pattern bounded by regions of relatively weak radiation intensity." [5].

The main lobe (or main beam or major lobe) is the lobe containing the direction of maximum radiation. There is also usually a series of lobes smaller than the main lobe. Any lobe other than the main lobe is called a minor lobe. Minor lobes are composed of side lobes and back lobes. Back lobes are directly opposite the main lobe, or sometimes they are taken to be the lobes in the half-space opposite the main lobe [6].

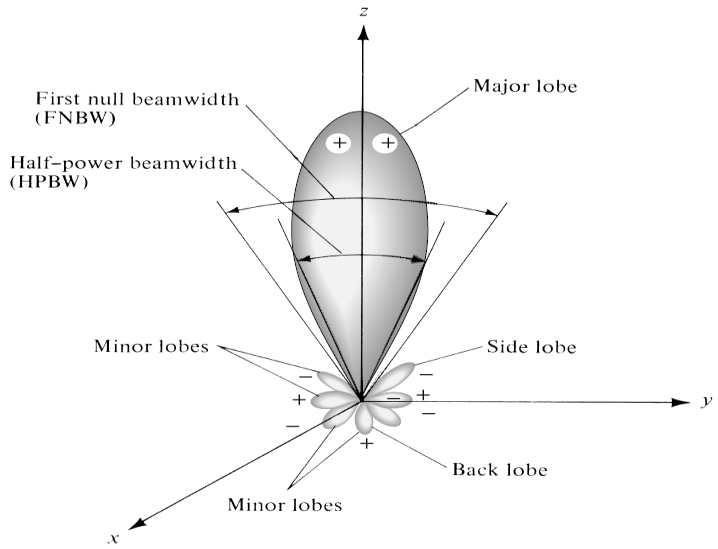

Figure 2.10 Radiation lobes and beamwidths of an antenna pattern [5].

There are three common radiation patterns that are used to describe an antenna's radiation property:

• **Isotropic**- A hypothetical lossless antenna having equal radiation in all directions.

• **Directional**- An antenna having the property of radiating or receiving electromagnetic waves more effectively in some directions than in others.

• **Omnidirectional**- An antenna having an essentially non-directional pattern in a given plane and a directional pattern in any orthogonal plane.

Directional or omnidirectional radiation properties are needed depending on the practical application. Omnidirectional patterns are normally desirable in mobile and hand-held systems [5].

2.4.2 Beamwidth

The *beamwidth* of a pattern definition is the angular separation between two identical points on opposite side of the pattern maximum. In an antenna pattern, there are a number of beamwidths. One of the most widely used beamwidths is the *Half-Power Beamwidth* (*HPBW*), which is defined by IEEE as: "In a plane containing the direction of the maximum of a beam, the angle between the two directions in which the radiation intensity is one-half value of the beam". The angular separation between the

first nulls of the pattern is referred to as the *First-Null Beamwidth* (*FNBW*) as shown in figures 2.10 and 2.11 [5].

The beamwidth of an antenna is a very important issue and often is used as a trade-off between it and the side lobe level; that is, as the beamwidth decreases, the side lobe increases and vice versa. In addition, the beamwidth of the antenna is also used to describe the resolution capabilities of the antenna to distinguish between two adjacent radiating sources or radar targets [5].

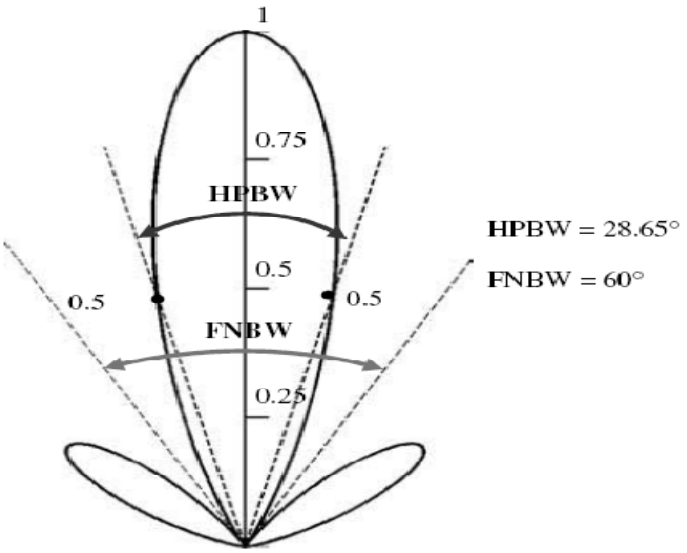

Figure 2.11 beamwidths of a directional antenna power pattern [5].

2.4.3 Directivity

The directivity of an antenna is defined as "the ratio of the radiation intensity in a given direction from the antenna to the radiation intensity averaged over all directions." In other words, the directivity of a nonisotropic source is equal to the ratio of its radiation intensity in a given direction, over that of an isotropic source [5,6].

Radiation intensity is the power radiated in a given direction per unit solid angle and has units of watts per square radian (or steradian, sr). The advantage of using radiation intensity is that it is independent of distance *r* [6].

$$D = \frac{U}{U_i} = \frac{4\pi U}{P_r} \tag{2.4}$$

Where *D* is the directivity of the antenna; *U* is the radiation intensity of the antenna; U_i is the radiation intensity of an isotropic source; and P_r is the total power radiated.
Sometimes, the direction of the directivity is not specified. In this case, the direction of the maximum radiation intensity is implied and the maximum directivity is given as

$$D_{\max} = \frac{U_{\max}}{U_i} = \frac{4\pi U_{\max}}{P_r} \tag{2.5}$$

where $D_{\max}$ is the maximum directivity and $U_{\max}$ is the maximum radiation intensity.

The directivity of an antenna can be easily estimated from the radiation pattern of the antenna. An antenna that has a narrow main lobe would have better directivity than the one that has a broad main lobe; hence, this antenna is more directive.

2.4.4 Antenna Efficiency

Antenna efficiency is the measure of the antenna's ability to transmit the input power into radiation. Antenna efficiency is the ratio between the radiated power to the input power [5,6]:

$$e = \frac{p_r}{p_{in}} \tag{2.6}$$

There are a number of antenna efficiencies; the total antenna efficiency e_0 is used to take into account losses at the input terminals and within the structure of the antenna as shown in Figure 2.12. Such losses may be due to [5]:

1. reflections because of the mismatch between the transmission line and the antenna
2. I^2R losses (conduction and dielectric)

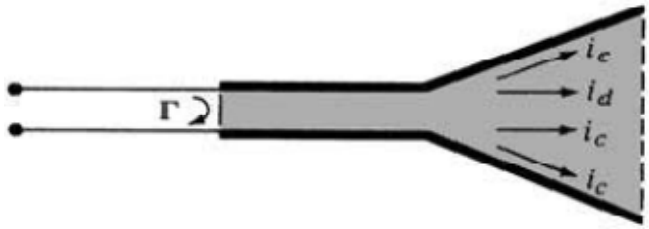

Figure 2.12 antenna losses (Reflection, conduction and dielectric) [5].

In general, the overall efficiency can be written as:

$$e_o = e_r e_c e_d \tag{2.7}$$

where
e_o = total efficiency
e_r = reflection(mismatch) efficiency
e_c = conduction efficiency
e_d = dielectric efficiency

2.4.5 Gain

The gain of an antenna (referred to a lossless isotropic source) depends on both its directivity and its efficiency. If the efficiency is not 100 percent, the gain is less than the directivity [2]. Thus, the gain

$$G = e_o D \tag{2.8}$$

Where k = efficiency factor of antenna ($0 < e_o < 1$).

Gain of an antenna (in a given direction) is defined as "the ratio of the intensity, in a given direction, to the radiation intensity that would be obtained if the power accepted by the antenna were radiated isotropically. The radiation intensity corresponding to the isotropically radiated power is equal to the power accepted (input) by the antenna divided by 4π." [5]. Gain can be expressed as

$$\text{Gain} = 4\pi \frac{\text{radiation intensity}}{\text{total input (accepted) power}} = 4\pi \frac{U(\theta,\phi)}{p_{in}} \tag{2.9}$$

2.4.6 Polarization

The polarization of an antenna is the polarization of the wave radiated in a given direction by the antenna when transmitting. When the direction is not stated, the polarization is taken to be the polarization in the direction of maximum gain. The polarization of a radiated wave is the property of an electromagnetic wave describing the time varying direction and relative magnitude of the electric field vector [5].

If the polarization of the receiving antenna is not the same as the polarization of the incoming (incident) wave, there is polarization mismatch resulting in power loss. The requirement of the antenna polarization depends on the applications [5-6]. Polarization can be categorized as linear, circular and elliptical as shown in Figure 2.13.

• **Linear polarization:** If the electric field vector moves back and forth along a line it is assumed to be linearly polarized. A linearly polarized wave is considered as horizontally polarized if the electric field is parallel to the earth and vertically polarized if the electric field is perpendicular to the earth. For a linearly-polarized antenna, the radiation pattern is taken both for a co-polarized and cross-polarized response.

Co-polarization represents the polarization the antenna is intended to radiate (receive), **Cross-polarization** represents the polarization orthogonal to a specified polarization (co-polarization).

• **Circular polarization:** If the electric field vector remains constant in length but rotates around in a circular path then it is considered circularly polarized. For circular polarization, the fields components have same magnitude and the phase between two components is 90 degree.

• **Elliptical polarization:** describes an antenna when its electric field vector at a far field point is such that traces elliptical curves constantly with time. Moreover, both the circular and elliptical polarizations are characterized for being right-hand (RH) or left-hand (LH) polarized, depending on the sense of the field; if the field is flowing in the clockwise direction, the field will be right hand polarized; otherwise it will be left hand polarized [5].

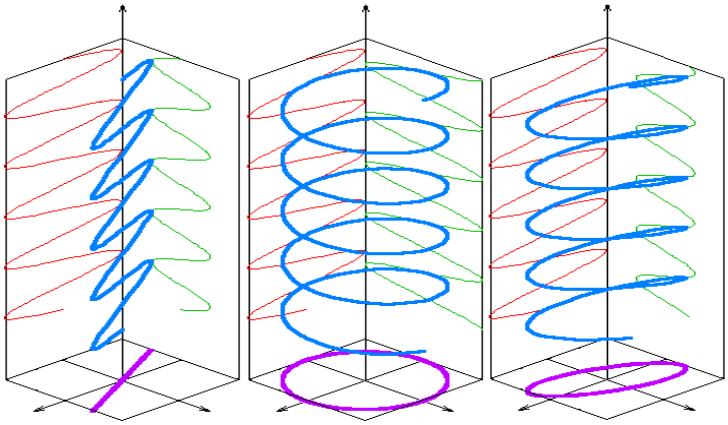

Figure 2.13 Three types of polarization (linear, circular and elliptical) [7].

2.4.7 Input Impedance

Input impedance is defined as "the impedance presented by an antenna at its terminals or the ratio of the voltage to current at a pair of terminals or the ratio of the appropriate components of the electric to magnetic fields at a point." [5]. The input impedance will be affected by other antennas or objects that are nearby, but we assume that the antenna is isolated. Input impedance is composed of real and imaginary parts [6]:

$$Z_{in} = R_A + jX_A \tag{2.10}$$

The input resistance R_A represents dissipation, which occurs in two ways. Power that leaves the antenna and never returns (i.e., radiation) is a form of dissipation. There are also ohmic losses associated with heating on the antenna structure, but on many antennas ohmic losses are small compared to radiation losses. However, ohmic losses are usually significant on electrically small antennas, which have dimensions much less than a wavelength. The input reactance X_A represents power stored in the near field of the antenna. As a consequence of reciprocity, the impedance of an antenna is identical during reception and transmission [6].

Frequency makes the impedance vary constantly with its value. For lower frequencies (higher wavelengths) the length of the transmission line is not significant when compared to wavelength, so the result is a short line. Although for higher frequencies where the transmission line is slightly a big fraction of a wavelength, it can be a problem because the input impedance will be influenced in a large scale by the length of the transmission line. Therefore, the term impedance matching becomes important, because in this case the length of a transmission line is not significant when compared to the wavelength. The input impedance of an antenna will be matched with a transmission line if both impedances are the same ($Z_A = Z_O$).

If an antenna is mismatched, the loss of power can be very high, because the power generated by the source will be reflected back. As a measure related with power, input impedance is a crucial quantity for the power that an antenna will receive. Thus, as a definition, a maximum power will be delivered from the source to the antenna, if the input impedance is equal to the conjugate of the impedance generated by the source $Z_A = Z_S^*$. Therefore, no power will be transmitted when Z_A is much smaller or much superior than Z_S as shown in Figure 2.14 [5,6].

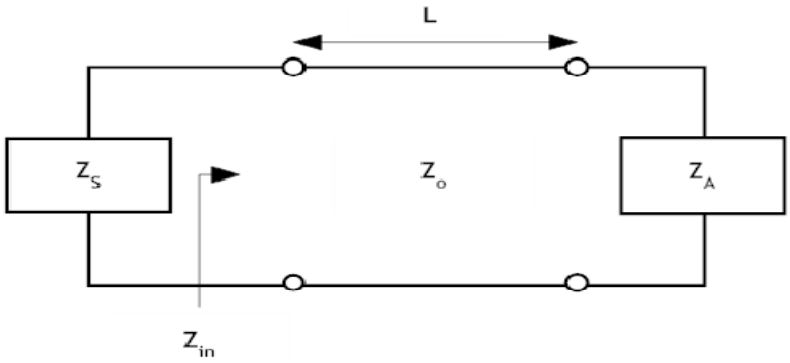

Figure 2.14 Circuit representing input impedance at the entrance terminals of the transmission line.

2.4.8 Bandwidth

The term bandwidth specifies the range of frequencies which an antenna can achieve, in order to obtain a desirable behavior of a certain characteristic. The bandwidth can be considered to be the range of frequencies, on either side of a center frequency (usually the resonance frequency for a dipole), where the antenna characteristics such as (input impedance, radiation pattern, beamwidth, polarization, side lobe level, gain, beam direction, radiation efficiency) are within an acceptable value of those at the center frequency (at -10 dB). It is classified as the first required condition before building an antenna, because it is a measure of how acceptable the performance of an antenna can be. However, as a range, two boundaries define the lower and upper frequency limits, and the ratio of its size to the centre frequency as a percentage define the percent bandwidth for a narrowband antenna – thus occupying a small space quantity on the RF spectrum – given by equation (2.11); otherwise, for a

broadband (or wideband) antenna the bandwidth is defined as the ratio of the upper to lower frequencies as written in equation (2.12). Both expressions are analytically represented as [5,8]:

$$B_f = \frac{f_H - f_L}{f_c} \times 100 \tag{2.11}$$

$$B_r = \frac{f_H}{f_L} \tag{2.12}$$

Where:

B_f – Fractional bandwidth in Hz percentage;

B_r – Bandwidth ratio;

f_H – Upper frequency in Hz;

f_L – Lower frequency in Hz;

f_c – Centre frequency in Hz.

Usually, the described parameters of an antenna may have a satisfactory value of those at the centre frequency; therefore a bandwidth involving it, for which those parameters are able to have a good performance. In fact, all the parameters can be influenced by frequency in a different way, what gives a different meaning to the bandwidth of each. Especially analyzing the radiation pattern and input impedance bandwidth differences, the useful bandwidth of a designed antenna can be related to both, despite of the disparity on those differences. In some cases the satisfactory bandwidth for radiation pattern goes above the one for input impedance, or vice-versa [5,8].

2.5 Antennas for Body Area Networks

Antennas play an important role in optimizing the radio system performance. The design of a power-efficient and reliable on-body communication system requires suitable antennas which therefore require accurate understanding of the human body effects on the antenna performance parameters and radio propagation channels [9].

For BAN applications, the antenna design is a difficult task because the antenna is required to be small in size with suitable feeding structure for proper integration in small-sized body-worn devices and having good antenna parameters performance on human body; The antennas can detune when mounted on the body which depends upon the antenna and tissue type [10].

One of the main issue in BAN antenna design is the health hazard associated with electromagnetic radiation very close to the human body and, as a result, the absorption of energy by the human tissues. The amount of energy absorbed is usually measured in Specific Absorption Rate (SAR), which is the maximum allowable power absorbed per unit mass of the body tissue. This level is 2.0 W/kg [11]. Careful consideration is required to design the wearable antennas and other circuits, as there are limitations on the maximum power to which the human body can be exposed. It is, for this reason, very important to keep the transmitted power as low as possible for body-worn devices and use antennas with very low or no back radiation.

The radiation pattern of the antenna is another important parameter to be considered. For on-body applications, the radiation pattern should be such that the maximum beam direction is along the surface of the body. This means that the antenna should be able to launch waves, which can travel along the body surface. These waves propagate along the surface of the body as creeping waves [12]. The antennas with omnidirectional radiation pattern in the plane tangential to the surface of the body are

considered suitable for BAN applications. The radiation pattern of the antenna is changed compared to the free space radiation pattern when the antenna is placed on the body. In some cases, the gain of the antenna on the body is significantly reduced compared to the free space gain. Hence, the antenna design requires careful consideration [10].
Currently the field of antennas for BAN has resolved itself into the following categories, narrowband, wideband, implantable, fabric and multiple antennas. The sensitivity of antenna performance to body proximity and in particular patch antennas working in a variety of modes has been investigated in [13].

Ultra wideband (UWB) systems are considered to be potentially useful, and the transient performance of such antennas on the body has been investigated in [14], as well as in [9] where M. M. Khan investigated many antennas from narrowband and UWB; The UWB and narrowband systems show nearly the same trends of path loss for different on-body locations of different test subjects.

There are many publications on implantable antennas, such as a novel chandelier meandered design for ingestible devices, [15], optimized antennas for rat implantation, [16], also Alomainy *et al.* presented a study of a compact antenna used in sensors aimed at healthcare applications in the 2.45 GHz ISM band [17]. A thorough numerical investigation of the antenna performance, including full sensor details and the presence of the human body, was performed. The results demonstrated that the power radiated from the compact embedded antenna is comparable to the one of an external monopole.

For flexibility, antennas were integrated into garments, antennas made out of textile materials have been proposed [18-24]. In [23], a patch antenna integrated into protective clothing for fire-fighters was introduced. The antenna was printed on a flexible pad of foam, which is commonly used in protective clothing. In [20, 21], narrowband antennas were printed above Electromagnetic Band Gap (EBG) structures to reduce the radiation towards the human body, and minimize the detuning effect. In [21], Langley *et al*. proposed a flexible dual-band patch antenna (2.45 and 5.5 GHz) printed on an EBG textile substrate made of felt. Results demonstrated that by introducing the EBG, the radiation into the body is reduced by over 10 dB, and the antenna gain is improved by 3 dB. However, the antenna is big in size (120 x 120 mm). Salonen *et al.* has presented a flexible planar inverted F antenna (PIFA) that can be applied to smart clothing intended for use with wearable computers as part of WBANs [24].

Multiple antenna systems for diversity and MIMO in [25] showed improved capacity performance over single antenna links. Work in channel modeling continues, with the difficult problem of modeling of non-stationary channels, being addressed in [26] using autoregressive transfer functions. Also in [10] I. khan investigated the usefulness of multiple antennas at the receiver side for the on-body channels and quantify the achievable improvement due to the use of diversity techniques, and he concluded that receive diversity has been found to be very effective in combating the fading caused by the environment and the body movement.

2.5.1 Literature Review for Narrowband Antennas for BAN

There are two basic requirements for antennas for on-body links. First, the antenna needs to be insensitive to the proximity of the body; and second, the antenna needs to have a radiation pattern shape that minimizes the link loss [12].

Many studies have been made on the operation of antennas located in close proximity of the body; In [27] a parametric study to evaluate how the antenna-body spacing affects the antenna performance has been presented. The further the antenna is

from the body, the lower is the absorption from the human body. The use of a lossy material to keep this spacing is beneficial, as it leads to SAR reduction, since part of the power is dissipated in the lossy material rather than in the body tissues.

Peter Hall *et al.* have done extensive studies on narrowband antennas (2.45 GHz) [28,29] for on-body applications and found that, for communication over the body surface, wire monopole antennas shows good performances with respect to path loss, due to their omnidirectional radiation pattern in the azimuth plane.

In [30] Scanlon *et al*. presented a set of higher-mode microstrip patch antennas operating at 2.45 GHz. The antennas are excited at the higher TM_{21} resonant mode, which has the advantage of having a vertical monopole-like radiation pattern. With a total antenna height of only $\lambda/20$, the on-body coupling performance is comparable to that achievable with a quarter wavelength monopole and significantly higher than that measured with a fundamental microstrip patch antenna.

In [31] a dual-band (2.4 GHz, 5.2 GHz) button antenna for WLAN applications was presented by John Batchelor. The antenna has the size of a standard metal button used in denim jeans, and can be easily integrated in clothes. The antenna has monopole-like radiation performances in both frequency bands of operation.

On-body radio propagation has been studied and investigated for narrowband (2.45 GHz) communication [12, 28, 32, 29]. In [12, 28, 29], on-body channel characterization was presented at the unlicensed frequency band of 2.45 GHz, with the human body standing, various body positions and postures and body movements, using different kinds of antennas (such as Wire Monopole on large ground plane, Loop, Dipole, Patch and Patch array). Results show that the Monopole-Monopole combination gives the lowest link loss (lowest path loss) for all on-body channels of positions and postures scenarios. The Wire Monopole antenna has a quite omnidirectional radiation pattern in the horizontal plane with the maximum gain, which provides good coverage over the body surface when it is placed on the human body.

Although there were some studies of the human body effects on the antenna parameters, they were not thorough and the antennas were limited. However, a complete parametric study addressing the effects of the human body on the performance parameters for a wider number of antennas are shown in [9], as it will be discussed in next section

2.5.2 Comparison between Five Antennas at 2.45 GHz for the On-body Performance Parameters

In [9], M. M. khan investigated and compared the on-body performance parameters of five different narrowband antennas at 2.45 GHz, specially the Wire Monopole, Patch, Printed Monopole, Inverted L and Loop antennas as shown in Figure 2.15. It provides an understanding of the human body effect on antenna parameters such as frequency detuning, impedance bandwidth, gain, impedance, radiation pattern, polarization and radiation efficiency. The effects of body-worn antenna types on the on-body radio channels are also investigated.

The size and volume of the narrowband antennas used in the study are shown in Table 2.2. All antennas are printed on FR4 substrate, except for the Patch (RT/Duroid) and Wire Monopole. Out of the five antennas, two (Patch, Wire Monopole) have a full ground plane at the back and the other three (Printed Monopole, Loop, Inverted L) have partial ground plane. Out of the five antennas, the Loop has the smallest ground plane size; in comparison, the Wire Monopole has the highest volume.

Antenna	Substrate L×W (mm^2)	ε_r	Ground Plane L×W (mm^2)	Height (mm)	Volume L×W×H (mm^3)	Antenna Element L×W(mm^2)
Patch	80×60	3	80×60	1.524	80×60×1.524	74.2×39.5
Wire Monopole	-	-	90×90	29.3	90×90×29.3	23.3×0.35
Printed Monopole	70×80	4.6	43×73	1.6	70×80×1.6	64×3
Inverted L	70×50	4.6	45×50	1.6	70×50×1.6	54.5×20.3
Circular Loop	60×60	4.6	10×60	1.6	60×60×1.6	47.5×33

Table 2.2 Comparison of volume and size of the narrowband antennas used in the study in [9].

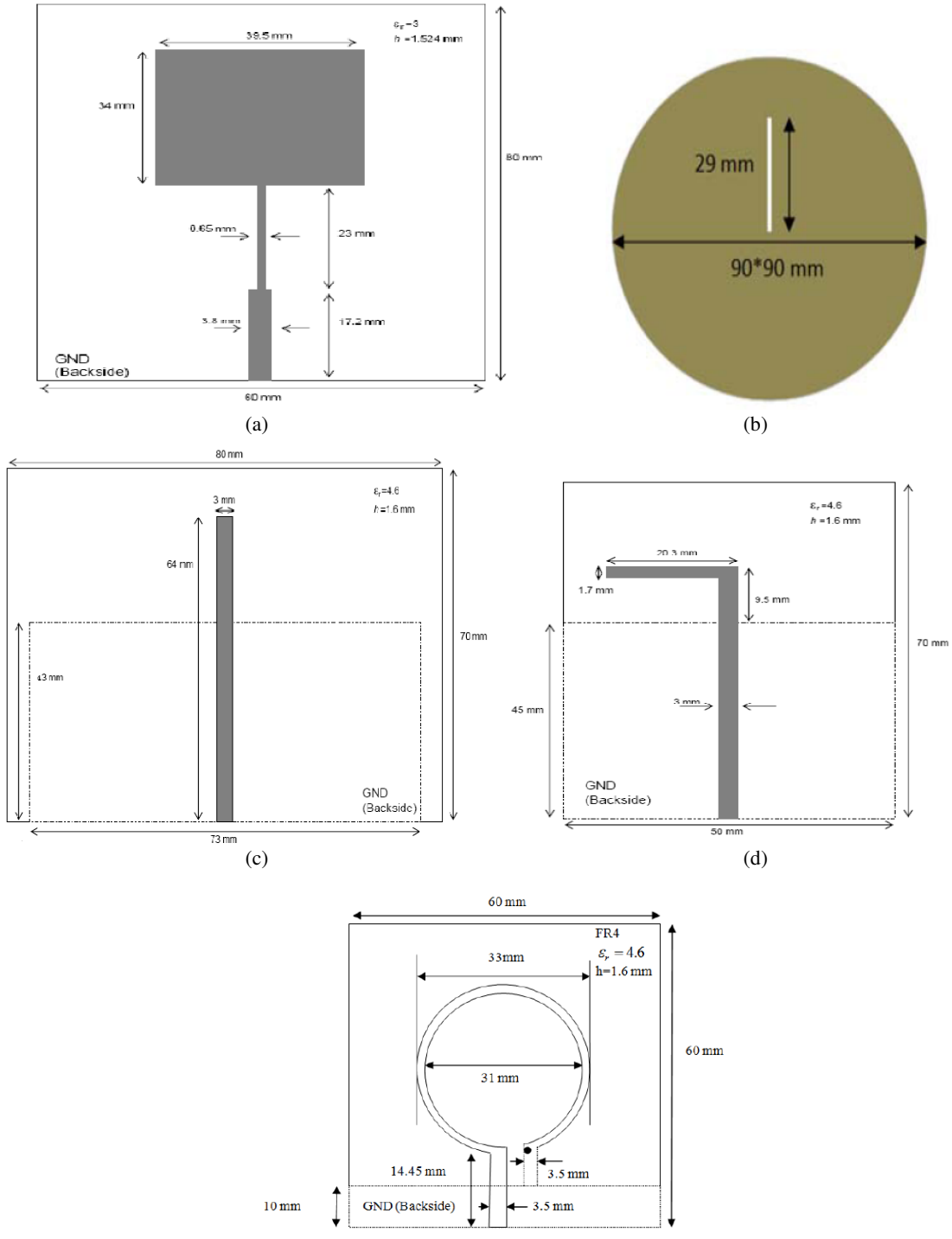

Figure 2.15 The five narrowband antennas (a) Patch, (b) Wire Monopole, (c) Printed Monopole, (d) Inverted L and (e) Circular Loop compared at [9].

During the measurement, the antennas were placed directly on the body, and then placed at 1, 4, 8 and 16 mm away from the body. Due to the back feed, the Wire Monopole antenna was placed at 16 mm away from the body only.

Figure 2.16 presents the percentage of frequency detuning from free space resonance for the different antennas when placed at various distances away from the body (left side of the waist). The resonance frequency detunes from the free space value, up to maximum of 33 % (Inverted L antenna), when the antenna placed on the body. The frequency detuning is due to the changes in the antennas effective length, caused by the presence of the human lossy tissue. The antennas with partial ground plane (Printed Monopole, Loop, and Inverted L) experience the highest frequency detuning, while the antennas with full ground plane (Patch and Wire Monopole) do not experience any frequency detuning. The ground plane acts as a shield between the antenna and the body, resulting in no frequency detuning for patch and wire monopole antennas. Results show that, as the distance between the antenna and the body increases, the frequency detuning reduces.

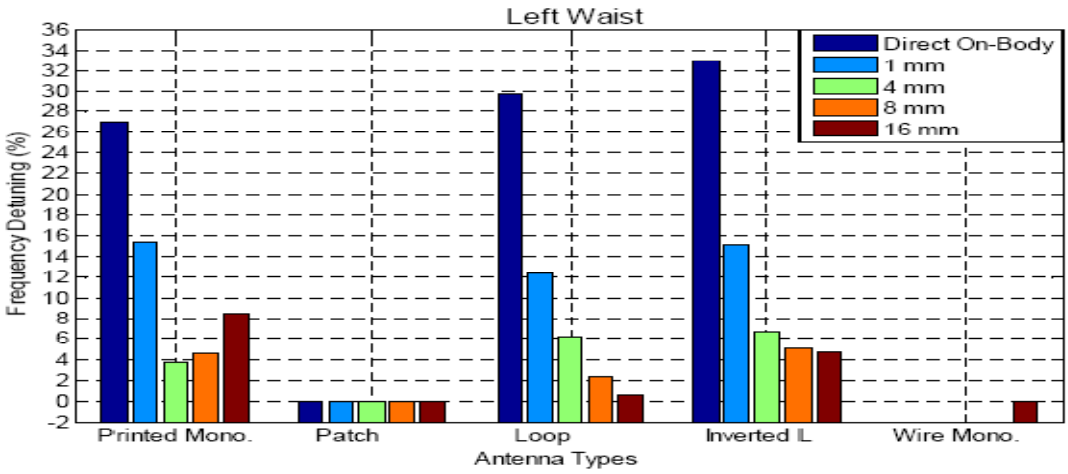

Figure 2.16 Comparison of frequency detuning in percentage for five narrowband antennas when placed at different distances from the left side of the waist [9].

The impedance bandwidth of the five antennas was extracted from the measured S11 results. For the study, impedance bandwidth was calculated for a return loss of -10 dB. Figure 2.17 shows a comparison of impedance bandwidth as a percentage for the five antennas, with respect to distance from the body (right side of the chest). When antennas were placed on the body, the impedance bandwidth mostly increased from the free space value, up to a maximum of 84.52% (Printed Monopole antenna). On the body, the impedance bandwidth of the antenna increases due to the loss from the human body. The impedance bandwidth increase is significant for the antennas with partial ground plane. The use of Printed Monopole, Inverted L and Loop antennas on the body, the frequency detunes from free space significantly; however, the impedance bandwidth increases greatly.

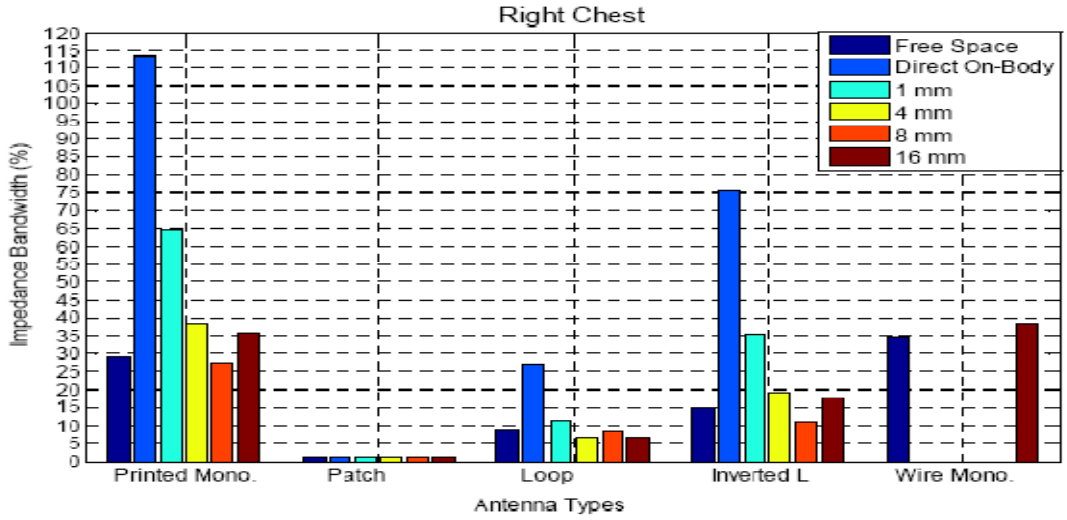

Figure 2.17 Comparison of impedance bandwidth in percentage for five different narrowband antennas when placed at different distances from the right side of the chest [9].

Varying the distance between the antenna and the body does not affect the impedance bandwidth much for the Patch antenna, whereas the impedance bandwidth varies to a large extent with separation for the Printed Monopole, Inverted L and Loop. Out of these five antennas, the Patch antenna shows the lowest on body impedance bandwidth (maximum up to 1.38 %).

The antenna radiation efficiency parameter was extracted from the simulation results. The antenna was simulated placing in free space and then at 1, 4, 8 and 16 mm away from the human phantom (right side of the chest) using CST microwave studio.

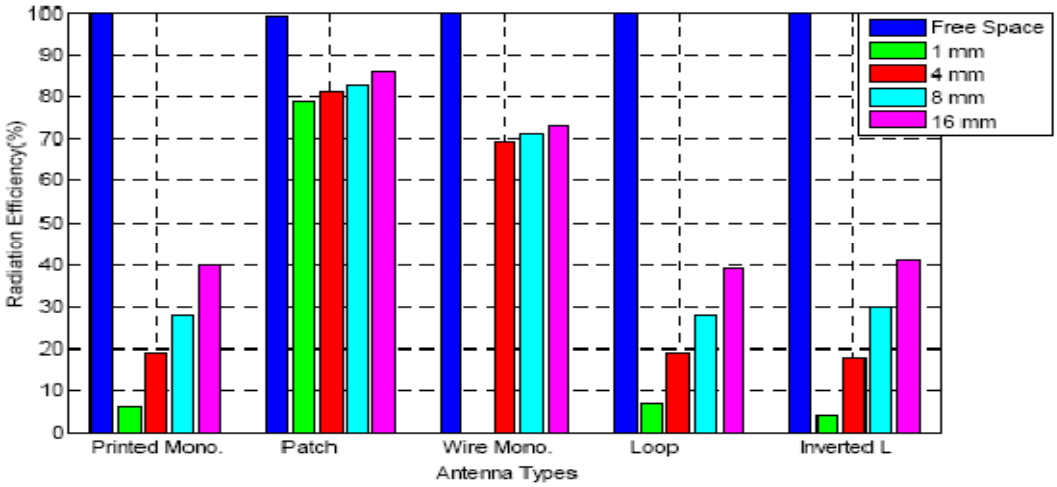

Figure 2.18 Comparison of radiation efficiency in percentage for five different narrowband antennas when placed on various distance from the body on right side of the chest [9].

Due to power absorption by the human lossy tissues, the radiation efficiency for all antennas reduces from free space when placed on the body. Figure 2.18 shows the reduction of radiation efficiency from that of free space (in percentage) for the narrowband antennas when placed at various distances from the body (right side of the chest). Placing the antennas at 1 mm away from the body, the highest radiation efficiency reduction of 96 % is noticed for the Inverted L, while the lowest is noticed for the Patch (20%). The Loop, Inverted L and Printed Monopole show nearly the same trends of the radiation efficiency reduction. Due to having full ground plane at the back, the radiation efficiency reduces less for the Patch and Wire Monopole. For all

narrowband antenna cases, as the distance between the body and the antenna increases the radiation efficiency reduces the less. Results show that regardless of the antenna type, reasonable on-body radiation efficiency is noticed when placed at 8 mm away from the body. However, for the antenna with full ground planes, reasonable radiation efficiency is still achieved at very lower distance (1 mm).

The gain parameter in free space and 1, 4, 8 and 16 mm away from the body of five antennas as in Figure 2.19 shows the comparison of free space and on-body gain for the presented five antennas, when placed at different distances on the body (right side of the chest). Placing the antenna on the body, the gain drops by a maximum of 12.39 dB (Inverted L); however, gain increases by a maximum of 1.6 dB for the Wire Monopole. On the human body, the gain drops for the antennas with partial ground planes (Printed Monopole, Inverted L and Loop) and increases mostly for the antennas with full ground plane (Patch and Wire Monopole). For the antennas having partial ground plane, higher power absorption occurs from the human lossy tissues resulting in a dramatic decrease of antenna gain. When the antenna placed on the human body, the curvature of the human body contributes to improve the directivity of the antenna which results higher gain for some on-body antennas.

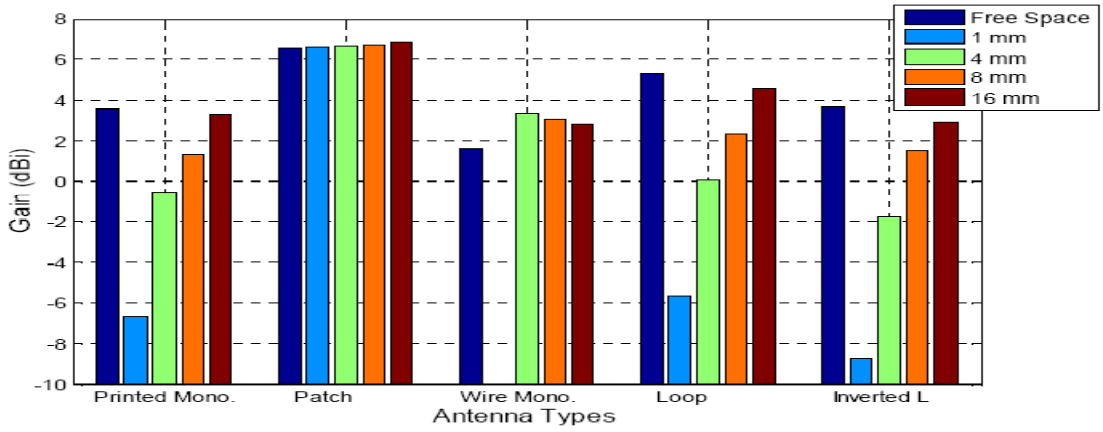

Figure 2.19 Comparison of gain for five different narrowband antennas when placed at various distances from the body on right side of the chest [9].

For on-body applications, if we do not want the full ground plane at the back of the wearable antennas, they need to be placed at 8 or 16 mm away from the body, because at these distances the antennas show acceptable gain . The optimum distance to place the narrowband antenna from the body is therefore recommended to be 8 mm or 16 mm.

The free space radiation pattern of the Wire Monopole antenna is quite omnidirectional over the body surface (in the XZ plane) and there is a presence of null in the Y direction [28,33] while the free space radiation of the Patch antenna is directive towards the Y direction (off-body direction) [32]. The Printed Monopole and Inverted L antennas show nearly the same free space radiation performances as omnidirectional in the XY plane. There is a presence of null to the Z direction in the radiation pattern of the Printed Monopole and Inverted L antennas [34,35]. The free space radiation pattern of the Loop antenna is directive towards the Z direction; however, it also radiates omnidirectional in the XY direction with slight loss in the radiation pattern in both direction of X [36]. Placing the narrowband antennas on the body, the radiation patterns do not deform for the Patch and Wire Monopole antennas while for the Printed monopole, Inverted L and Loop antennas, the radiation patterns deform notably (the radiation patterns become directive towards off-body direction).

The radiation pattern was investigated as a function of distance between the antenna and the human body. In this case, the Patch and Printed Monopole have been chosen as suitable examples. Figures 2.20 (a) and (b) show the simulated XZ plane co- and cross-polar radiation patterns of the Printed monopole and Figures 2.20 (c) and (d) show the simulated XZ plane co-and cross-polar radiation patterns of the Patch. Results show that varying the distance between the antenna and the body does not distort the radiation pattern but changes the power level.

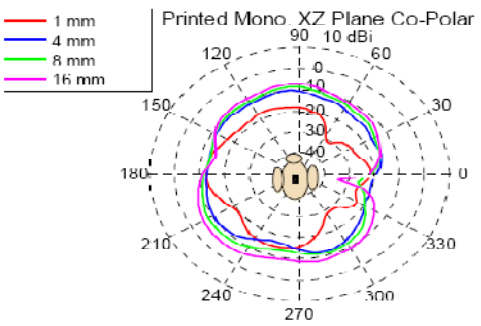

(a) Printed Monopole, XZ plane co-polar

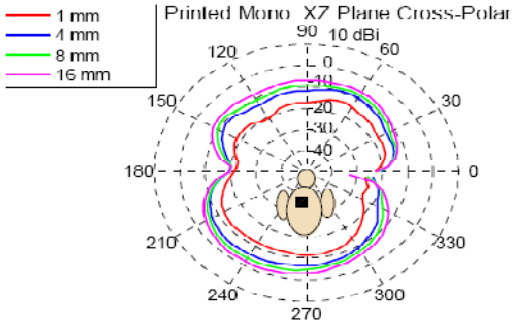

(b) Printed Monopole, XZ plane cross-polar

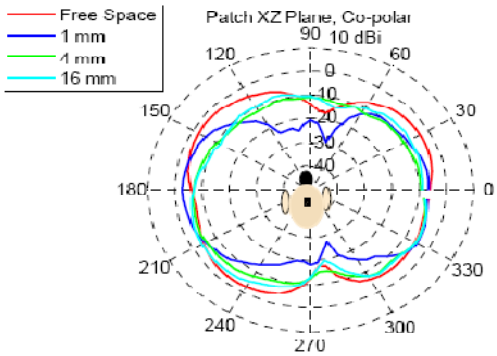

(c) Patch, XZ plane co-polar

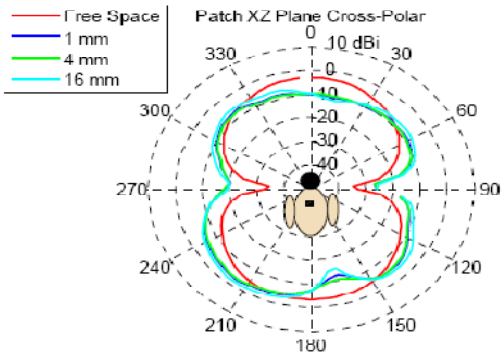

(d) Patch, XZ plane cross-polar

Figure 2.20 (a) XZ plane co-polar radiation patterns of the Printed Monopole, (b) XZ plane, cross-polar radiation patterns of the Printed Monopole, (c) XZ plane co-polar radiation patterns of the Patch, (d) XZ plane cross-polar radiation patterns of the Patch [9].

It was observed that the performances of the Printed Monopole, Inverted L and Loop antennas degrade significantly in close proximity to the human body except the increase of the bandwidth, so they need to be placed far away from the human body in order to get good on-body performance. The overall on-body performances of the Inverted L, Printed Monopole and Loop are comparable, while slight improve performance is noticed for the Printed Monopole antenna as shown in the results of the study in [9].

The performance of the Wire Monopole and Patch antenna is less sensitive to the presence of the human body due to having full ground plane at the back. These two antennas show very good (nearly stable) performance even very close to the body. The wire monopole antenna has the advantage of performance compared with the Patch (in terms of impedance bandwidth, gain and radiation pattern). It has omnidirectional radiation pattern with higher on-body gain over the body surface plane while the patch has the radiation towards the off-body direction with higher gain as shown in the results of the study in [9].

The major drawback of the wire monopole is the shape which is not conformal to the body. In addition, the volume of the wire monopole is the highest compared with other four antennas.

References

[1] C. A. Balanis, "Antennas," in Antenna theory : analysis and design, pp. 1 – 10, 3rd ed., New York: Wiley, 2005.

[2] J. D. Kraus, "Basic Antenna Concepts," in Antennas, pp. 17 – 82, 2nd ed., New York: McGraw-Hill, 1988.

[3] J. D. Kraus and R. J. Marhefka, "Antenna Basics," in Antennas for all Applications, pp. 11-92, 3rd ed., New York: McGraw-Hill, 2002.

[4] Y. Huang and K. Boyle, Antennas: From Theory to Practice,1st ed., John Wiley & Sons, 2008.

[5] C. A. Balanis, " Fundamental Parameters of Antennas," in Antenna theory: analysis and design, pp. 27 – 86, 3rd ed. New York: Wiley, 2005.

[6] W. L. Stutzman, G. A. Thiele, " Antenna Fundamentals and Definitions," in Antenna theory and design, PP. 1-52, 2nd ed., New York: Wiley, 1998.

[7] http://en.wikipedia.org/wiki/Polarization_(waves).

[8] J. L. Volakis, "Fundamentals of Antennas, Arrays, and Mobile Communications," in *Antenna engineering handbook*, pp. 13 – 14, 4th ed. New York: McGraw-Hill, 2007.

[9] M. M. Khan, "Antenna and Radio Channel Characterization for Low-Power Personal and Body Area Networks", PhD thesis, University of London, February 2012.

[10] I. Khan, "Diversity and MIMO for Body-Centric Wireless Communication Channels", PhD thesis, University of Birmingham, September 2009.

[11] IEEE, "IEEE Recommended Practice For Determining The Peak Spatial-Average Specific Absorption Rate (SAR) In The Human Head From Wireless Communications Devices: Measurement Techniques", IEEE Std. 1528-2003, 2003.

[12] P. S. Hall, Y. Hao, "Antennas and Propagation for Body-Centric Wireless Communications", Artech House, London, 2006.

[13] S. L. Cotton and W. G. Scanlon, "Channel Characterization for Single- and Multiple-Antenna Wearable Systems Used for Indoor Body-to-Body Communications", IEEE Trans AP, Vol. 57, No. 4, Part 1, pp 980 –990, April 2009.

[14] A. Alomainy, A. Sani, A. Rahman, J.G. Santas, and Y. Hao, "Transient Characteristics of Wearable Antennas and Radio Propagation Channels for UWB Body-Centric Wireless Comms.", IEEE Trans AP, Vol. 57, No. 4, Part 1, pp 875 –884, April 2009.

[15] P. Izdebski and Y. Rahmat-Samii, "Antenna design for medical biotelemetry applications: small antennas for ingestible capsules," Dig. URSI-USNC National Radio Science Meeting, Boulder, CO, Jan. 3-6, 2008.

[16] T. Karacolak, R. Cooper, E. Topsakal, "Electrical Properties of Rat Skin and Design of Implantable Ants for Medical Wireless Telemetry", IEEE Trans AP, Vol. 57, No. 9, pp. 2806 -2812, Sept. 2009.

[17] A. Alomainy, Y. Hao and F. Pasveer, "Numerical and Experimental Evaluation of a Compact Sensor Antenna for HealthCare Devices,'' *IEEE Transaction on medical circuits and systems,* Vol.1, No.4, December 2007.

[18] P. Salonen, Y. Rahmat-Samii, and M. Kivikoski, "Wearable antennas in the vicinity of human body," *IEEE Antenna and Propagation Society Symposium*, Vol. 1, pp. 467–470, June 2004.

[19] P. Salonen and Y. Rahmat-Samii, "Textile antennas: effects of antenna bending on input matching and impedance bandwidth," *IEEE Aerospace and Electronic Systems Magazine*, Vol. 22, No. 3, pp. 10–14, 2007.

[20] S. Zhu and R. Langley, "Dual-band wearable antennas over EBG substrate," *Electronics Letters*, Vol. 43, No. 3, pp. 141–142, 2007.

[21] S. Zhu, "Dual-band wearable textile antenna on an EBG substrate," *IEEE Transactions on Antennas and Propagation*, Vol. 57, No. 4, pp. 926–935, 2009.

[22] C. Hertleer, A. Tronquo, H. Rogier, L. Vallozzi, and L. Van Langenhove, "Aperturecoupled patch antenna for integration into wearable textile systems," *IEEE antennas and wireless propagation letters*, Vol. 6, 2007.

[23] C. Hertleer, H. Rogier, L. Vallozzi, and L. van Langenhove, "A textile antenna for off-body communication integrated into protective clothing for fire-fighters," *IEEE Transactions on Antennas and Propagation*, Vol. 57, No. 4, pp. 919–925, 2009.

[24] P. Salonen and J. Rantanen, "A dual-band and wide-band antenna on flexible substrate for smart clothing," *27th Annual Conference of the IEEE Industrial Electronics Society*, 2001.

[25] I. Khan and P. S. Hall, "Experimental Evaluation of MIMO Capacity and Correlation for Narrowband Body-Centric Channels" IEEE Trans AP, Vol. 58, No. 1, pp 195 – 202, 2010.

[26] S. L. Cotton, G. A. Conway, W. G. Scanlon, "A Time Domain Approach to the Analysis and Modeling of On-Body Propagation Using Synchronized Measurements at 2.45 GHz", IEEE Trans AP , Vol. 57 , No. 4 , Part: 1, pp 943 – 955, 2009.

[27] A. Alomainy, Y. Hao and D. M Davenport, "Parametric Study of Wearable Antennas Varying Distances from the Body and Different On-Body Positions,'' *Antennas and Propagation for Body-Centric Wireless Communications,* pp. 84 – 89, *2007, IET Seminar on* 24-24 April 2007.

[28] P. S. Hall, Y. Hao, Y. I. Nechayev, A. Alomainy, C. C. Constantinou, , C. G. Parini, M.R Kamruddin, T. Z. Salim, D. T. M. Hee, R. Dubrovka, A. Wadally, W. Song, A. Serra, P. Nepa, M. Gallo, and M. Bozzetti, "Antennas and propagation for on body communication systems," *IEEE Antenna Technology and Propagation Magazine,* Vol. 49, No. 3, June 2007.

[29] M. R. Kamruddin, Y. Nechayev, and P.S. Hall, "Performances of Antennas in the On-Body Environment," *IEEE Antennas and Propagation Society International Symposium*, Page(s): 475-478 vol. 3A, 2005.

[30] G. A. Conway and W. G. Scanlon, "Antennas for over Body- Surface Communication at 2.45 GHz,'' *IEEE Transactions on Antennas and Propagation.* Vol. 57. No. 4, April 2009.

[31] B. Sanz-Izquierdo, F. Huang, and J. C. Batchelor, "Covert dual-band wearable button antenna,'' *IEEE Electron. Lett.* Vol. 42, No.12, pp. 3-4, 2006.

[32] A. Alomainy, Y. Hao, A. Owadally, C. G. Parini, P. S. Hall, and C. C. Constantinou, " Statistical analysis and performance evaluation for on-body radio propagation with microstrip patch antennas," *IEEE Transactions on Antenna and Propagation*, Vol. 55, No. 1, pp. 245–248, January 2007.

[33] P. S. Hall, Y. Nechayev, Y. Hao, A. Alomainy, M. R. Kamruddin, C. C. Constantinou, R. Dubrovka, and C. G. Parini, "Radio channel characterization and antennas for on body communications," *Proceeding of Loughborough Antennas and Propagation Conference, Loughborough, UK,* pp. 330-333, April 2005.

[34] M. N. Suma, P. C. Bybi, and P. Mohanan, "A wideband printed monopole antenna for 2.45 GHz WLAN applications,'' *Microwave and optical technology letter*, Vol. 48, No. 5, pp 871-873, May 2006.

[35] H. D. Chen, J. S. Chen, Y. T. Chen, "Modified inverted-L monopole antenna for 2.4/5 GHz dual-band operations'', *Electronics Letters*, Volume 39, Issue 22, pp: 1567-1568, October 2003.

[36] L. Akhoondzadeh-Asl, I. Khan, Y. I. Nechayev, P. S. Hall, "Investigation of polarization in on-body propagation channels,'' *Antennas and Propagation*, pp. 466–469, *EuCAP 2009*, 3rd European Conference, 2009.

Chapter 3

Monopole and PIFA Antennas

The most important requirements for antennas for on-body communications are the antenna sensitivity to the human body and the proximity to the human body. Diversity antenna of monopole and PIFA are used to satisfy these two factors that can minimize the channel loss.

The monopole antennas are chosen due to their advantages in providing omnidirectional patterns with maximum radiation along the surface, but with H and E fields normal to the surface, respectively. These will be suitable for paths where the surface wave dominates so monopole antennas has a polarization, which matches that of the surface wave. Since patch antenna produces strong radiation in the direction that normal to the radiating patch so it is more suitable for the free space channels [1].

Also the PIFA antennas have many advantages which make them suitable for WBAN, their radiation patterns do not have significant dips in directions normal to the body surface and are thus sensitive to both E_θ and E_ϕ polarizations. As a consequence, they will be particularly suitable to receive fields scattered by the walls, ground, and pieces of furniture in an indoor environment [2].

In this chapter we will define and analyze the monopole and PIFA antennas as well as their properties, types and applications.

3.1 Monopole Antenna

Monopole antennas have found extensive applications in many wireless communication systems, such as airborne and ground-based communication systems, over a wide range of frequencies. This is because of their desirable features; pure vertical polarization and an omnidirectional radiation pattern in the horizontal plane.

Monopole antenna is theoretically half a dipole, when the ground plane is infinite, planar and perfectly conducting (i.e. perfect ground). However, it is impossible to have an infinite plane, even a large ground plane results in a different radiation pattern from that of an infinite plane. In addition, the capacitance between the base of the monopole and the ground plane differs from that between two halves of a dipole [3].

Monopole antenna is well known for its compact size, great bandwidth, vertical polarization, desired impedance level, or particular physical characteristics. When a monopole is a quarter wavelength long a resonant action occurs and the resonant resistance is compatible with conventional transmission line feeders. When its electrical size is less than the quarter of the wavelength then matching and efficiency problems occur and the feed radiation can ruin the total pattern characteristic [4].

3.1.1 Fundamentals of Monopole Antenna

The linear monopole antenna is half the length of the dipole antenna. However, when this monopole is mounted on a “perfect” ground plane (i.e. planar, infinite in extent, and perfectly conducting) the characteristics of the antenna can be derived from dipole antennas. W. L. Stutzman and G. A. Thiele worked on the perfect ground characteristics and the image of the antenna’s fields due to the reflection from perfect ground, which were based on the Snell’s law of reflection. This work is called “Image Theory” [5].

The following analysis of the monopole characteristics, on a perfect ground, is also based upon “Image Theory” as shown in Figure 3.1.

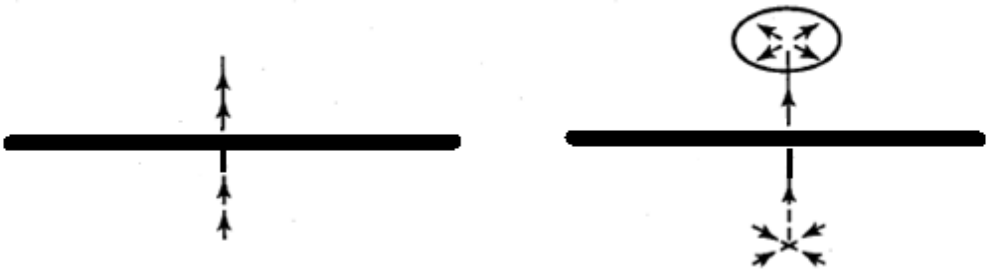

(a) Monopole antenna (b) Capacitor plate monopole

Figure 3.1 Monopole antennas over perfect ground planes with their images "dashed" [5].

The current (I_m) and the charges on a monopole antenna are the same as on the upper half of a dipole (I_{dip}). The voltage of the monopole (V_m) is half the voltage of the dipole (V_{dip}), because the electric field is the same but the length of the antenna is half, hence the same electric field over the half distance gives half the voltage. Therefore, the impedance of the monopole (Z_m) antenna is half that of the dipole (Z_{dip}):

$$Z_m = \frac{1/2 V_{dip}}{I_{dip}}$$

$$Z_m = \frac{1}{2} Z_{dip} \tag{3.1}$$

The radiation resistance ($R_{r,m}$) of the monopole is half that of the dipole ($R_{r,dip}$), due to the monopole radiation power ($P_{r,m}$), which emits only over the upper hemisphere. Hence, it is half of the radiation power of the dipole ($P_{r,dip}$) that radiates over a full sphere.

$$R_{r,m} = \frac{1}{2} R_{r,dip} \tag{3.2}$$

The directivity (D_m) of the monopole antenna is double the directivity of the dipole (D_{dip}). The reason for this is that the radiated power of the monopole is half that of the dipole for the same current levels. The radiation intensity in the free space for the monopole (ϕ_m) is the same with the dipole one (ϕ_{dip}), due to the unchanged current. Since there are 4π steradians in the total solid angle the monopole directivity is [6]:

$$D_m = \frac{\phi_m}{p_m / 4\pi} = \frac{\phi_{dip}}{\frac{1}{2} p_{dip} / 4\pi} = 2 D_{dip} \tag{3.3}$$

Accordingly from the above equations, the impedance of a quarter-wavelength ($\lambda/4$) monopole antenna ($Z_{m,\lambda/4}$) is half the impedance of the half-wavelength ($\lambda/2$) dipole antenna ($Z_{dip,\lambda/2}$). Thus

$$Z_{m,\lambda/4} = \frac{1}{2} Z_{dip,\lambda/2}$$

$$Z_{m,\lambda/4} = \frac{1}{2}(72 + j42.5)$$

$$Z_{m,\lambda/4} = (36 + j21.3)\Omega \tag{3.4}$$

Similarly the directivity of a quarter-wavelength ($\lambda/4$) monopole antenna ($D_{m,\lambda/4}$) is double the directivity of the half-wavelength ($\lambda/2$) dipole antenna ($D_{dip,\lambda/2}$) [5].

$$D_{m,\lambda/4} = 2D_{dip,\lambda/2}$$
$$D_{m,\lambda/4} = 2 \times 1 \cdot 64$$
$$D_{m,\lambda/4} = 3 \cdot 28 = 5 \cdot 16 dB \quad (3.5)$$

3.1.2 Types of Monopole Antenna

There are different types of monopole antennas. However, monopole antennas are classified in five groups which are described and analyzed below.

1. **Linear Monopole**

The simplest (structurally) and most widely used antenna is the linear monopole as shown in Figure 3.2. This type of monopole has radiation resistance ($R_r=40\lambda^2(h/\lambda)^2$), where h is the height of the antenna from the ground plane and λ is the wavelength. The linear monopole is highly capacitive and it has low efficiency when it is matched due to power losses in the matching network (typically 30-70%) [7].

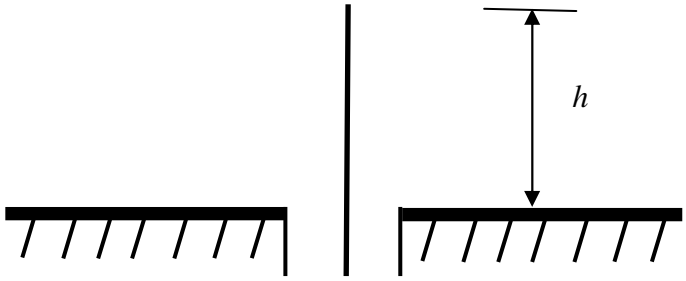

Figure 3.2 Linear monopole.

2. **Folded Monopole**

This monopole is used as a director and reflector in directional antennas. The radiation resistance of this monopole is around 10–15 Ω . The most common structure of this antenna is the "Open Folded" monopole as shown in Figure 3.3. The radiation resistance of this antenna is around 10 Ω . The advantages of using this type of monopole are the protection of radio equipment from lightning strikes and the ability to carry shielded cables to a warning light on the top of the antenna without any important effect on the antenna characteristics [3].

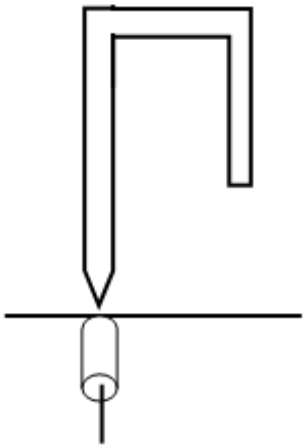

Figure 3.3 Open folded monopole [3].

3. Active/Passive Loaded Monopole

These monopoles are loaded with active (transistor, tunnel diode, varactor, etc.) and passive (inductor, capacitor, resistance or combinations) elements. The load is used to increase the radiation resistance, the effective bandwidth and to modify the radiation pattern of the linear monopole. The performance of the monopole changes according to the position of the load on the antenna's conductor [8].

Some examples of this group of monopole antennas are the "Diode Loaded", "Transistor Loaded", "Inductively Loaded" and the "Capacitively Loaded". "Diode Loaded" monopole as shown in Figure 3.4 uses the properties of the varactor diode. Varying the D.C. biasing of the diode can control the effective height of the antenna. The structure of the monopole can be reciprocal, when the diode operates linearly [8].

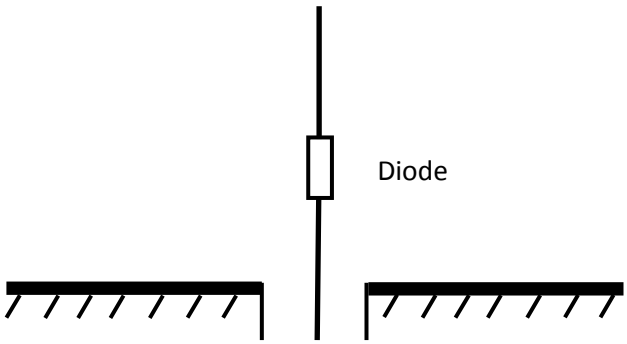

Figure 3.4 Diode loaded monopole [8].

A "Transistor Loaded" antenna as shown in Figure 3.5 is used to reduce the resonance frequency. Consequently it reduces the effective height of the antenna.

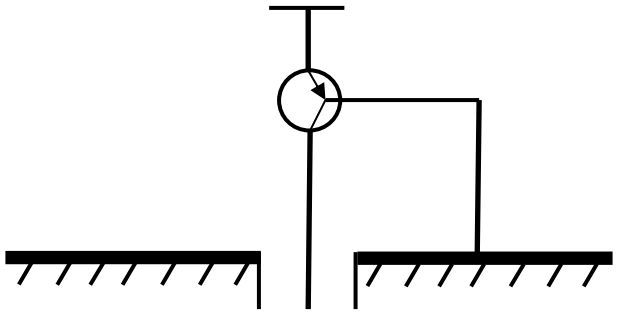

Figure 3.5 Transistor loaded monopole [8].

The "Inductively Loaded" version as shown in Figure 3.6 increases the efficiency of the antenna from 50 to 70%. The bandwidth of the same antenna can be increased nearly 2%, by choosing an appropriate value for the Quality factor of the coil. The radiation resistance of inductively loaded antennas starts from 4 to 23 Ω [7].

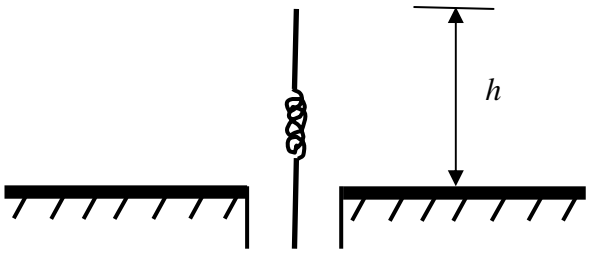

Figure 3.6 Inductively loaded monopole [7].

4. Sleeve Monopoles

"Sleeve" monopole as shown in Figure 3.7 is used to increase the radiation resistance of the antenna and to reduce the height of the antenna. R. A. Burberry has calculated the input resistance of the sleeve monopole of height $l = \lambda/4$ compared to a linear one [3]:

$$R_s = \frac{R_m}{\cos^2 \beta h} \tag{3.6}$$

where R_S is the resistance of the sleeve monopole, R_m is the resistance of the linear monopole, h is the height of the feed-point of the monopole from the ground and β is the phase constant ($\beta = 2\pi / \lambda$ rad/m).

Other monopole structures, which belong into this group, are "Bent Sleeve", "Broadband Sleeve" and "Double-band Sleeve". These monopoles are used at VHF and UHF bands [3].

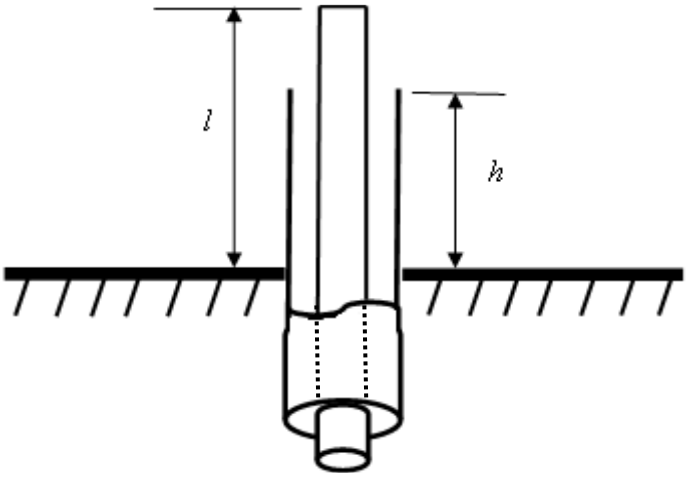

Figure 3.7 Sleeve monopole [3].

5. Top Loaded Monopole

In this category there are several wire loaded antennas. These antenna structures increase the current in the vertical portion of the antenna and this generates a decrement of the radiation resistance (R_r) and a deduction of the input impedance (Z_{in}). The radiation resistance (R_r) becomes very small and the efficiency of the antennas becomes an important factor. The radiation resistance (R_r) was computed by Laport, who defined that the R_r is related to the area 'A' (Ampere-Degree) of the plot of current distribution on the radiating surface. For example when the current at the base of the monopole is 1 A then the $R_r = 0.01215\ A^2$ [3].

"Inverted-L" as shown in Figure 3.8 is considered as a top loaded monopole antenna. The characteristic of this design is the uniform current distribution along the antenna's conductor. A consequence of this uniform distribution is to increase the radiation resistance (R_r). This type of antenna is used at high frequency (HF) and its input impedance is about 5 Ω [7].

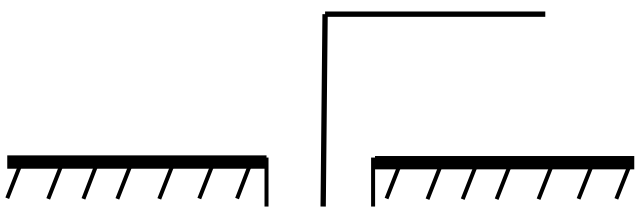

Figure 3.8 Inverted-L monopole [8].

Another type of top loaded monopole is the "Two or Four Element" top loaded monopole as shown in Figure 3.9. The radiation resistance of these structures is almost the same as the radiation resistance of the inverted-L monopole. However, these antennas need tuning and matching networks because they are frequently operated below self-resonance [7].

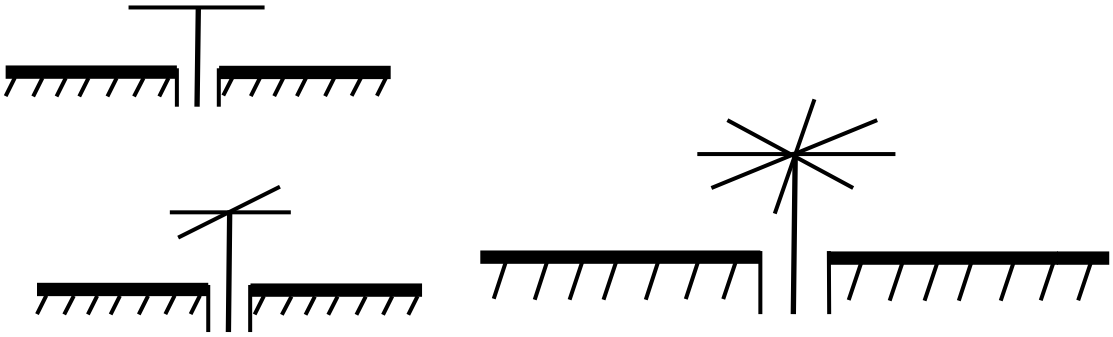

Figure 3.9 (a) Two/Four-element top loaded monopole [7], (b) N-element top loaded monopole [3].

"Spiral" top loaded monopole as shown in Figure 3.10 belongs, also, to this group of monopoles. It is also self resonant as most top loaded monopoles are. Therefore, it does not need a matching network for tuning. The efficiency of the "spiral" loaded monopole is low, about 10%, when it is placed over lossy ground and its height is around 0.02λ . The input impedance of this structure is nearly $6\ \Omega$. It is used at HF and VLF [7].

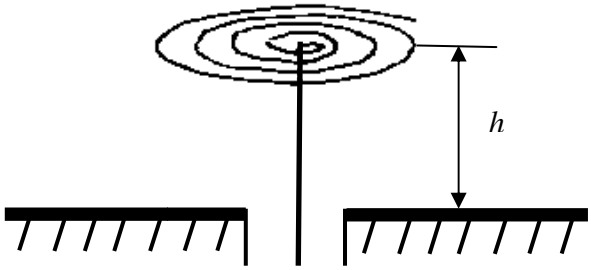

Figure 3.10 Spiral top loaded monopole [7].

Another top loaded monopole is the "Disk loaded" or "Capacitor Plate" monopole as shown in Figure 3.11. It is well known for its great radiation resistance. This antenna has a radiation resistance four times more than that of the linear monopole ($R_r = 160\,\lambda^2\,(h/\lambda)^2$), where h is the height of the antenna from the ground plane and λ is the wavelength [7].

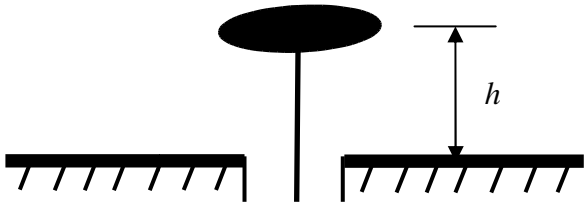

Figure 3.11 Capacitor plate loaded monopole [7].

3.1.3 Disk Loaded Monopole Antenna

End Loaded antennas have a long history. Heinrich Hertz used a dipole antenna with large conducting spheres attached to each end as the transmitter/oscillator source in the first successful demonstration of electromagnetic waves in 1886 [9]. The transmission of very low frequency (VLF) signals in the earliest applications of radio was accomplished with top loaded antennas, and the U.S. Navy continues to employ large top loaded antennas today for VLF communications [10].

In 1947, Wheeler clearly defined the relation between size and performance of electrically small antennas which he defined it as one with a maximum geometrical dimension much less than the radian length. The radian length is a distance measurement equal to $\lambda/2\pi$. This is a convenient definition because a sphere with diameter equal to the radian length contains most of the stored near-field energy of the electrically small antenna [11]. Drawing on experience and insight, he expressed the limitations related to small size with a few simple formulas for the two types: the electric type, a parallel-disk capacitor, and the magnetic type, a helical-coil inductor, each occupying the same cylindrical volume. Although the design process has changed dramatically since 1947, with high-speed computer programs virtually replacing trial and error empiricism, the physical basis of electromagnetic radiation remains unaltered; the significance of Wheeler's concepts remain valid. Much effort has been expended in the intervening years in the continuing search for improved performance under the constraint of reduced size. The method of moments (MoM) was used in [12] to analyze the disk loaded monopole to show the usefulness of Wheeler's design criteria applied to the design of electrically small antennas [12].

3.2 PIFA Antenna

The PIFA has become one of the most popular antennas in recent years, bringing much attention to the research in this area, Applications where the PIFA have been used are: satellite/terrestrial communications, various cellular communications equipment such as handset terminals/base stations, GPS devices, biomedical transceivers and implantable applications, WLAN transceivers and Bluetooth devices, and MIMO systems, The number of applications of the PIFA and PIFA-derived antennas continues to grow rapidly [13].

3.2.1 PIFA Evolution

PIFA referred to as a hybrid microstrip antenna [14] (rectangular PIFA as shown in Figure 3.12, or a half-disk antenna semicircular PIFA as shown in Figure 3.13) is one of the most compact microstrip patch antennas. It can provide the same resonant frequency at less than half size of conventional patch antenna. It is in its essence a half of the usual patch antenna with one of its radiating edges shorted to ground-plane along zero potential line.

Therefore, the PIFA has the advantage of being more compact than the conventional patch , while providing very good bandwidth capabilities with comparable antenna gain and efficiency. It is also capable of multi-band frequency operation, which makes it an ideal candidate for wireless communications devices and systems.

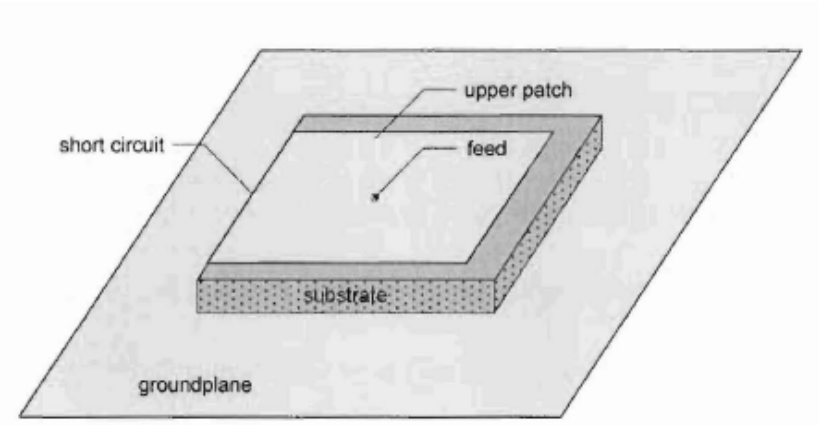

Figure 3.12 the rectangular PIFA on finite ground plane [13].

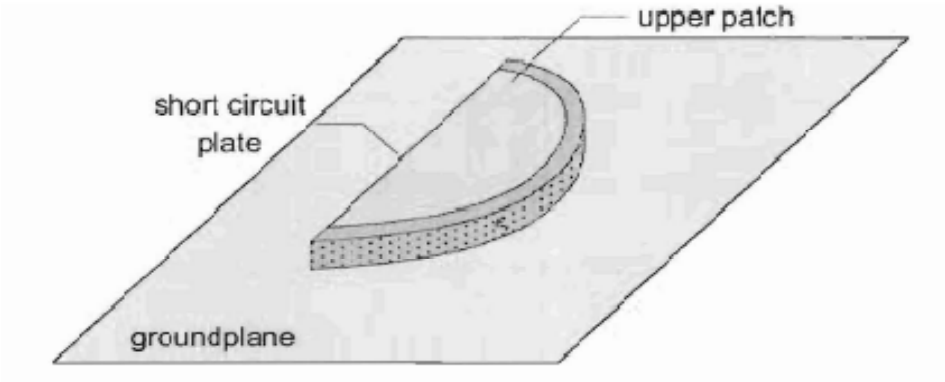

Figure 3.13 semicircular PIFA on finite ground plane [13].

PIFA Antenna Evolved Gradually from ILA and IFA antennas in order to overcome certain limitations in its preceding structure, as shown in figure 3.14 [15].

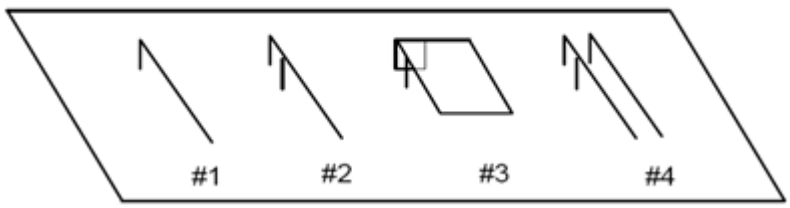

Inverted-L Antenna	**Inverted-F Antenna**	**Planar Inverted-F Antenna**	**Dual Inverted-F Antenna**

Figure 3.14 The various geometries of inverted antennas [15].

The Inverted-L Antenna (ILA) in Figure 3.14 #1 consists of a short vertical monopole with the addition of a long horizontal arm at the top. Its input impedance is nearly equivalent to that of the short monopole with the addition of the reactance caused by the horizontal wire above the ground plane [16].

The ILA is generally difficult to impedance match to a feed line since its input impedance consists of a low resistance and high reactance. Since loss due to mismatch decreases radiation efficiency, it is desirable to modify the structure of the ILA to achieve a nearly resistive input impedance that is easily matched to a standard coaxial line.

The ILA structure is commonly modified by adding another inverted-L element to the end of the vertical segment to form the Inverted-F Antenna (IFA) shown in Figure 3.14 #2.

One disadvantage of an IFA constructed using thin wires is low impedance bandwidth. Typically, a single IFA element experiences an impedance bandwidth of less than 2% of the center frequency [16]. One way to increase the bandwidth of the IFA is to replace the top horizontal arm with a plate oriented parallel to the ground plane to form the Planar Inverted-F Antenna (PIFA) as in Figure 3.14 #3 which will be analyzed in section 3.2.3.

The Dual Inverted-F Antenna (DIFA) in Figure 3.14 #4 is formed by adding a second inverted-L element to the Inverted-F Antenna (IFA). The second element is parasitic and is not directly fed so impedance bandwidth is increased if the resonant frequencies of the two elements are closely spaced [17].

3.2.2 Parameter Effects on PIFA Performance

The performance of PIFA shown in Figure 3.15 can be expressed in terms of the following parameters [18]:

- the geometric shape of the radiating plate: L,W
- the height of the radiating plate: H
- the size and shape of the ground plane: L_g,W_g
- the location and structure of the feeding stem
- the location and size of the shorting strip: H,*w*
- the material used to support or load the radiating plate, if any
- lump loading (such as an LCR) or a distributed loading (such as a slot or a notch at the radiating plate, if any).

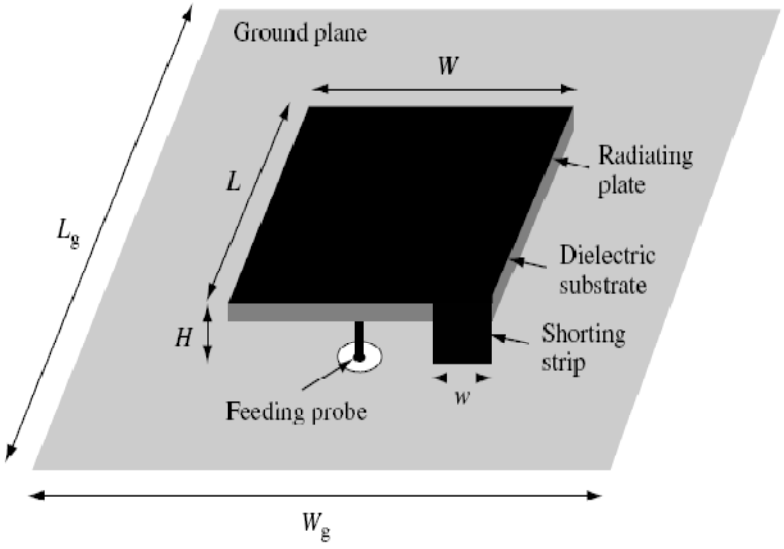

Figure 3.15 Geometry of a planar inverted-F antenna [18].

Design considerations for a PIFA include the resonant frequency, the impedance bandwidth, radiation patterns, gain and size [19]. Important observations include:

- The greater the height H, the broader is the bandwidth, and the lower is the resonant frequency.
- The greater the ratio, *w*/W is (≤1), the higher is the resonant frequency, and the broader is the bandwidth.
- The greater the ratio of W/L, the lower is the resonant frequency, and the broader is the bandwidth.

• The locations of feed point and shorting strip, as well as the width *w* of the shorting strip, control the radiation polarization characteristics.

3.2.3 PIFA Analysis

Most recent treatments of the PIFA and PIFA-derived antennas include numerical solutions using expensive electromagnetic software packages and conventional experimental iterations design techniques, Both these methods are time consuming and expensive.

Tools are needed to estimate accurately the basic characteristics of the antenna performance, in particular, the behavior of the pattern, impedance, bandwidth and polarization.

The most popular approaches in microstrip antennas analysis are proved to be the cavity model (CM), transmission line model (TLM) and the full wave analysis (integral equations and/or Method of Moments (MoM), Finite Element Method (FEM), Finite Difference Time Domain (FDTD) methods and Spatial Network Method (SNM)) [13].

The transmission line model is the easiest of all of the above mentioned approaches, and it gives fair physical insight into microstrip radiation mechanisms, it lacks accuracy and flexibility in dealing with coupling effects of patches. The classic two-slot transmission line model, which was initially proposed for a rectangular patch antenna [20], is not accurate when applied to the PIFA. It was later improved by [21] for the rectangular PIFA by replacing the classic two-slot arrangement with the variable uniformly radiating slot and short circuit arrangement, paired with the two fixed radiating side slots of the PIFA, which helped to provide accurate information about the PIFA impedance only across its center.

The cavity model is more accurate, yet at the same time, more computationally complex. Calculations based on the cavity method are the most useful for analysis of microstrip antennas. The cavity model offers both the simplicity of computations and a great physical insight in radiation mechanisms of microstrip structures. Again, the classic two-slot cavity model was initially proposed for a rectangular [22] and circular [23] patch antennas, however, later it was successfully applied to various patches with different geometries. An attempt has been made in [21] to describe electric vector potentials for the PIFA three equivalent magnetic currents.

In general, the full wave models are accurate and flexible, if properly applied. They can provide adequate results for variety of different microstrip radiators, arrays of elements of different shape, and coupling effects. However, they give less physical insight if compared to the cavity model as well as they are the most analytically and numerically complex of all described models [24-26].

As our antenna design include rectangular PIFA and the cavity model cover the physical mechanisms of microstrip, we are going to analyze the rectangular PIFA by cavity model from [13] in the next section.

3.2.3.1 Cavity Model for Rectangular PIFA

To simplify the analysis of electromagnetic field distribution inside PIFA radiator, the configuration of the feeding structure is neglected. The feed electromagnetic discontinuity will have a minor effect on the field configuration inside PIFA resonator, so the boundary conditions at the edges of the cavity should remain fit.

The cavity model for the PIFA consists of a description of the region between the microstrip and the ground plane, bounded by perfect electric and magnetic walls along the edges and by perfect electric walls from above and below, loaded with a

dielectric material of permittivity ε_r as shown in Figure 3.16, the upper and the lower (the ground plane) plates of the cavity as well as the vertical shorting plate are assumed to be *perfect electric conductors* (PEC). All other vertical perimeter walls are treated as *perfect magnetic conductors* (PMC).

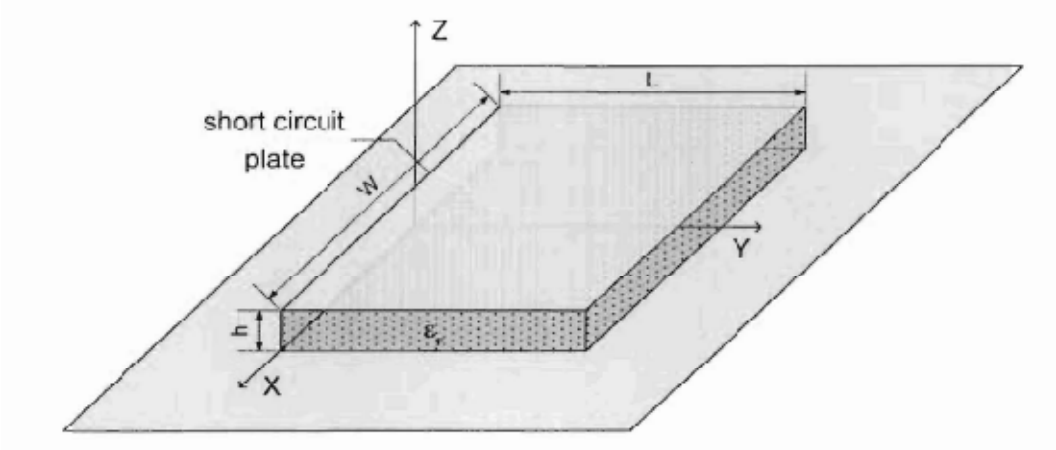

Figure 3.16 Cavity model for PIFA element shown with a finite ground plane [13].

The ground plane surface is assumed to be infinite but in reality, the ground plane is always finite, when the electric and magnetic fields inside the cavity get calculated, the radiated fields of the PIFA are found readily by replacing magnetic walls with equivalent radiating sources, using the vector potential theory and Maxwell equations [27].

When the far fields of the PIFA get found, many important characteristics of the antenna can be easily determined such as radiated power, directivity, Quality factor, frequency bandwidth, input impedance etc .

- **PIFA Field Distribution (TM-modes)**

As the height of the microstrip is usually very small ($h << \lambda$, where λ is the wavelength inside the dielectric) , the fields along the height of the PIFA are considered constant. Also, the fringing fields around the edges of the PIFA are small because of the thin substrate. Therefore, the electric fields are considered to be normal to the surface of the PIFA patch. Consequently, only TM_{mn} *(transverse magnetic modes)* field configurations should be considered in the model.

The cavity is treated as a lossless, source-free, linear, isotropic homogeneous media in which the electric field satisfies the following condition :

$$\nabla^2 \mathbf{E} + k^2 \mathbf{E} = 0 \tag{3.7}$$

where $\mathbf{E}$ is the vector electric field , $k = 2\pi/\lambda$ is the wave number. Equation (3.7) is known as the *homogeneous Helmholtz equation* [28].

Resonance length of the cavity resonator is in $\mathbf{a}_y$ direction, so cavity wave propagation is mostly $\mathbf{a}_y$ directed. The boundary conditions for the electric walls produce the electric field in the $\mathbf{a}_z$ direction, so the dominant modes excited in the PIFA cavity are TM_{mn} modes, also with the fringing fields effect neglected, and the electric field depending only on $\mathbf{a}_y$, the equation (3.7) become :

$$\frac{\partial^2 \mathbf{E}_z}{\partial y^2} + k^2 \mathbf{E}_z = 0 \tag{3.8}$$

And its general solution:

$$\mathbf{E}_z = E_1 e^{-jk_y y'} + E_2 e^{jk_y y'} \tag{3.9}$$

here the primed coordinate denotes a source point.
The electric currents should be zero on the open end of the cavity *(y′ = L).* From the electric current and magnetic field relation [28]:

$$\int_{\mathbf{c}} \mathbf{H}.\mathbf{dl} = \int_{\mathbf{s}} \mathbf{J} \cdot \mathbf{da} \tag{3.10}$$

the magnetic fields at y' = *L* should also be zero :

$$\mathbf{H}_{y'=L} = 0 \tag{3.11}$$

From the Maxwell equations we have:

$$\nabla \times \mathbf{E} = -jw\mu\mathbf{H} \tag{3.12}$$

The curl in (3.12) can be evaluated yielding:

$$\nabla \times \mathbf{E} = \nabla \times \mathbf{E}_z = -\frac{\partial E_z}{\partial y}\mathbf{a_x} \tag{3.13}$$

By substituting the boundary condition (3.11) into (3.13) we obtain :

$$\left(\frac{\partial E_z}{\partial y}\right)_{y'=L} = 0 \tag{3.14}$$

and the electric field is indeed finite at y' = *L*.
According to the electric wall boundary condition, the tangential electric field must disappear at the short circuit, thus, the boundary condition at *y′* = 0 :

$$\left(E_z\right)_{y'=0} = 0 \tag{3.15}$$

substituting the boundary condition (3.15) into (3.9) we obtain :

$$\mathbf{E}(y'=0) = E_1\mathbf{a_z} + E_2\mathbf{a_z} = 0 \Rightarrow E_1 = -E_2 \tag{3.16}$$

By Euler's identity, the general solution equation can be rewritten as follows :

$$\mathbf{E} = E_1 e^{-jk_y y'}\mathbf{a_z} - E_1 e^{jk_y y'}\mathbf{a_z} = -2jE_0 \sin k_y y'\mathbf{a_z} \tag{3.17}$$

Taking the differential of (3.17) with respect to *y* and inserting the boundary condition from (3.14) yields:

$$\frac{\partial E_x}{\partial y} = \left(-j2kE_o \cos k_y y'\right)_{y'=L} = -j2kE_o \cos k_y L = 0 \tag{3.18}$$

The general solution of this equation is an infinite number of resonant modes:

$$k_y L = \pm\frac{\pi}{2}(2l+1) \tag{3.19}$$

where k_y is the wave number along *y* direction corresponding to each mode.

the lowest radiating dominant mode is TM_{01} mode. Furthermore, solving for resonance length of the antenna and choosing *l* = 0 for the smallest radiator size, we obtain:

$$L = \frac{\pi}{2k_y} = \frac{\lambda}{4} \tag{3.20}$$

Equation (3.17) can be used now as an approximation of the electric fields inside the cavity.

Different modes of rectangular PIFA are depicted in Figure 3.17.

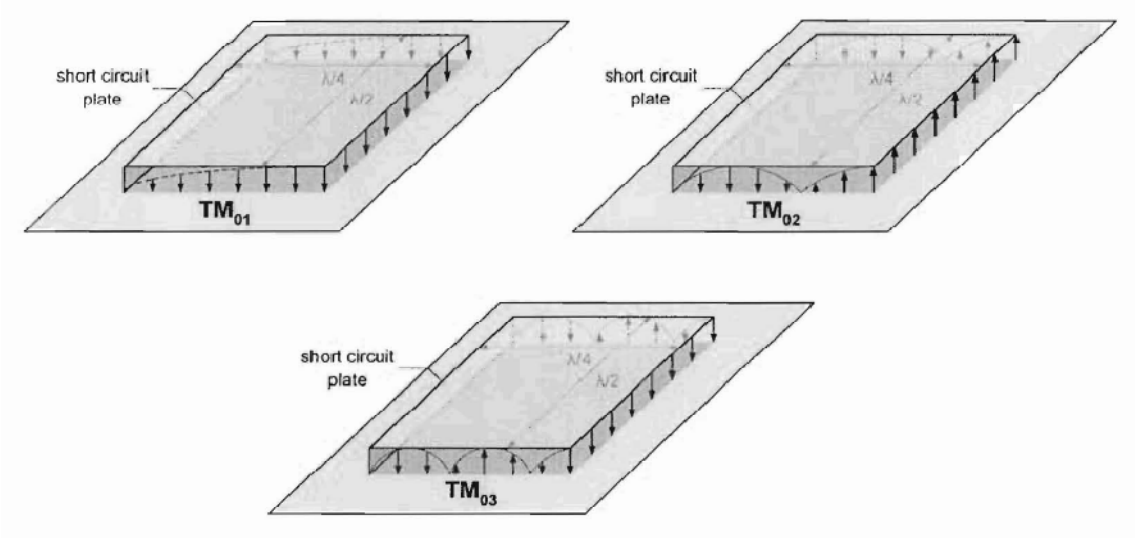

Figure 3.17 Electric field configurations (modes) for the rectangular PIFA [13].

Similarly, the magnetic field inside the cavity can be found from the following Maxwell equation :

$$\nabla \times \mathbf{E} = -jw\mu\mathbf{H}$$

$$\Rightarrow \mathbf{H} = -\frac{1}{jw\mu}\nabla \times \mathbf{E} \tag{3.21}$$

Performing the curl operator of $\mathbf{E}$ in (3.17):

$$\nabla \times \mathbf{E} = -\mathbf{a}_x\left(\frac{\partial E_z}{\partial y}\right) = j2E_0 k\cos ky'\mathbf{a}_x \tag{3.22}$$

By substituting (3.22) into (3.21) we get the magnetic field :

$$\mathbf{H} = -\frac{k}{\omega\mu}2E_0\cos ky'\mathbf{a}_x = -\frac{1}{Z_o}2E_0\cos ky'\mathbf{a}_x \tag{3.23}$$

Where $Z_o = \sqrt{\mu/\varepsilon}$ intrinsic impedance, and $k = \omega\sqrt{\mu\varepsilon}$.

It is clear from the equation (3.23) that the tangential magnetic field equals to zero at the open ends of the cavity. However, in order to radiate electromagnetic energy, the power flux of the electromagnetic wave excited in the radiator $\mathbf{P} = \mathbf{E} \times \mathbf{H}^*$ Have to be a nonzero value. The model has to be refined to account for this.

- **PIFA Bandwidth**

The PIFA as a member of microstrip antenna class is a strongly resonant device. Conventionally, it is the PIFA impedance, not the far filed pattern, serves as a limit on its bandwidth. When the microstrip antenna is matched to its feeding structure, the mismatch loss off the antenna's resonance is usually described by the Voltage Standing Wave Ratio (VSWR). The maximum tolerated value of the VSWR then defines the bandwidth of the antenna:

$$BW = \frac{100(VSWR-1)}{Q_T\sqrt{VSWR}}\% \tag{3.24}$$

This formula defines the usable bandwidth (in percents of the resonant frequency) as a relation to the total Quality factor of the antenna, for the *VSWR* ≥ *1,* but less than the certain value [13].

- **PIFA Input Impedance**

According to the cavity model, input impedance Z_{in} can be estimated by using both the far fields radiation pattern and resonant cavity electromagnetic fields for a rectangular patch antenna. The input impedance of a microstrip antenna can be found as follows [29]:

$$Z_{in} = \frac{0.5 v_o v_o^*}{P_T + j2\omega(W_e - W_m)} \tag{3.25}$$

Where P_T is the total power dissipated by the antenna

$$P_T = P_{rad} + P_c + P_d \tag{3.26}$$

P_{rad} - the power radiated by the antenna; P_c - ohmic (conductor) losses in the antenna; and P_d - losses in the dielectric of the cavity.

The averaged energy stored by the antenna resonating structure may be both electric energy and magnetic energy. These can be expressed as integrals over the antenna volume e.g. [21]:

$$W_e = \frac{1}{4}\int_v \varepsilon |E|^2 dv \tag{3.27}$$

$$W_m = \frac{1}{4}\int_v \mu |H|^2 dv \tag{3.28}$$

Also the patch edge voltage is [19]:

$$v_o = hE_z \tag{3.29}$$

- **PIFA Polarization**

The polarization of an arbitrary antenna is sensed from the plane wave transmitted by that antenna. The PIFA is inheritably a linearly polarized antenna. However, it is possible to find certain angular directions for which, the so called cross-polar and co-polar components of an electromagnetic wave, radiated by the PIFA have almost identical amplitudes, meaning that for these directions the circularly polarized (CP) radiation from the PIFA is achievable [13].

References

[1] M. R. Kamarudin, O. Abdul Aziz "Antenna Measurements In The On-Body Environment" in *Recent developments in small size antenna*, pp. 125-128, 1st edition, 2008.

[2] T. Alves, B. Poussot, and Jean-Marc Laheurte "PIFA–Top-Loaded-Monopole Antenna With Diversity Features for WBAN Applications, " IEEE Antennas and Wireless Propagation Letters, Vol. 10, No. 1, pp. 693–696, July 2011.

[3] R. A. Burberry, "Monopole Antennas", in *VHF and UHF Antennas*, pp. 24—58, London, U.K: Peter Peregrinus Ltd., 1992.

[4] K. Fujimoto and J. R. James, "Dipole Derivatives", in *Mobile Antenna Systems Handbook*, pp. 548—549, USA: Artech House, Inc., 1994.

[5] W. L. Stutzman, G. A. Thiele, "Antenna above a Perfect Ground Plane", in *Antenna Theory and Design*, pp.63—68, 2nd Ed. USA: John Wiley & Sons Inc., 1998.

[6] H. J. Strangeways, "Antenna Properties", in Lecture Notes of Radio Communication Techniques, University of Leeds, 1999—2000.

[7] K. Fujimoto, al. et, "Introduction", in *Small Antennas*, pp. 1—36, England: Research Studies Press Ltd., 1987.

[8] W. A. Kimball, "Active Antennas", University of Leeds, West Yorkshire, England, PhD Thesis 080/03, June 1972.

[9] J. H. Bryant, *Heinrich Hertz, the Beginning of Microwaves*: IEEE/MTT-S Hertz Centennial Celebration, 1988.

[10] T. L. Simpson, M. Roberts, and E. Berg, "Developing a broadband circuit model for the cutler VLF antenna," in *IEEE AP-S/URSI Int. Symp.*, Boston, MA, July 15–18, 2001.

[11] H. A. Wheeler, "Fundamental limitations of electrically small antennas," *Proc. IRE*, pp. 1479–1484, Dec. 1947.

[12] T. L. Simpson "The Disk Loaded Monopole Antenna, " IEEE Transactions on Antennas and Propagation, Vol. 52, No. 2, pp. 542–550, Feb. 2004.

[13] Vadim Antonchik, "Theory and experiment of planar inverted F-antennas for wireless communications applications,", Master thesis, pp. 9–62, 2007.

[14] J. R. James and P. S. Hall, "Handbook of Microstrip Antennas," London, Eng: Peregrinus, 1989.

[15] A. T. Gobien, "Investigation of Low Profile Antenna Designs for Use in Hand-Held Radios,", Master thesis, pp. 18–22, 1997.

[16] Fujimoto, K., Henderson, A., Hirasawa, K., James, J.R. *Small Antennas*, Section 2.4.1, Research Studies Press Ltd., London and John Wiley & Sons Inc., New York, 1987.

[17] Jensen, M. A., Rahmat-Samii, Y., "FDTD Analysis of PIFA Diversity Antennas on a Hand-Held Transceiver Unit,", pp. 814-817, *IEEE Antennas and Propagation Symposium Digest*, July 1993.

[18] Z. N. Chen and M. Y. W. Chia, "*Broadband Planar Antennas: Design and Applications*,", pp. 142-143, John Wiley & Sons, Chichester, UK, 2006.

[19] K. Hirasawa and M. Haneishi, " *Analysis, Design, and Measurement of Small and Low-profile Antennas*,", Boston, MA: Artech House, 1992.

[20] H. Pues and A. van de Capelle, "Accurate transmission-line model for the rectangular microstrip antenna," *IEE Proceedings H: Microwaves Optics and Antennas,* Vol. 131, pp. 334-340, dec. 1984.

[21] R. Vaughan and J. Bach Andersen, *"Channels Propagation and Antennas for Mobile Communications"*, Vol. 50, pp.753, London: Institution of Electrical Engineers, 2003.

[22] Y. La, D. Solomon and W. Richards, "Theory and experiment on microstrip antennas," *Antennas and Propagation, IEEE Transactions on [Legacy, Pre -* 1988*]*, Vol. 27, pp. 137-145, 1979.

[23] A. Derneryd, "Analysis of the microstrip disk antenna element," *Antennas and Propagation, IEEE Transactions on [Legacy, Pre –* 1988*]*, Vol. 27, pp. 660-664, 1979.

[24] P. Pinho and J. F. Rocha Pereira, "Design of a PIFA antenna using FDTD and genetic algorithms,", pp. 700-703, Vol. A, 2001.

[25] M. N. O. Sadiku and A. F. Peterson, "A comparison of numerical methods for computing electromagnetic fields,", pp. 42-47, Vol. I, 1990.

[26] M. N. O. Sadiku and C. N. Obiozor, "A comparison of finite difference time-domain (FDTD) and transmission-line modeling (TLM) methods,", pp. 19-22, 2000.

[27] C. A. Balanis, " *Antenna Theory :Analysis and Design.*,", pp. 1117, 3rd ed., Hoboken, NJ: John Wiley, 2005.

[28] R. F. Hanington, " *Time-Harmonic Electromagnetic Fields*,", pp.480, McGraw-Hill, 1961.

[29] W. Richards, Y. Lo and D. Harrison, "An improved theory for microstrip antennas and applications," *Antennas and Propagation, IEEE Transactions on [Legacy, Pre-I988],*vol. 29, pp. 38-46, 1981.

Chapter 4

Designs and Simulations of PIFA and Top Loaded Monopole Antennas

In the previous chapters, we described the types of monopole and PIFA antennas as well as their theoretical analysis. Also we have shown various antenna types used for WBAN at 2.45 GHz with the advantages and disadvantages for each of them.

PIFA and Top Loaded Monopole Antenna with Diversity Features in [1] was designed for WBAN Applications in ISM band (2.45 GHz) using the commercial electromagnetic simulation tool, the FEM based software, HFSS by ANSOFT. Where PIFA has a ground above the substrate with length of 35 mm and width of 30 mm while Top Loaded Monopole Antenna has ground below the substrate with length of 20 mm and with of 30 mm as shown in Figure 4.1.

The feeding method for PIFA is Coplanar Waveguide (CPW) and Microstrip line for Top Loaded Monopole Antenna. The return loss of the monopole and PIFA antennas as well as the isolation between them are shown in Figure 4.2, also the total gain and radiation pattern are shown in Figure 4.3.

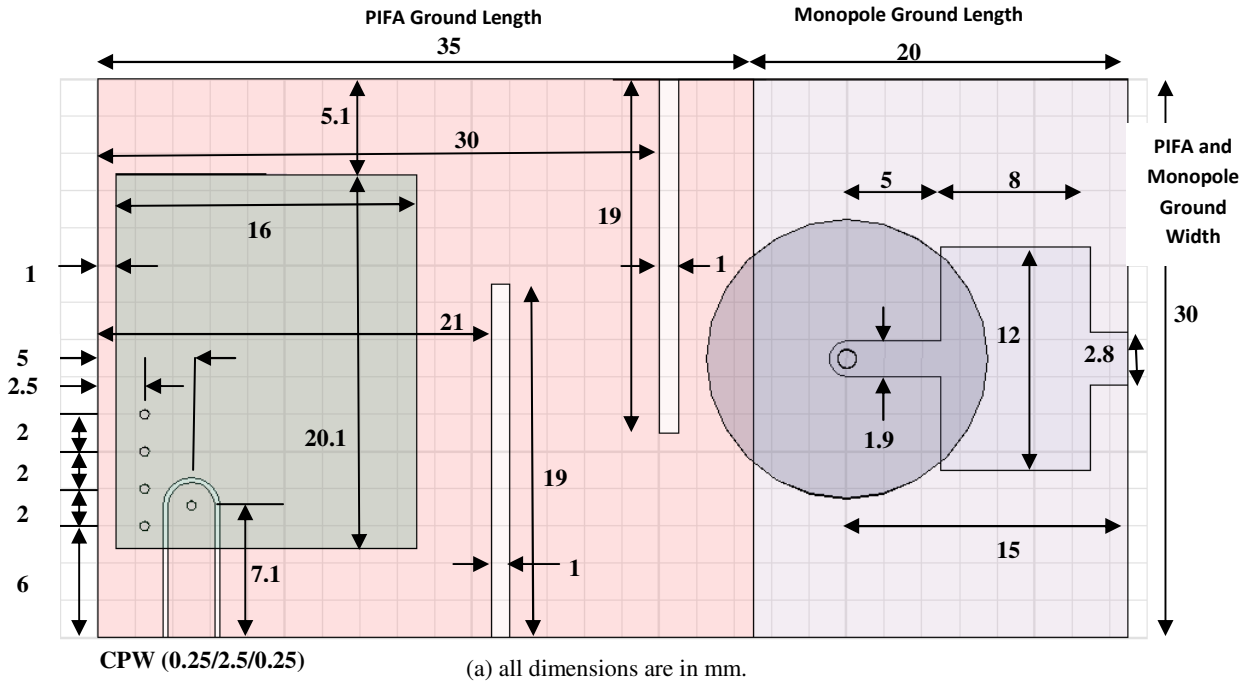

(a) all dimensions are in mm.

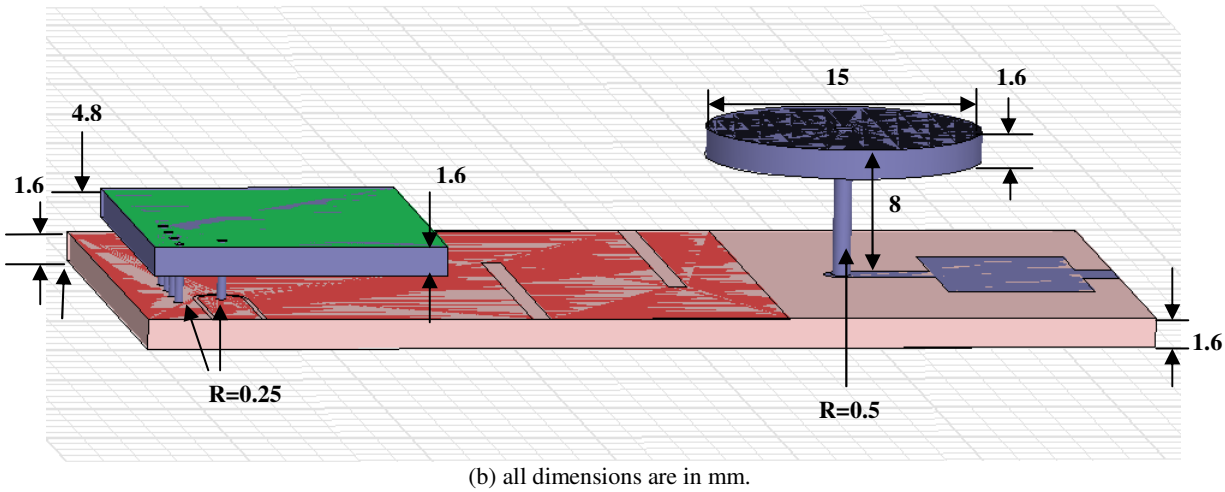

(b) all dimensions are in mm.

Figure 4.1 PIFA and Top Loaded Monopole Antenna With Diversity Features in [1] (a) Top view, (b)Side view.

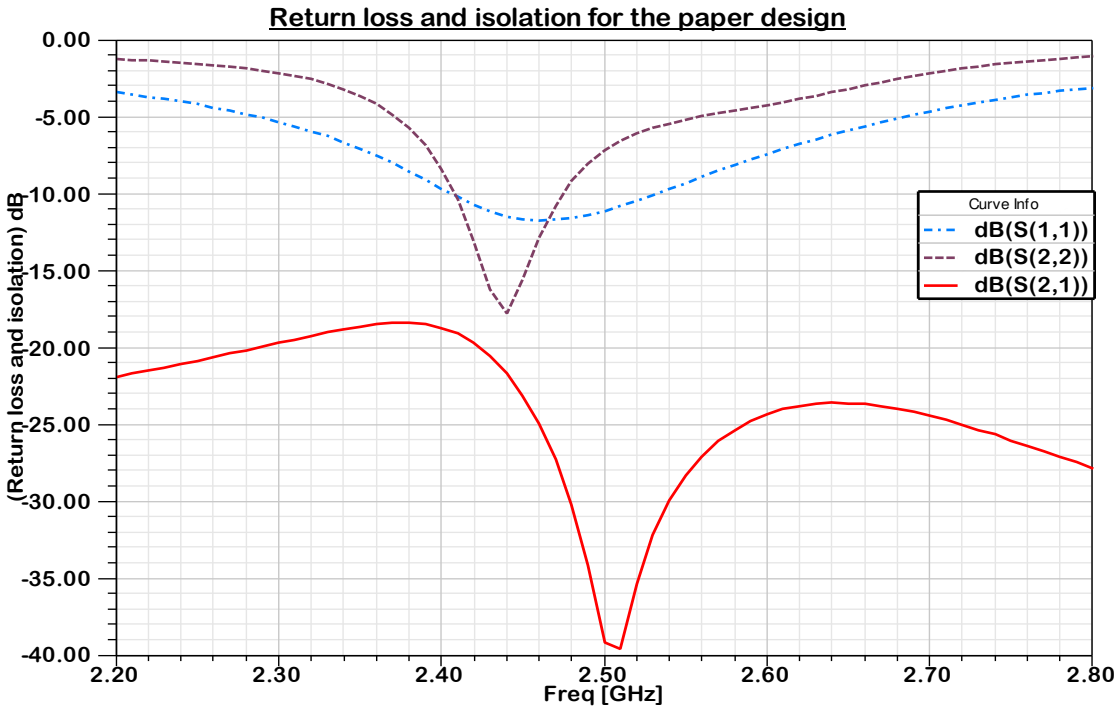

Figure 4.2 Monopole return loss S(1,1), PIFA return loss S(2,2), and isolation between them S(2,1) as in [1].

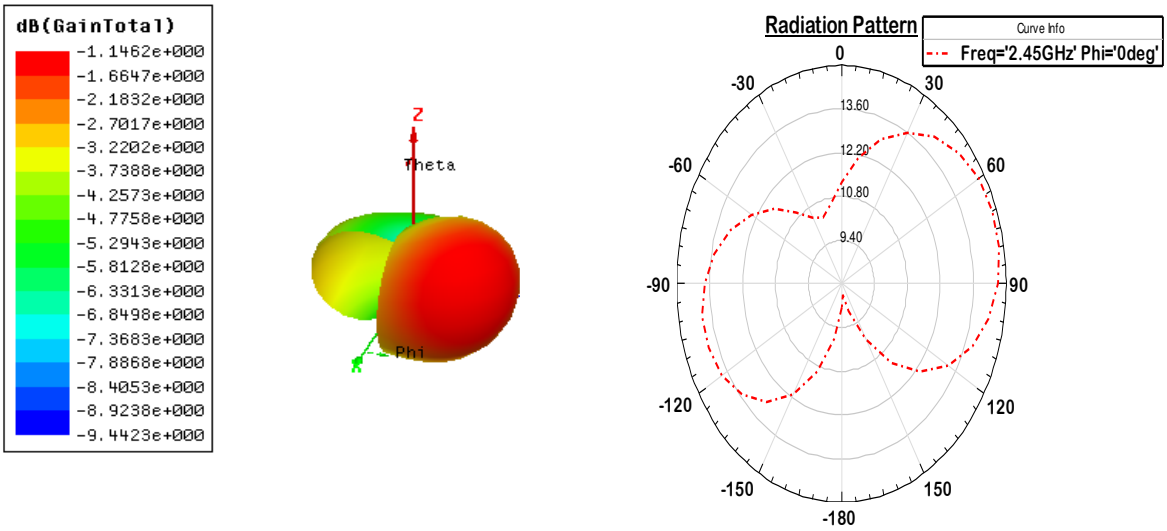

(a) (b)

4.3 (a) Total gain of the antenna design as in [1], (b) Radiation pattern for theta at phi=0.

In this chapter, we will analyze and design a structure that has better performance and size reduction for WBAN, starting from parametric study of the antenna elements to see the effect of each parameter on the antenna characteristic and also by using different techniques to achieve our goal for enhancement of the antenna performance.

4.1 Parametric Study of the Antenna

A comprehensive parametric study has been carried out to understand the effects of various dimensional parameters of the antenna.

Nine parameters have been investigated in this section, three of them are common for both monopole and PIFA (ground length, ground width, and substrate

material dielectric), another three parameters are for monopole antenna (monopole height, monopole radius, and monopole disc radius), and the last three parameters are for PIFA (PIFA height, PIFA length, and PIFA width) as shown in Figure 4.4.

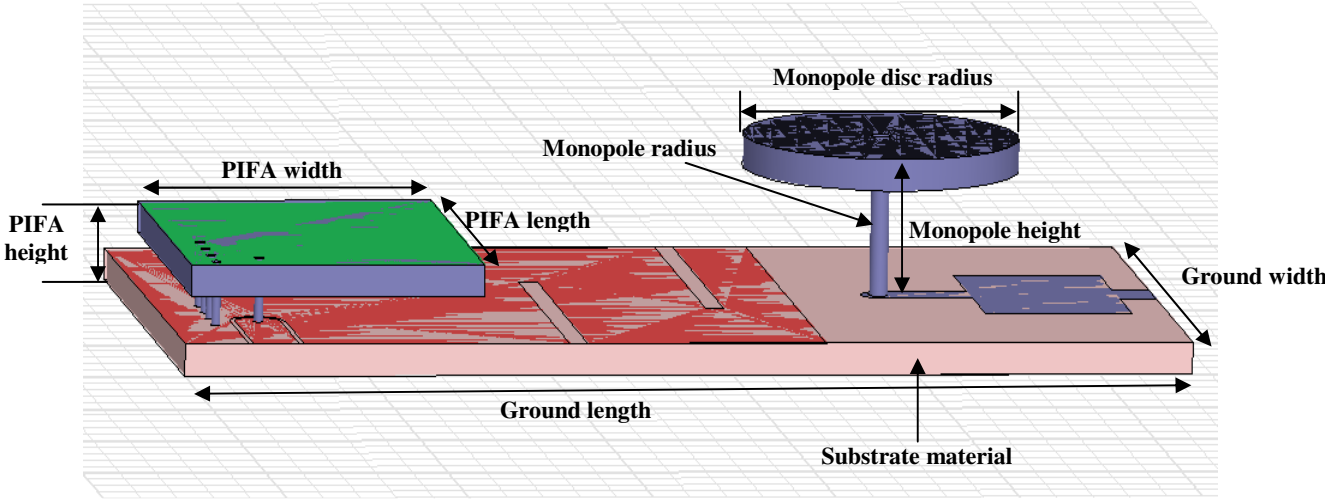

Figure 4.4 Parameters of PIFA Top Loaded Monopole Antenna.

Each of the parameters is going to be investigated thoroughly and its influence on monopole and PIFA resonant frequency, return loss, gain, and bandwidth will be studied. Also the isolation between the two antennas and how it is affected by the parameters will be considered.

4.1.1 Ground Length

Ground length variation means variation with the substrate length as well as monopole and PIFA antennas ground length for example, if we increased the ground length by 2 mm then the substrate increased 2 mm, the monopole increased 1 mm and the PIFA increased 1 mm. As it is shown in Figures 4.5 and 4.6, the PIFA is slightly affected by the ground length variation while monopole antenna is strongly affected which show that we cannot reduce the ground length because it highly degrades the return loss of the monopole antenna.

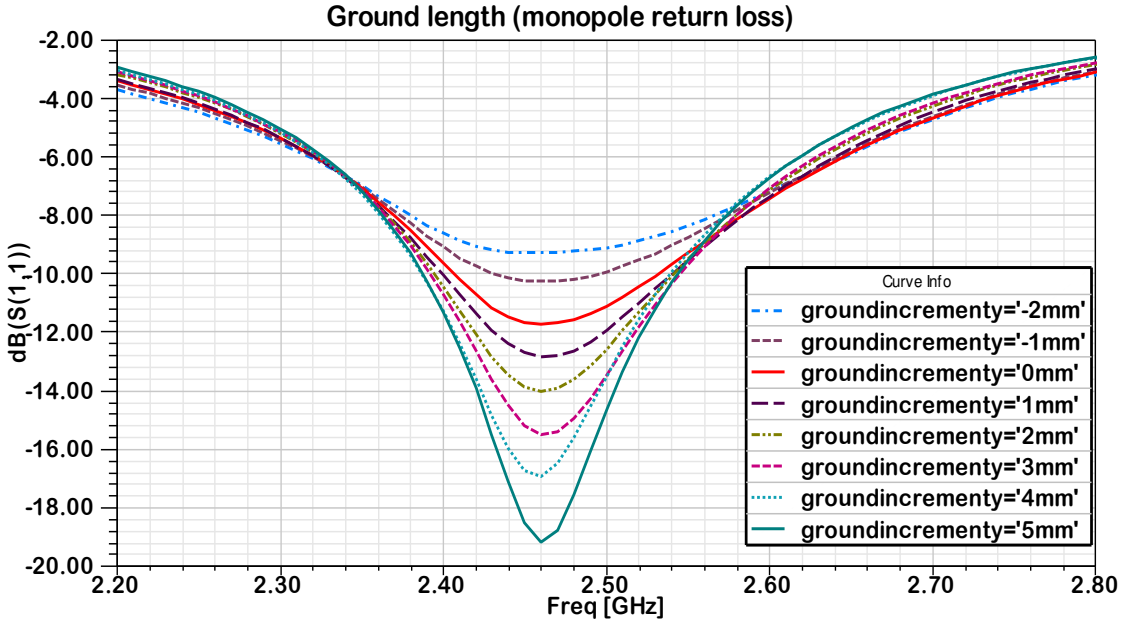

Figure 4.5 Monopole return loss with different values of the ground length.

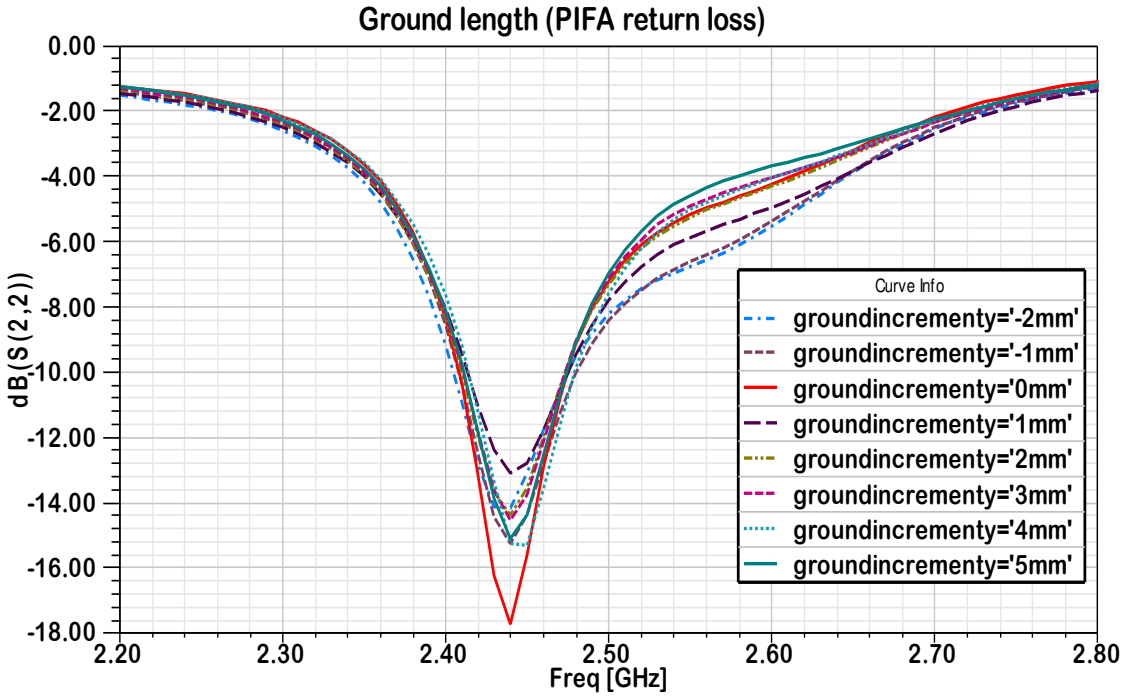

Figure 4.6 PIFA return loss with different values of the ground length.

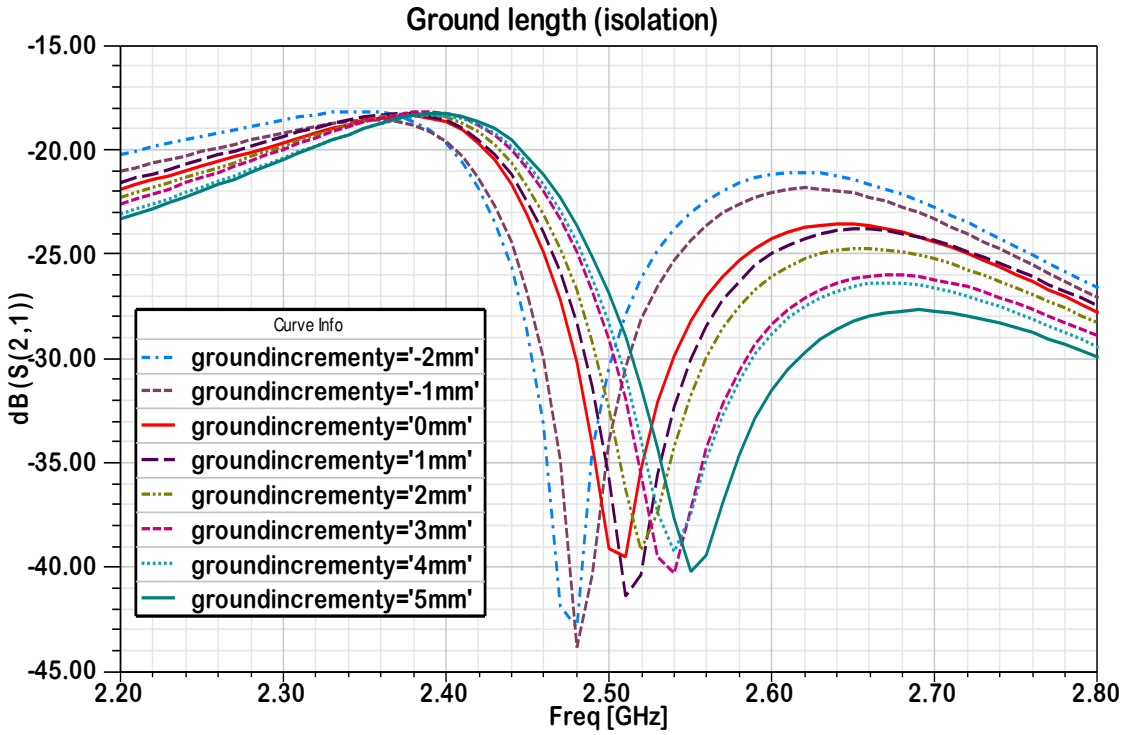

Figure 4.7 Isolation between the two antennas with different values of the ground length.

Also from Figure 4.7, the isolation was not affected by the ground length variation neither total gain at theta as shown in Figure 4.9 while total gain slightly decreased at phi with the ground length increment as shown in Figure 4.8. From the above discussion we see that we can improve the monopole return loss by increasing the ground length but it is not suitable for our design because we want the design to be compact in size.

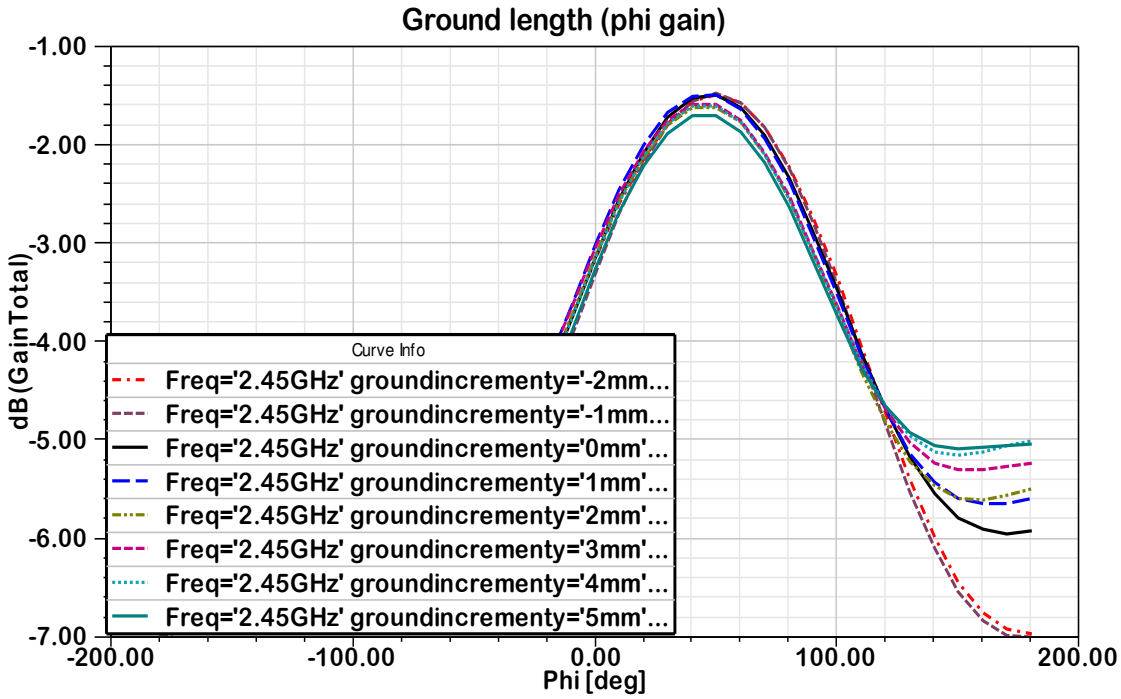

Figure 4.8 Maximum gain at phi with different values of the ground length.

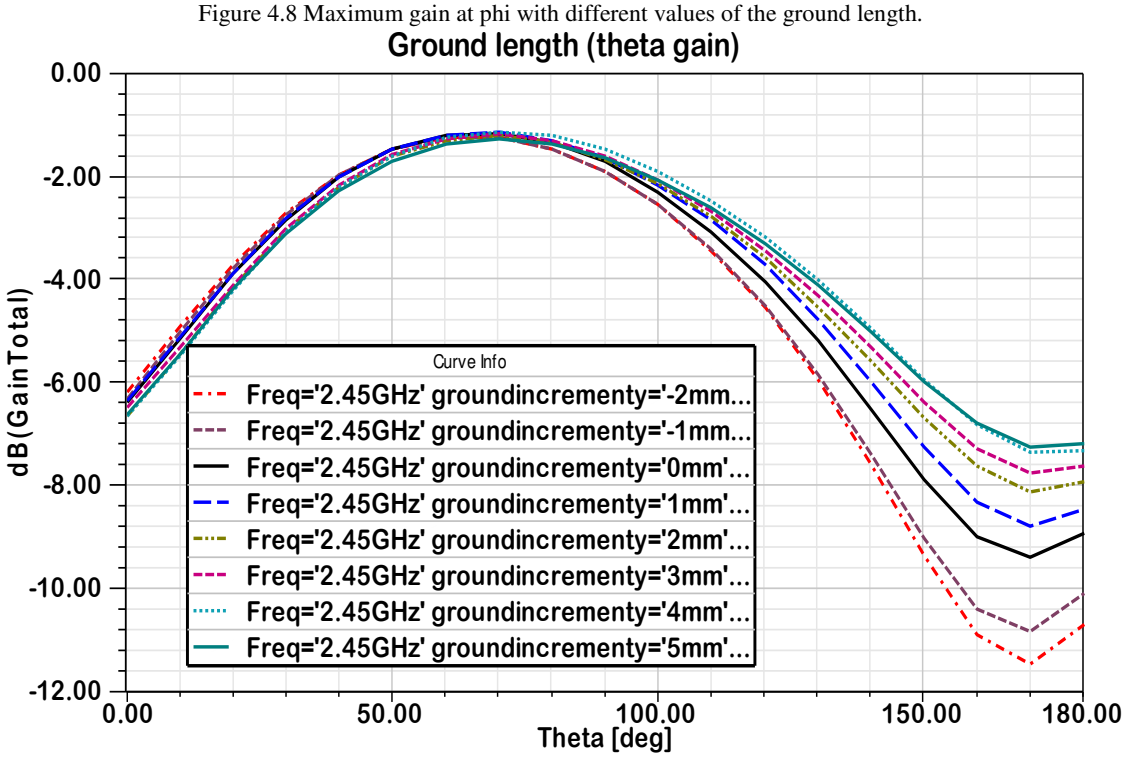

Figure 4.9 Maximum gain at theta with different values of the ground length.

4.1.2 Ground Width

Ground width variation has more influence in PIFA than in monopole antenna as shown in Figures 4.10 and 4.11. When we decrease the ground width, the resonant frequency of PIFA increases while with monopole antenna ground width variation slightly improves the return loss and impedance bandwidth.

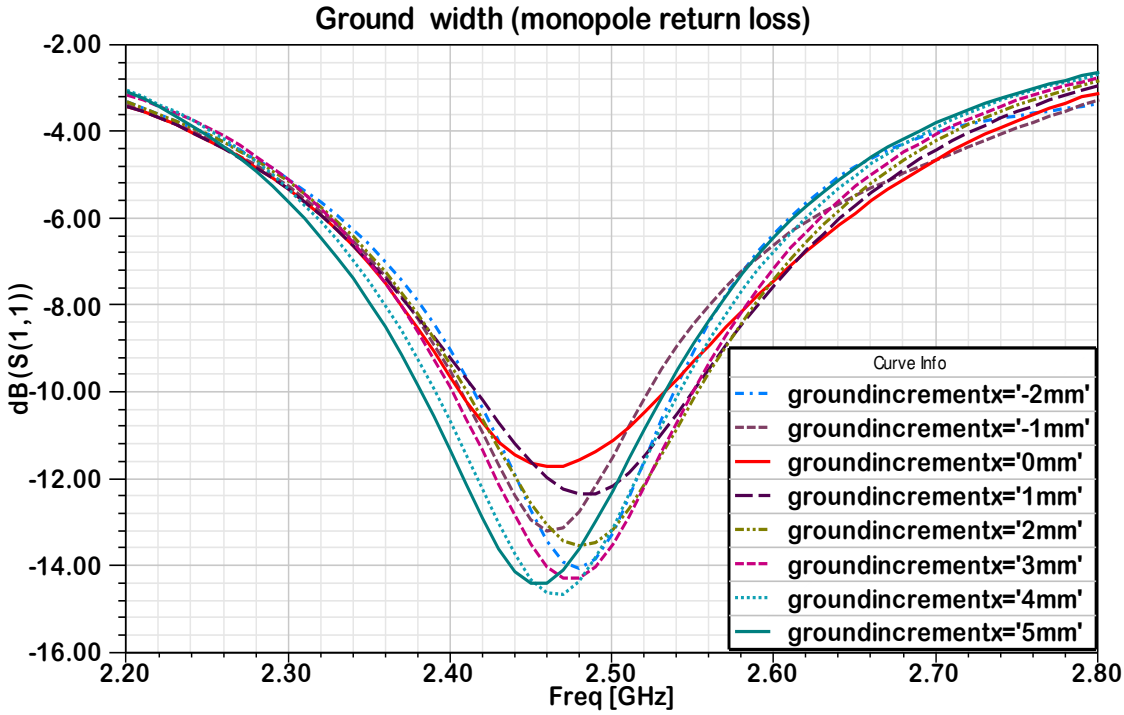

Figure 4.10 Monopole return loss with different values of the ground width.

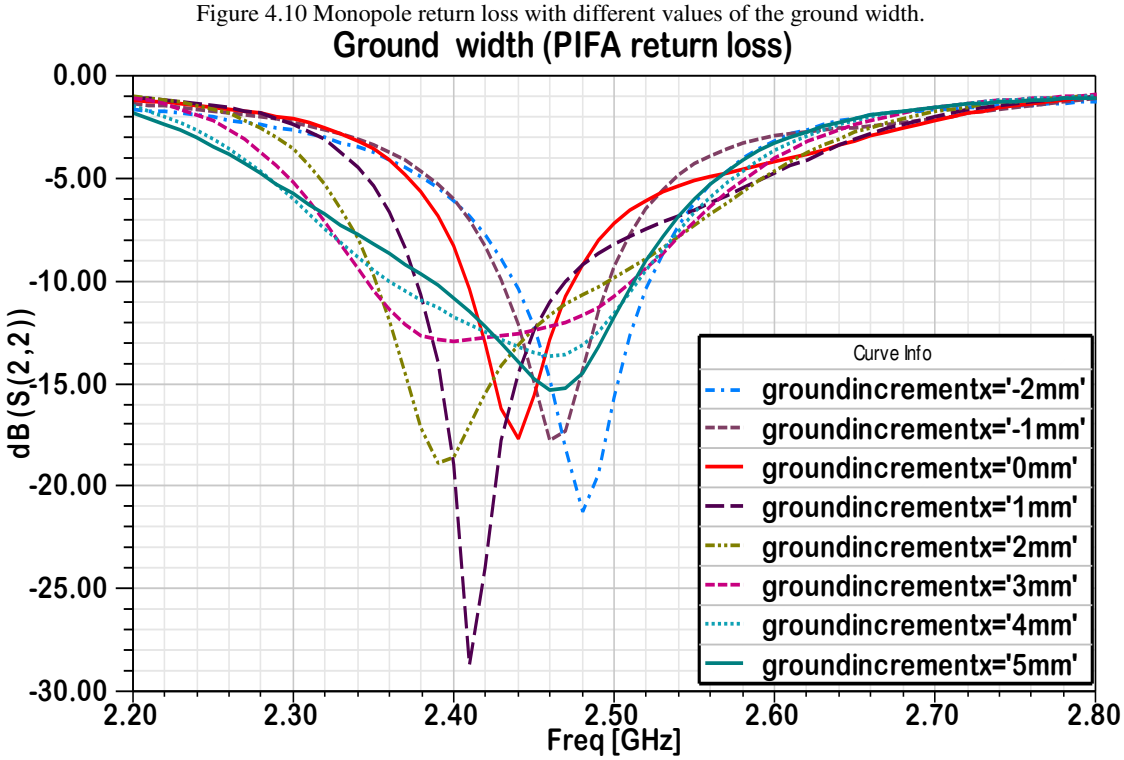

Figure 4.11 PIFA return loss with different values of the ground width.

Isolation improved with the increment in ground width as shown in Figure 4.12, while the total gain decreased with both variation in phi and theta as shown in Figures 4.13 and 4.14. Also ground width reduction cannot be used with our design because it decreases the isolation and shifts the resonant frequency.

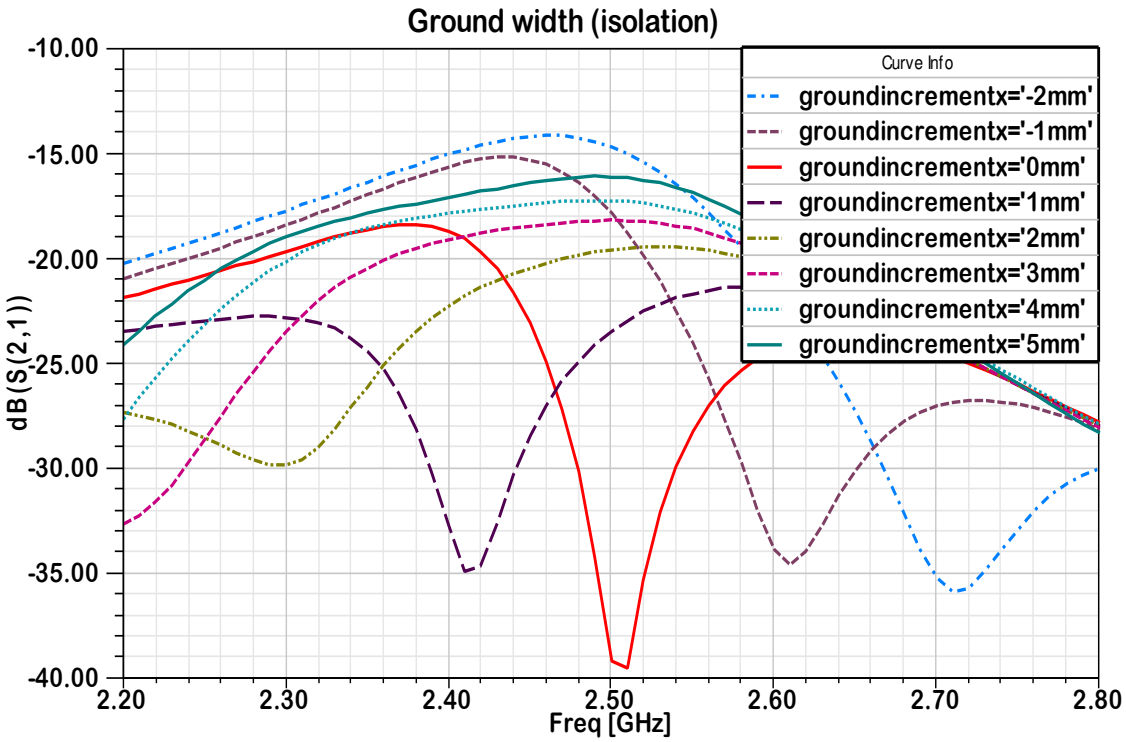

Figure 4.12 Isolation between the two antennas with different values of the ground width.

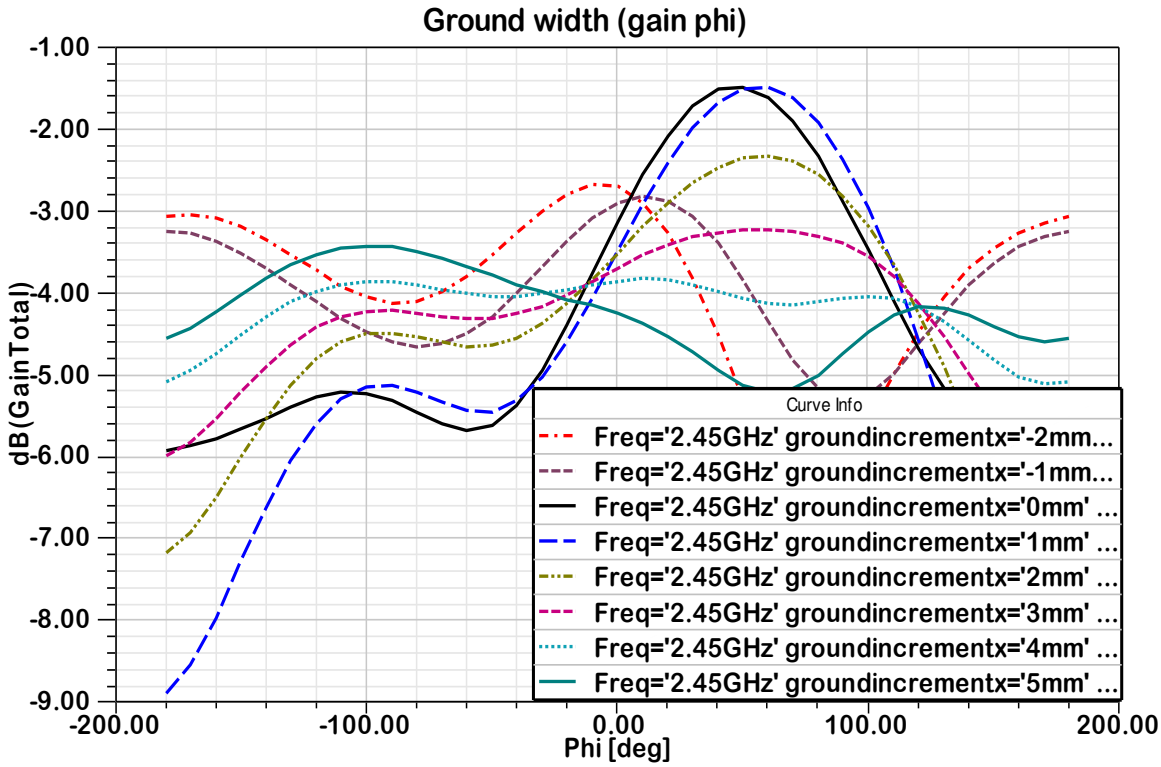

Figure 4.13 Maximum gain at phi with different values of the ground width.

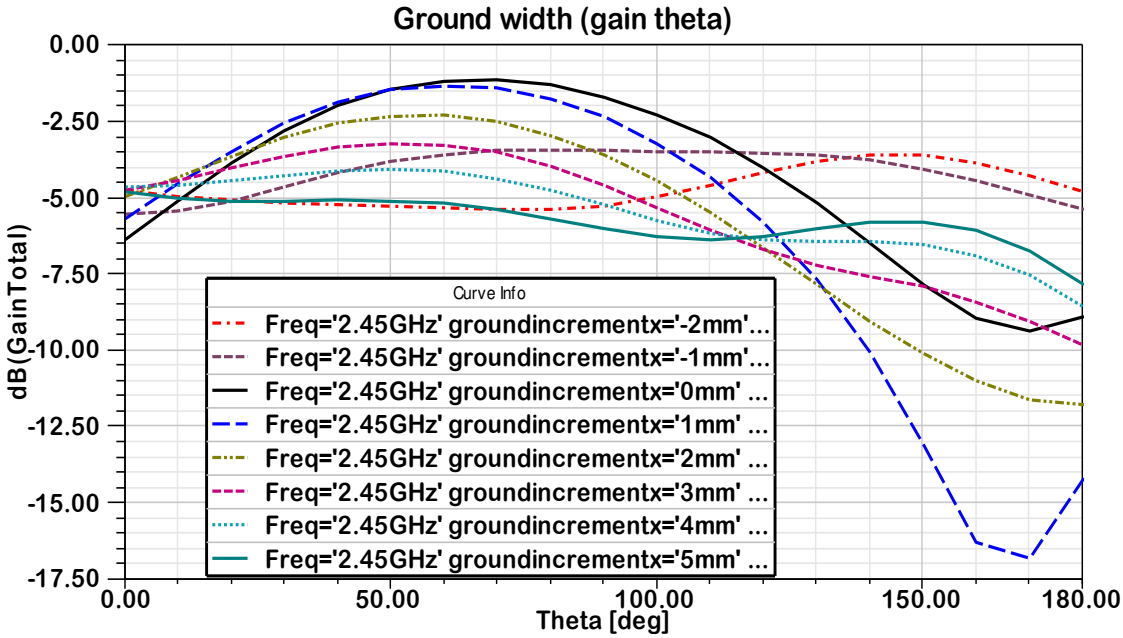

Figure 4.14 Maximum gain at theta with different values of the ground width.

4.1.3 Substrate Material

To investigate the substrate material of the antenna we used two different materials beside the basic design substrate of FR-4 material with the same thickness of 1.6 mm. FR-4 has a dielectric constant (ε_r=4.4). One with higher dielectric constant (ε_r=10.2) that is Roger 3010 which reduced the return loss of monopole S(1,1) for less than -10 dB, and also decreased resonant frequency and reduced the isolation as shown in Figure 4.15. However it increased the bandwidth of PIFA and resonant frequency and slightly improved the total gain of the antenna design from -1.15 dB (as shown in figure 4.3) to -0.9 dB as shown in Figure 4.16.

From the results it is possible to use high dielectric material with PIFA to increase the bandwidth and improve the gain but in our design we can not, because it reduced the isolation.

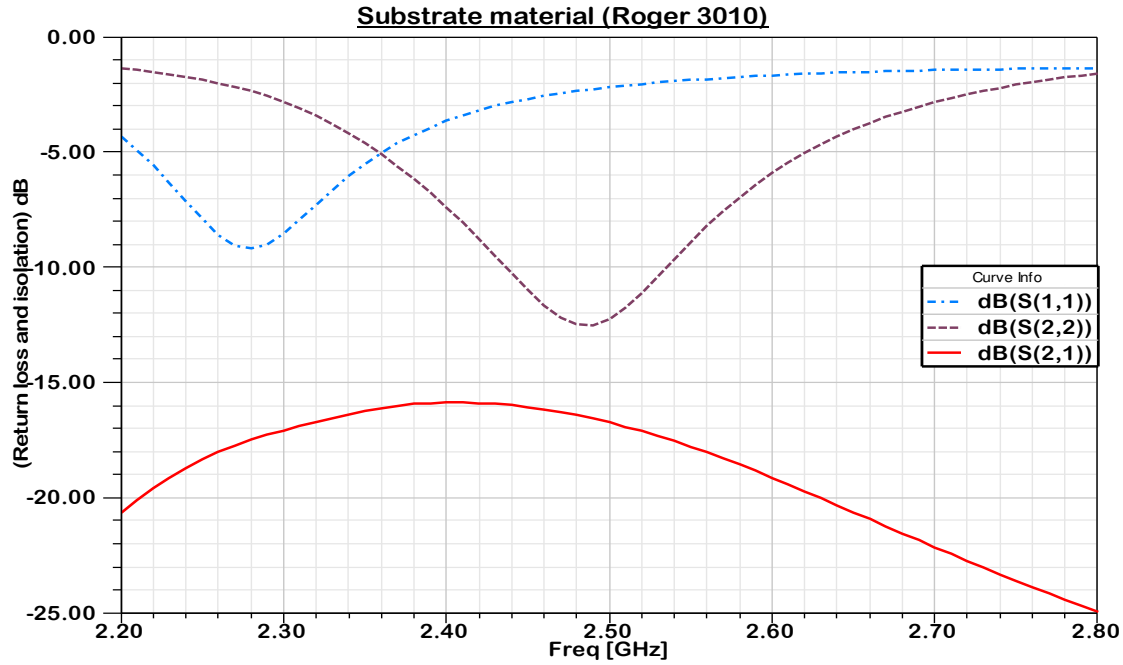

Figure 4.15 Monopole return loss S(1,1), PIFA return loss S(2,2), and isolation between them S(2,1) with substrate material (Roger 3010).

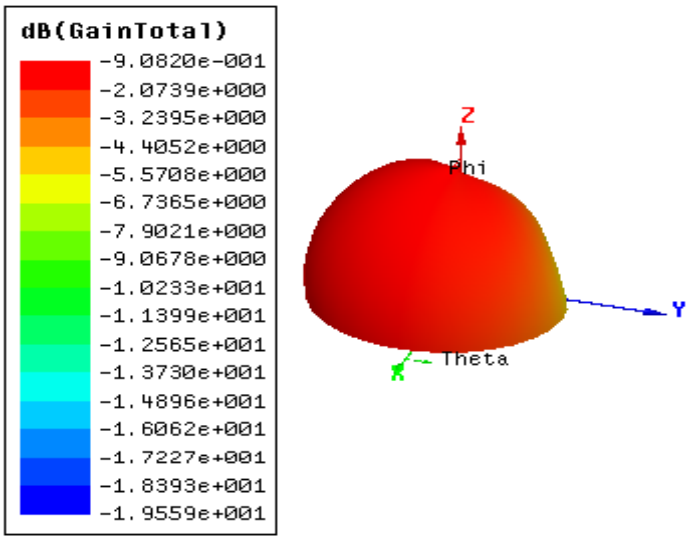

4.16 Total gain of the antenna with substrate material (Roger 3010).

While the use of the other material with lower dielectric constant (ε_r =2.2) that is Roger/Duriod 5880 increased the return loss of the monopole antenna S(1,1) and also increased its resonant frequency by more than 100 MHz while it shifted the resonant frequency of PIFA slightly toward higher frequency with small increment in the bandwidth. It is noticed that it reduced the isolation to unacceptable limit as shown in Figure 4.17 and reduced the total gain of the antenna slightly from -1.15 to -1.45 as shown in Figure 4.18.

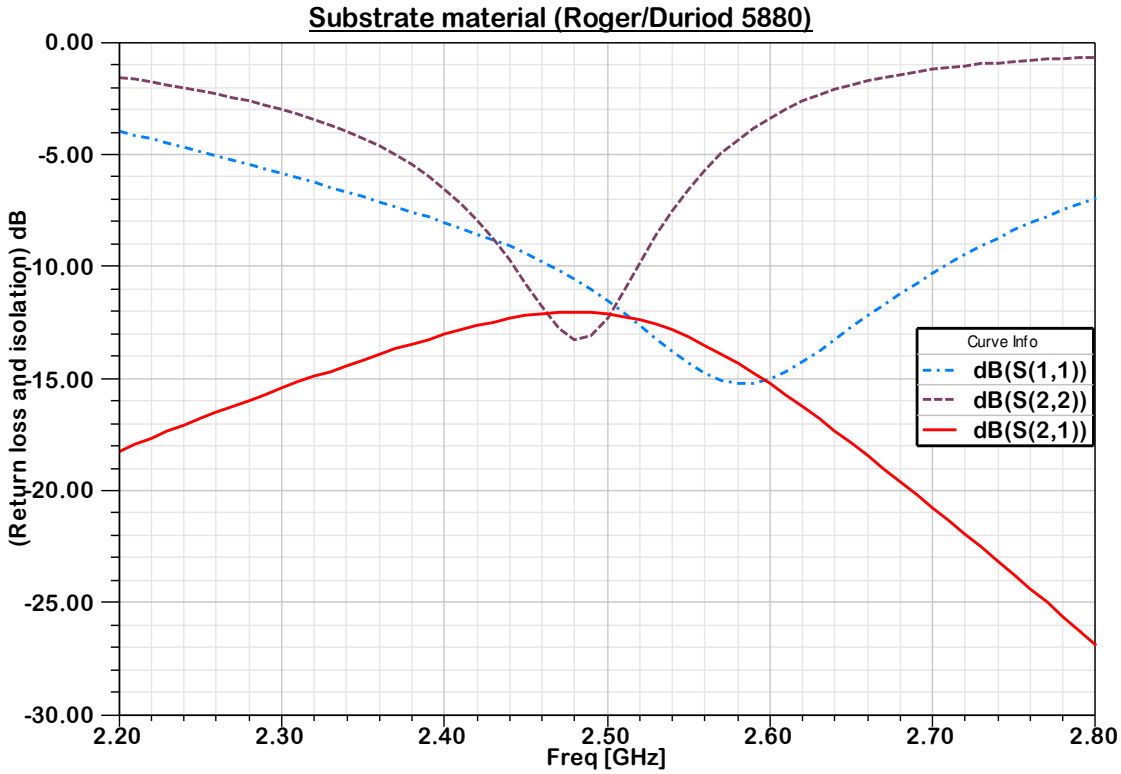

Figure 4.17 Monopole return loss S(1,1), PIFA return loss S(2,2), and isolation between them S(2,1) with substrate material (Roger/Duriod 5880).

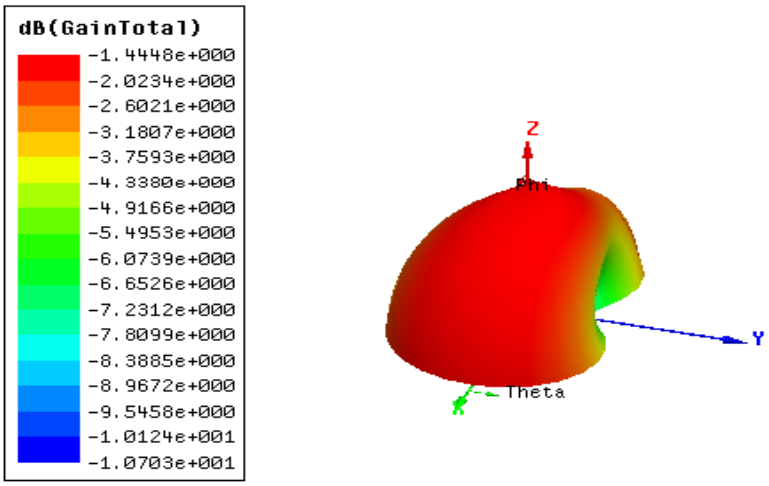

4.18 Total gain of the antenna with substrate material (Roger/Duriod 5880).

4.1.4 Monopole Radius

Monopole radius variation mainly influence the resonant frequency of the monopole antenna as shown in Figure 4.19. It is noticed that the resonant frequency increase as we increase the monopole radius, and that the return loss of PIFA changes with increase in monopole radius as shown in Figure 4.20.

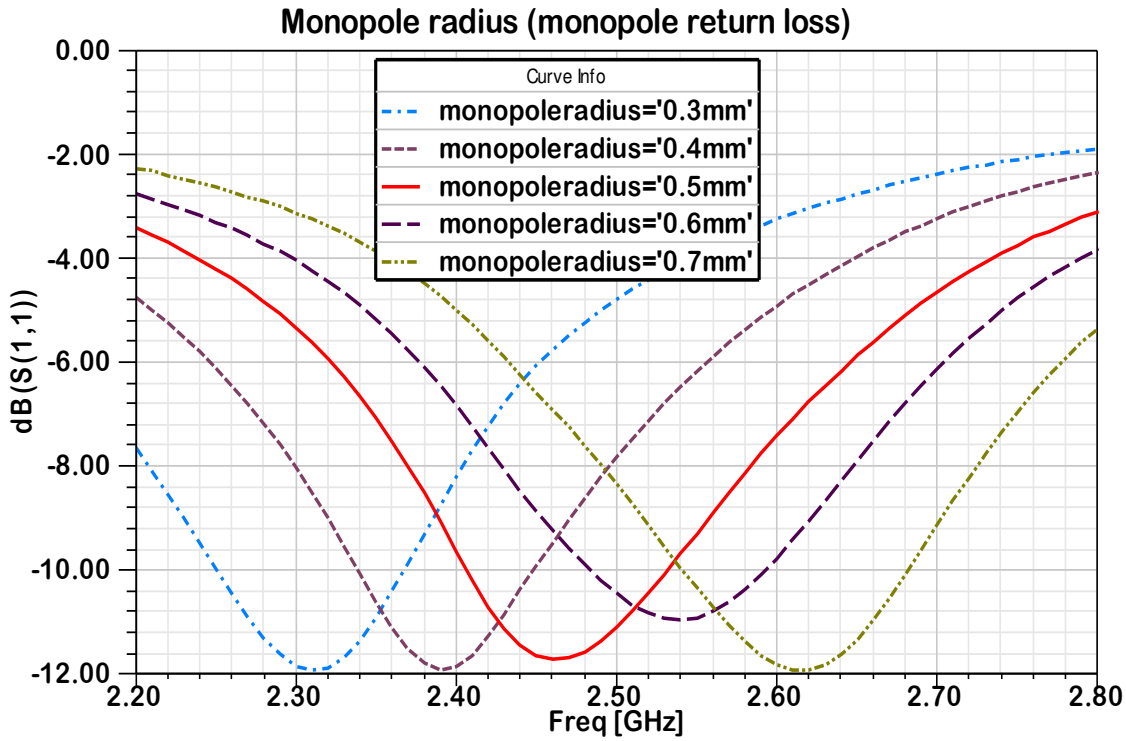

Figure 4.19 Monopole return loss with different values of the monopole radius.

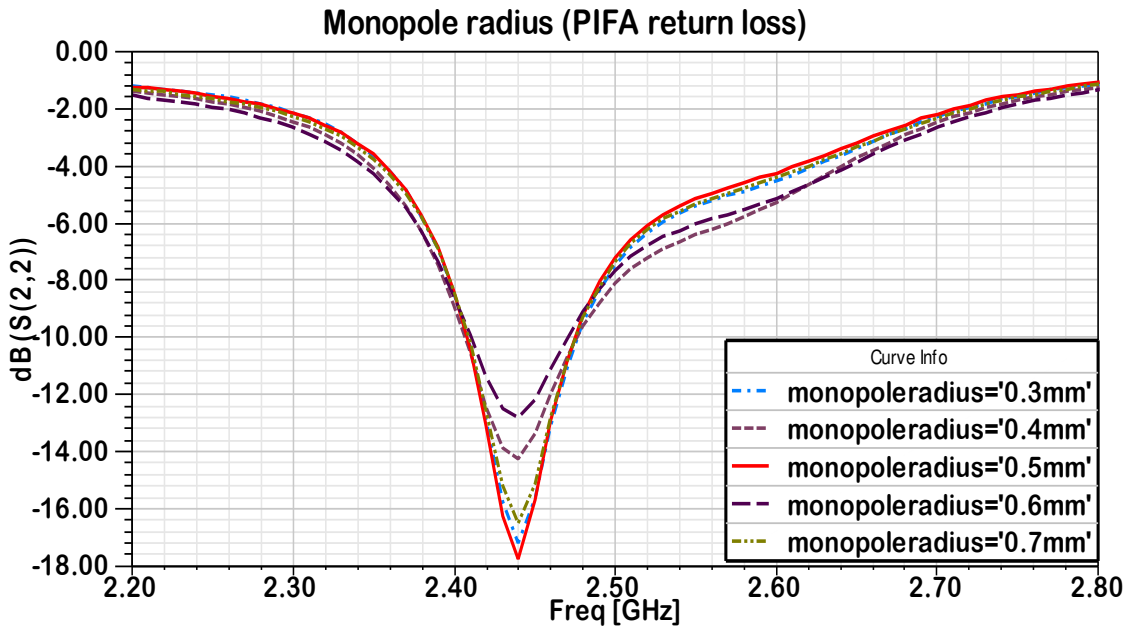

Figure 4.20 PIFA return loss with different values of the monopole radius.

Monopole radius slightly effects the isolation as shown in Figure 4.21. When the monopole radius is reduced, it reduces the isolation and when it is increased, it improves the isolation. It is noticed that Phi gain increases with the decrease in monopole radius as shown in Figure 4.22 and also theta gain increases with the decrease in monopole radius as shown in Figure 4.23. So monopole radius parameter is suitable when we want to reduce the resonant frequency because it reduces the resonant frequency and improves the total gain.

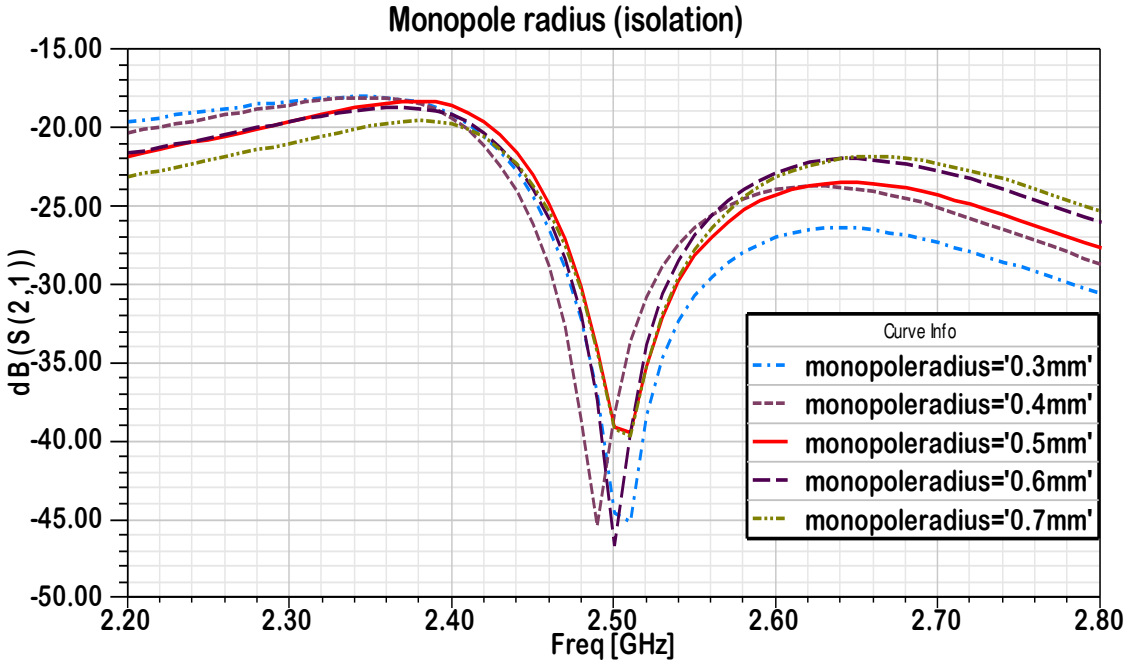

Figure 4.21 Isolation between the two antennas with different values of the monopole radius.

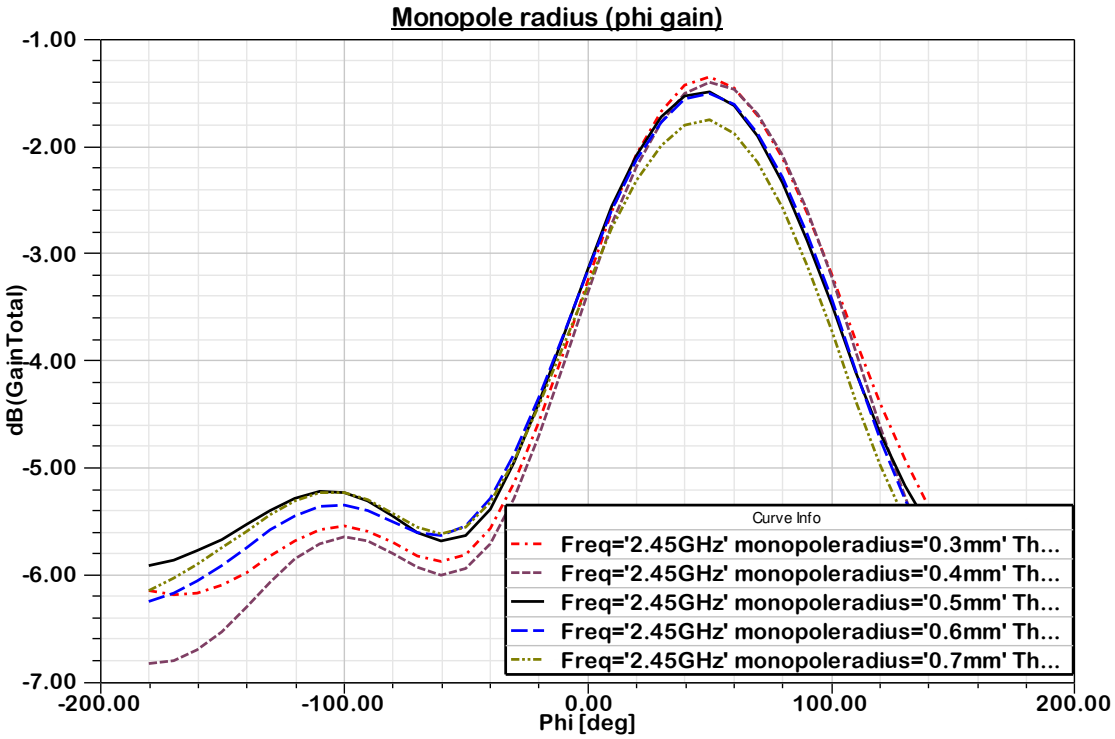

Figure 4.22 Maximum gain at phi with different values of the monopole radius.

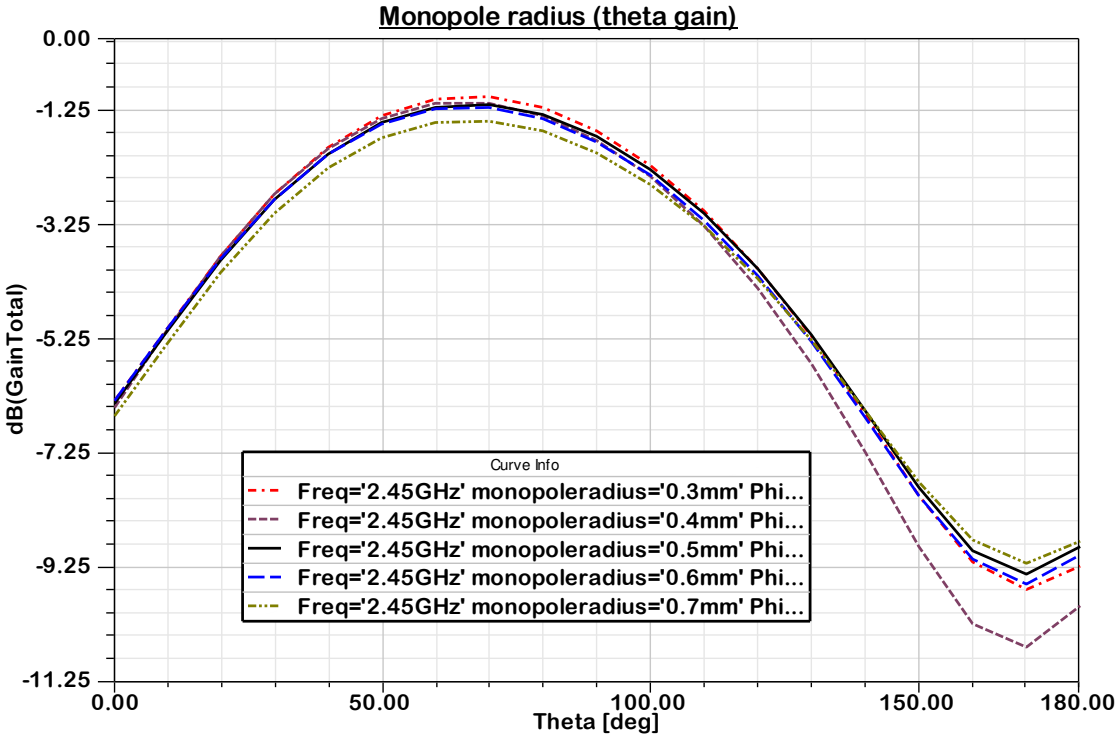

Figure 4.23 Maximum gain at theta with different values of the monopole radius.

4.1.5 Monopole Height

Monopole height is very effective parameter for monopole antenna return loss, resonant frequency and bandwidth as shown in Figure 4.24. When we decrease the height, it improves the return loss as well as the bandwidth and increase the resonant frequency while it has slight influence on PIFA as shown in Figure 4.25.

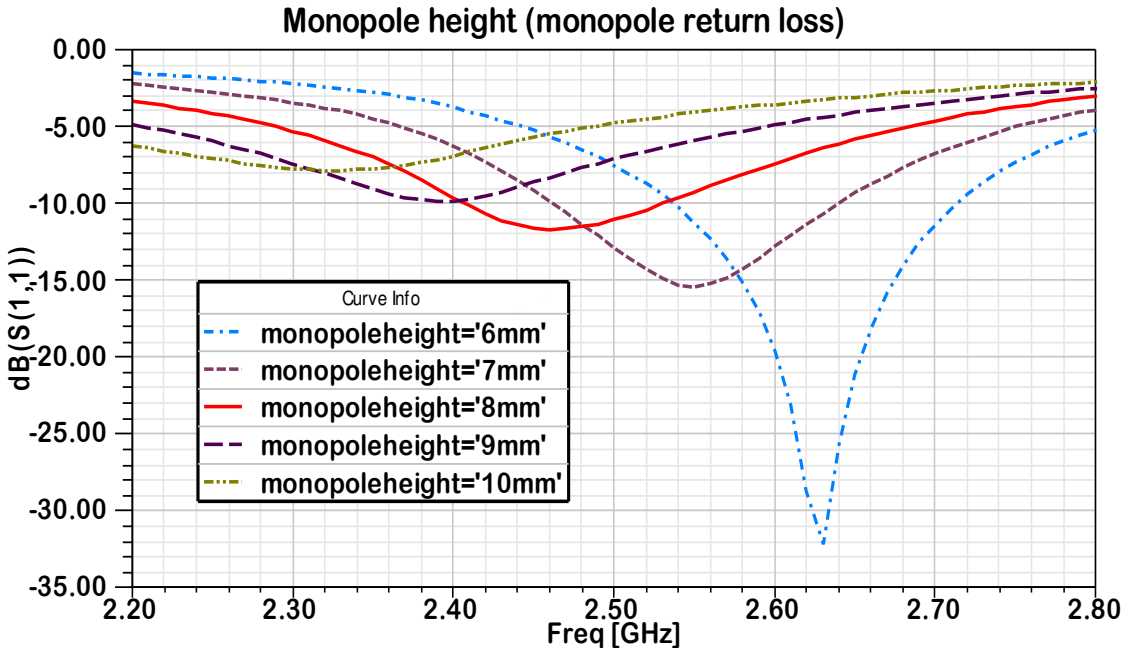

Figure 4.24 Monopole return loss with different values of the monopole height.

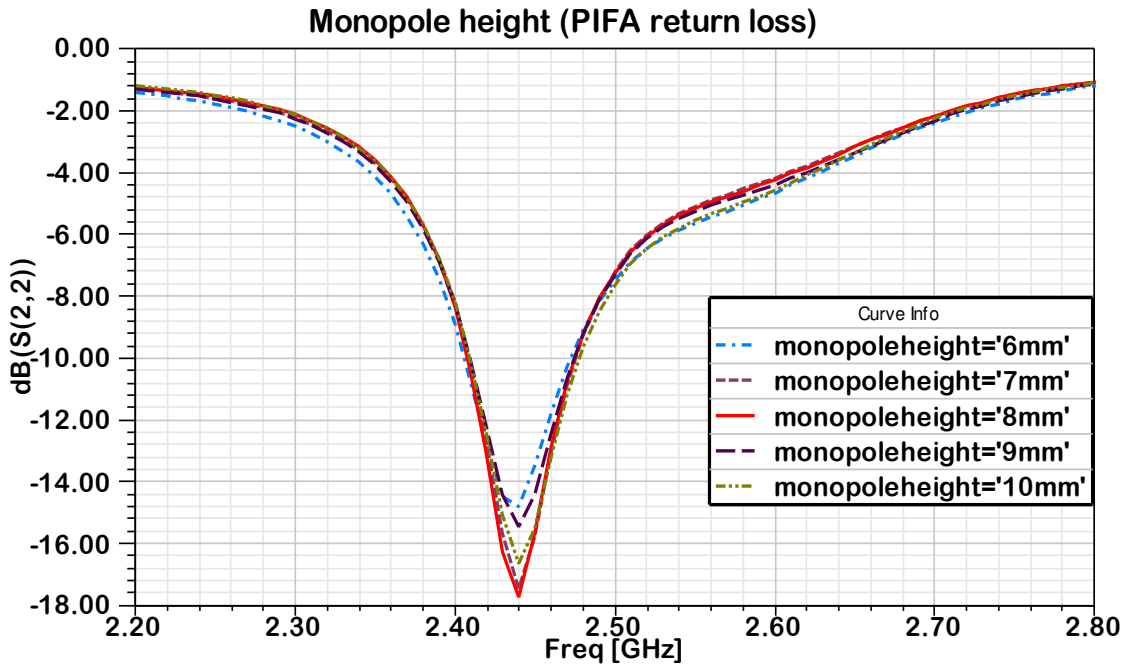

Figure 4.25 PIFA return loss with different values of the monopole height.

Monopole height slightly effects the isolation between the antennas and when the monopole height decreases the isolation improves at 2.45 GHz as shown in Figure 4.26 while it improves the gain of phi and theta slightly when the height increases as shown in Figures 4.27 and 4.28.

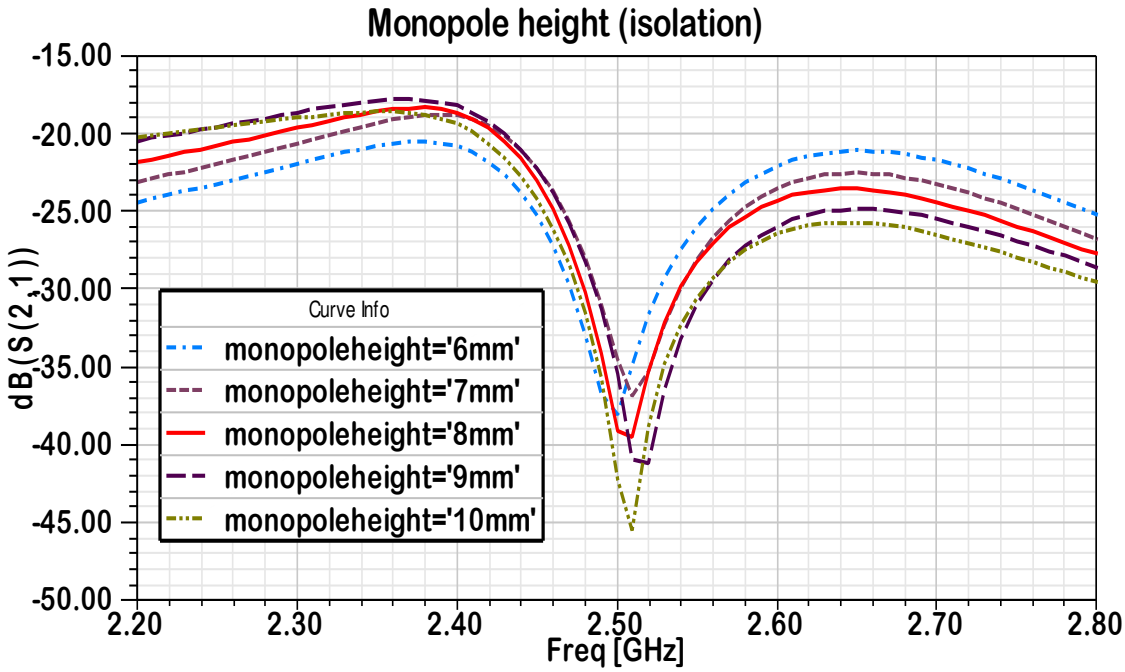

Figure 4.26 Isolation between the two antennas with different values of the monopole height.

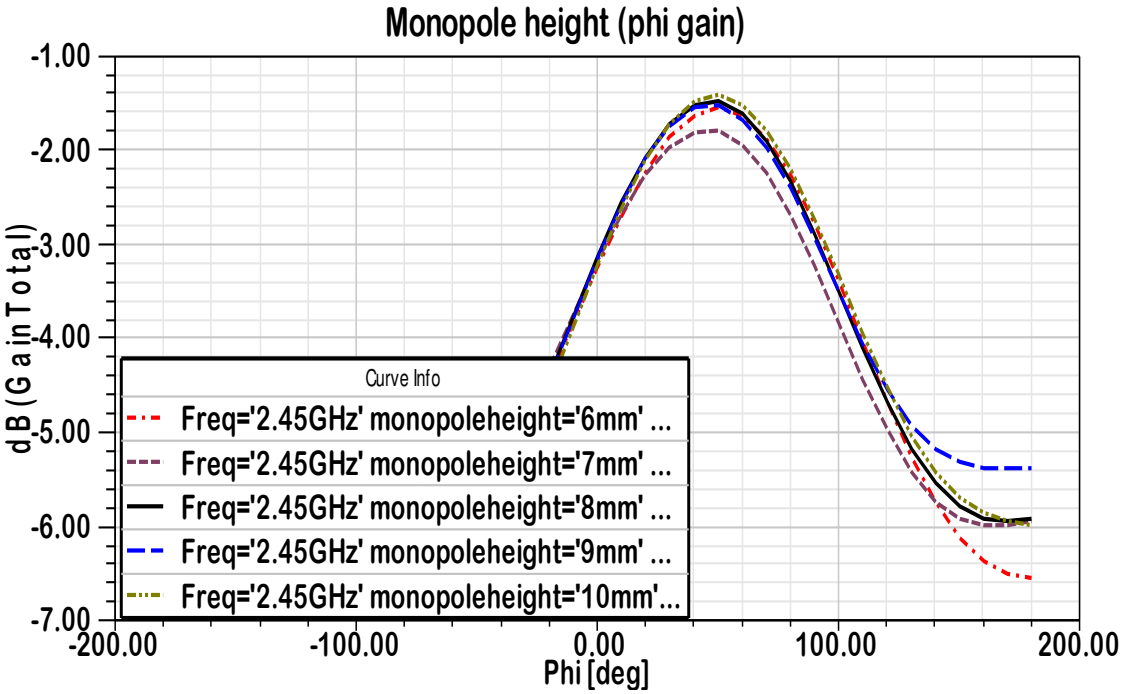

Figure 4.27 Maximum gain at phi with different values of the monopole height.

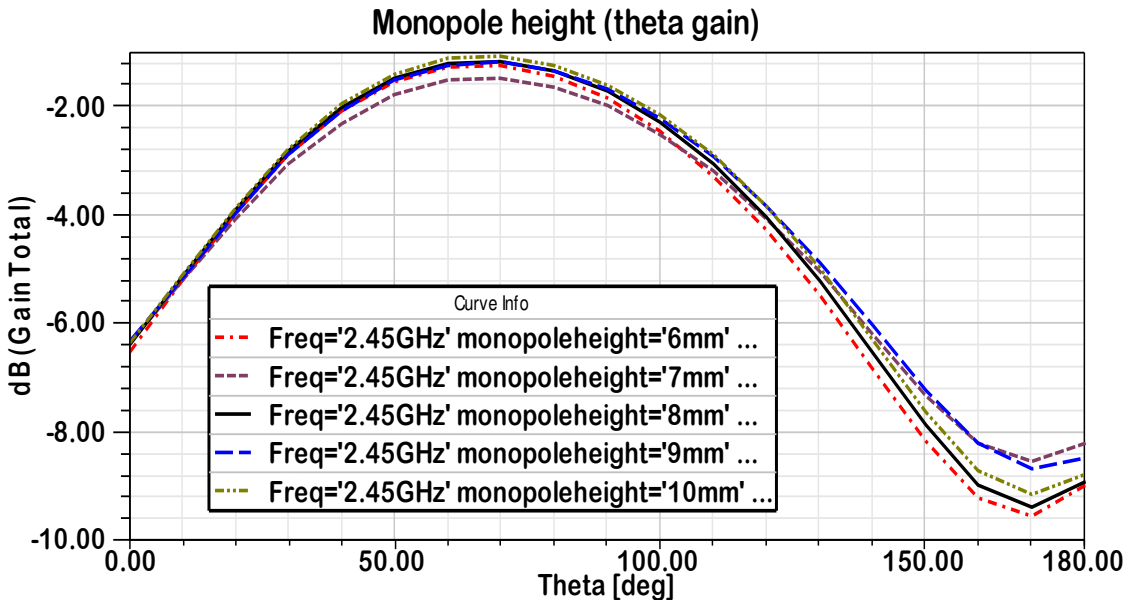

Figure 4.28 Maximum gain at theta with different values of the monopole height.

4.1.6 Monopole Disk Radius

Monopole disk radius is another important parameter which influences the characteristics of monopole antenna, as shown in Figure 4.29. When the disk radius increases it shifts the resonant frequency of the monopole antenna to a lower frequency but it slightly influence the return loss of PIFA by small reduction as shown in Figure 4.30.

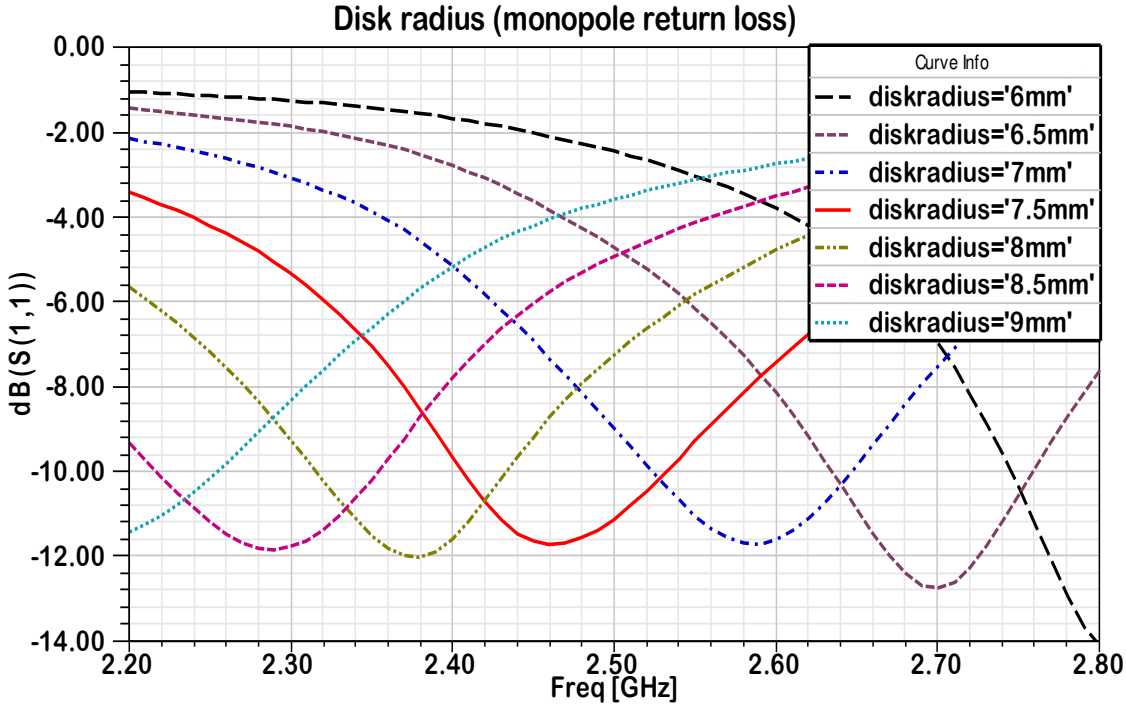

Figure 4.29 Monopole return loss with different values of the monopole disk radius.

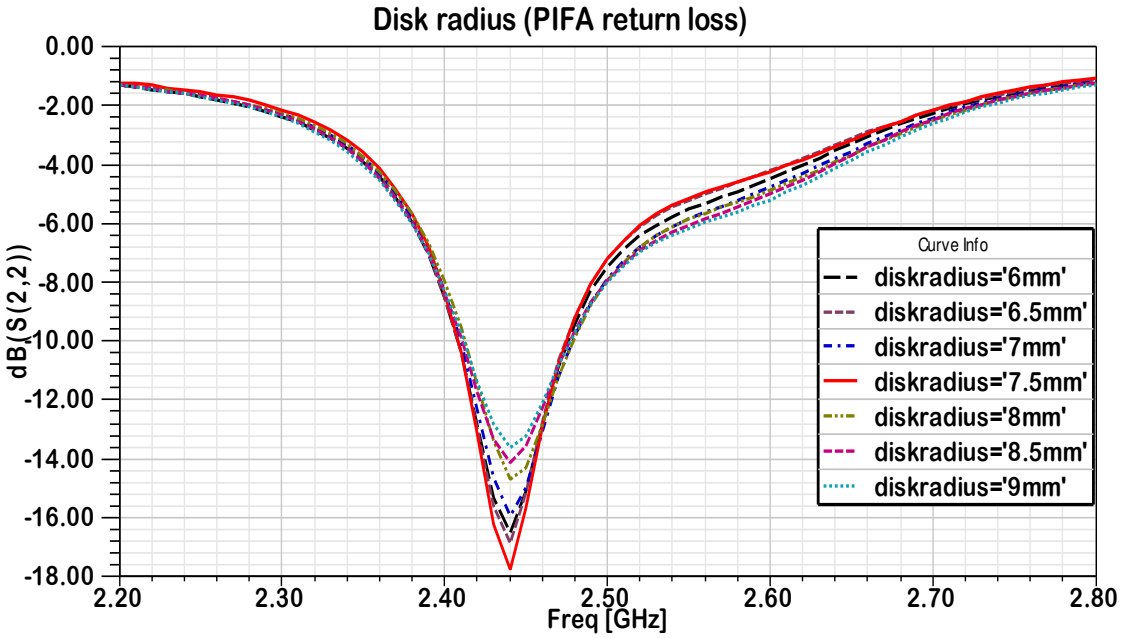

Figure 4.30 PIFA return loss with different values of the monopole disk radius.

Morever, the isolation improved by the reduction in the disk radius of the monopole antenna as shown in Figure 4.31, but the gain of phi and theta improved by increasing the disk radius of the monopole antenna as shown in Figures 4.32 and 4.33.

From the results, we have seen that increasing the disk radius is good in improving the gain of monopole antenna but in our design because we are using diversity technique, the increment in the disk radius reduces the isolation between the two antennas as shown in Figure 4.31.

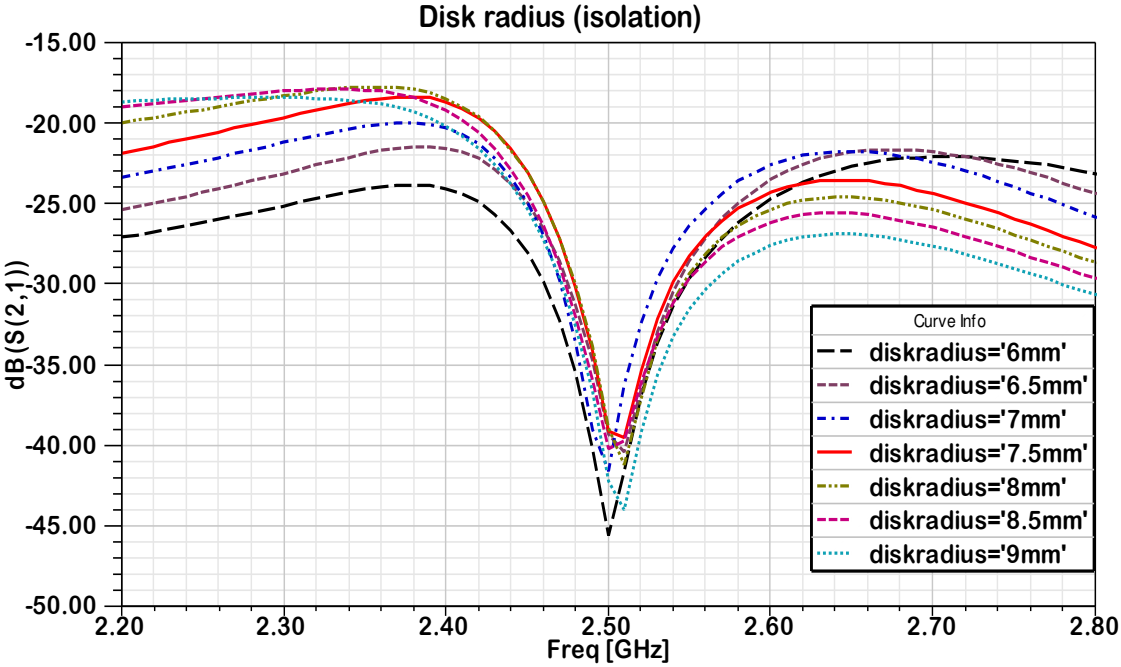

Figure 4.31 Isolation between the two antennas with different values of the monopole disk radius.

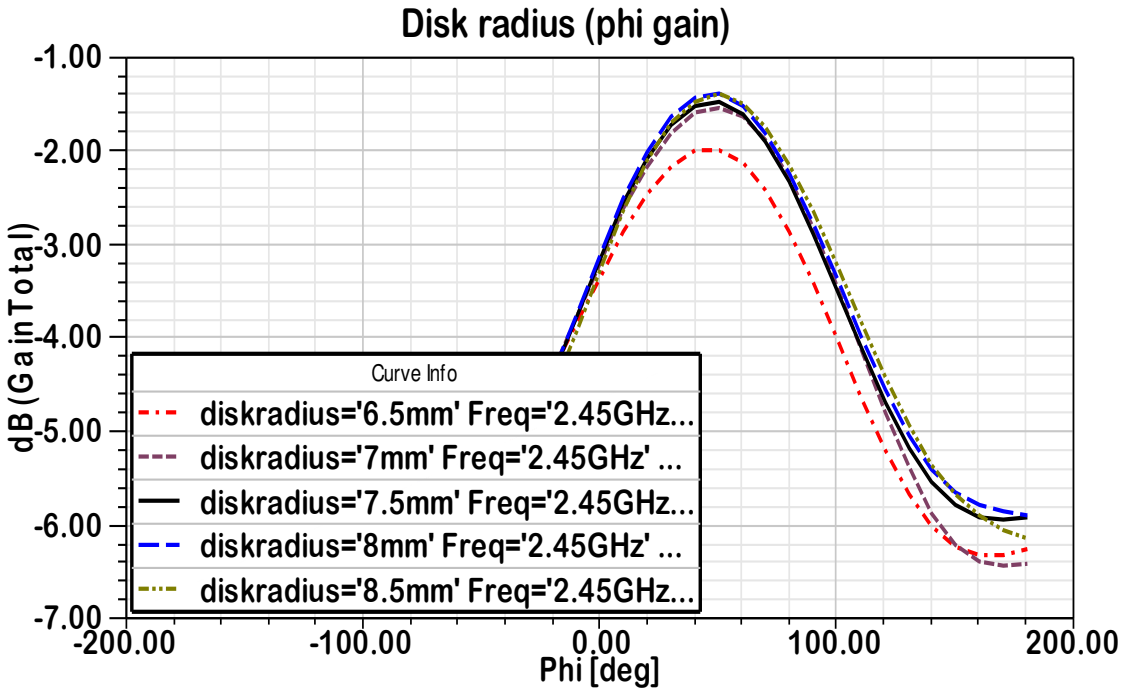

Figure 4.32 Maximum gain at phi with different values of the monopole disk radius.

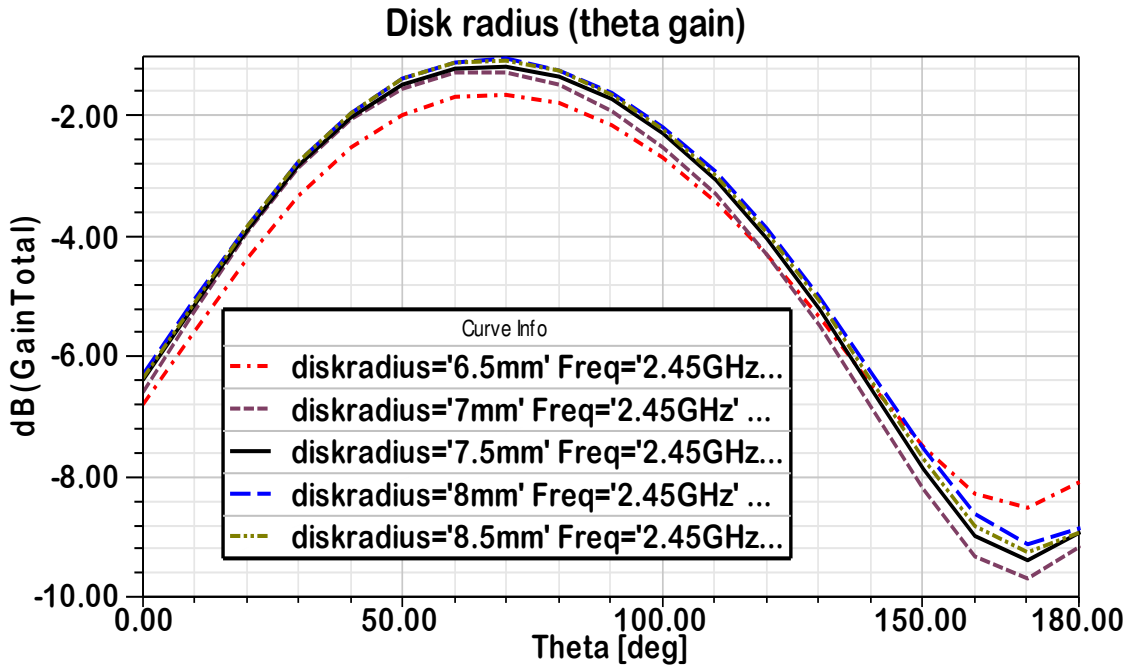

Figure 4.33 Maximum gain at theta with different values of the monopole disk radius.

4.1.7 PIFA Height

PIFA height parameter has a great influence in PIFA characteristics, as we increase the height the resonant frequency increases and the bandwidth increases as shown in Figure 4.35. But the height of PIFA is preferred to be small enough so that the antenna fits in the casing of small terminal device. PIFA height has a small effect on monopole antenna as shown in Figure 4.34, where the return loss and bandwidth of the monopole antenna increased slightly by increasing in PIFA height.

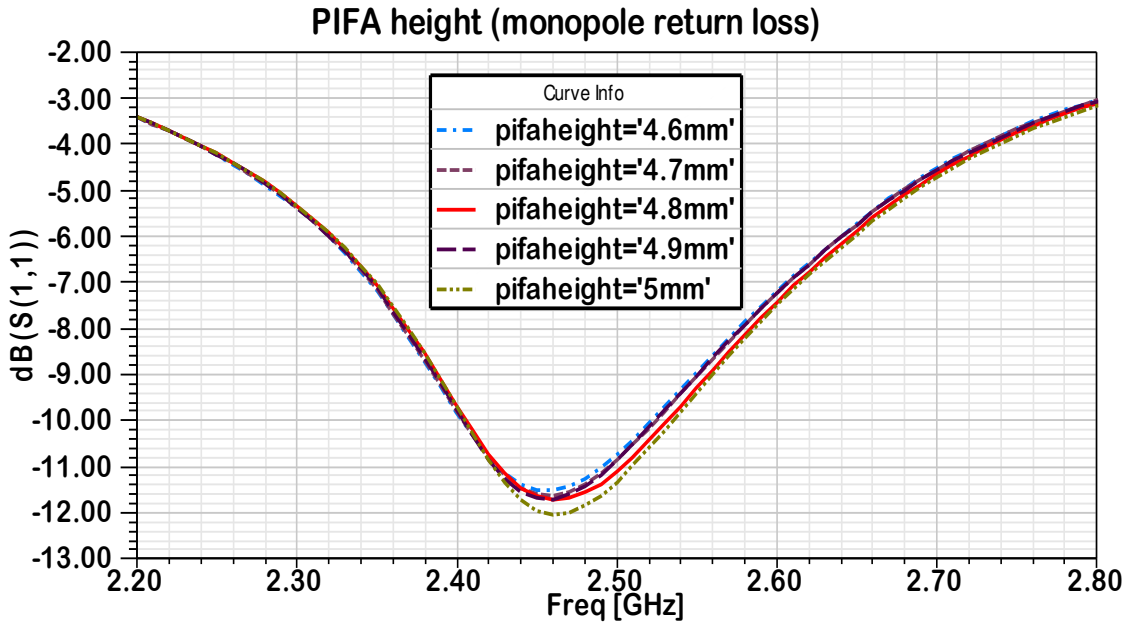

Figure 4.34 Monopole return loss with different values of the PIFA height.

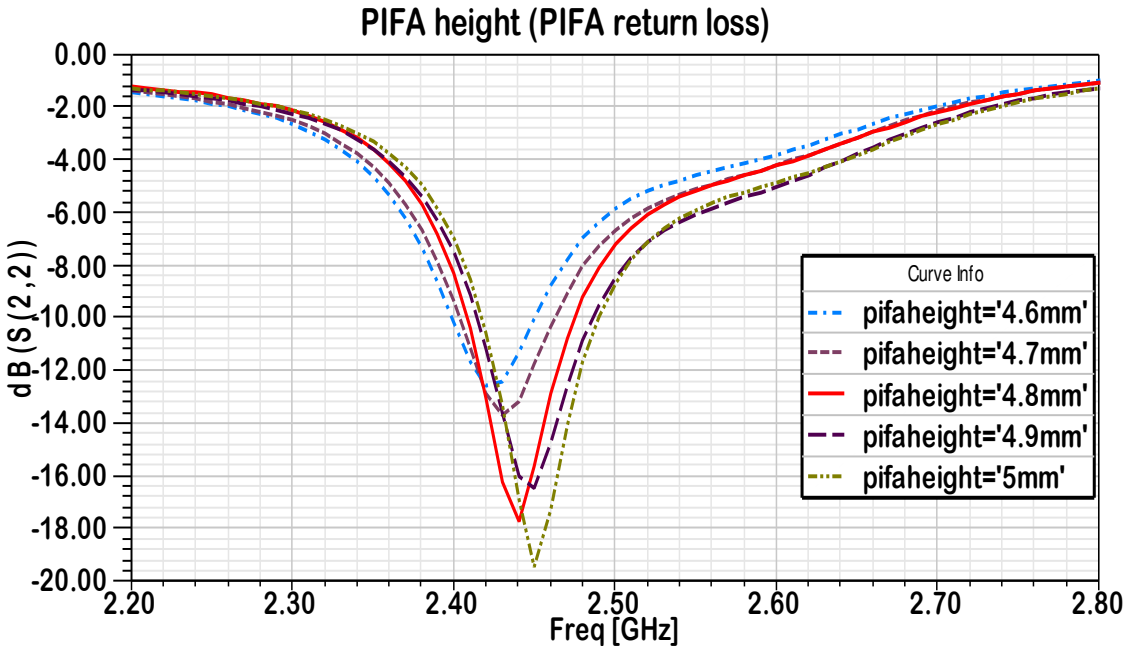

Figure 4.35 PIFA return loss with different values of the PIFA height.

PIFA height variation slightly reduces the isolation between the two antennas as shown in Figure 4.36, also the gain of phi and theta slightly reduces by the height variation as shown in Figures 3.37 and 3.38.

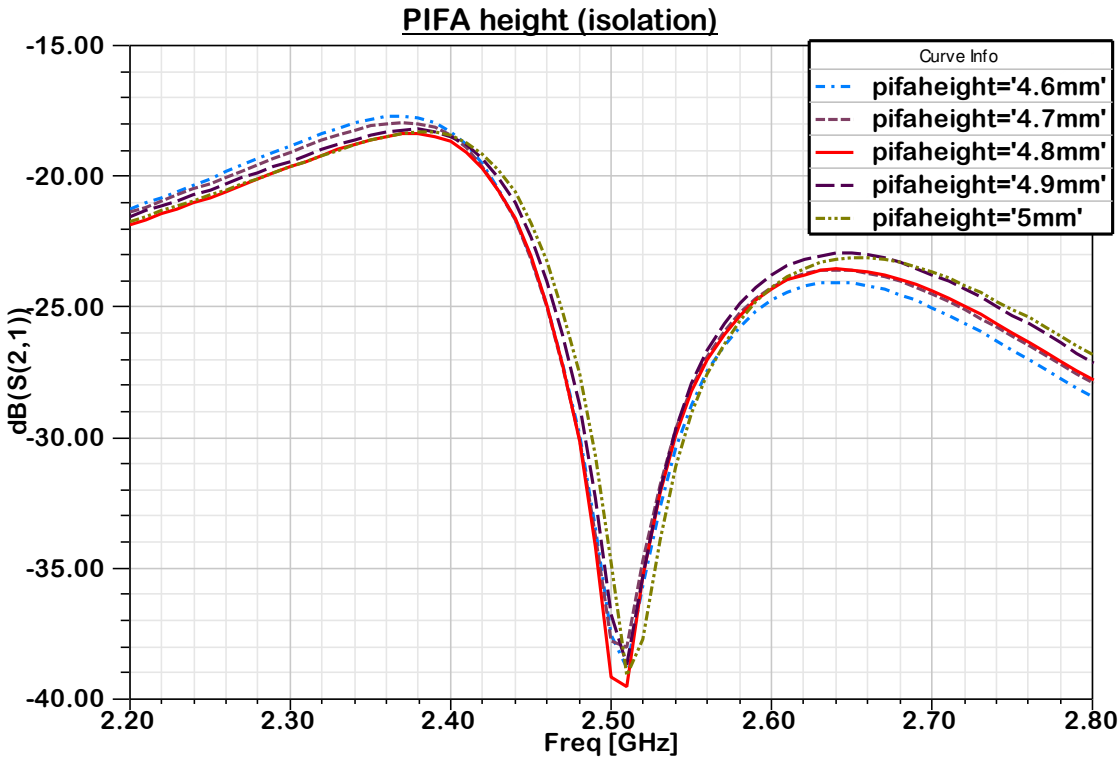

Figure 4.36 Isolation between the two antennas with different values of the PIFA height.

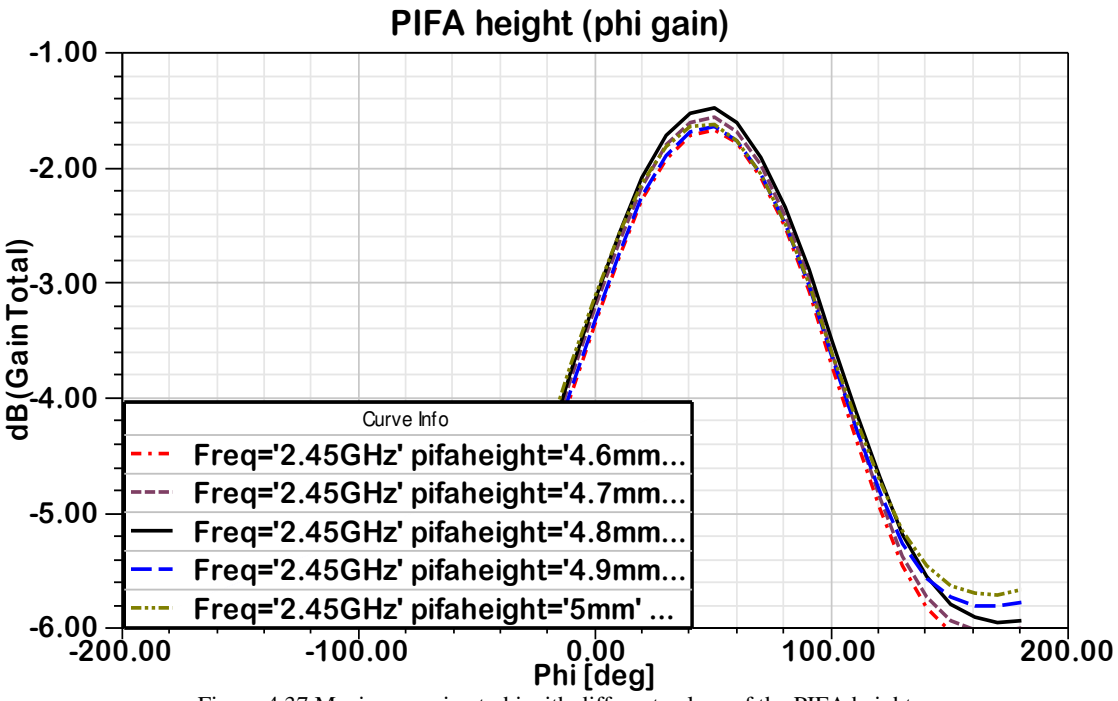

Figure 4.37 Maximum gain at phi with different values of the PIFA height.

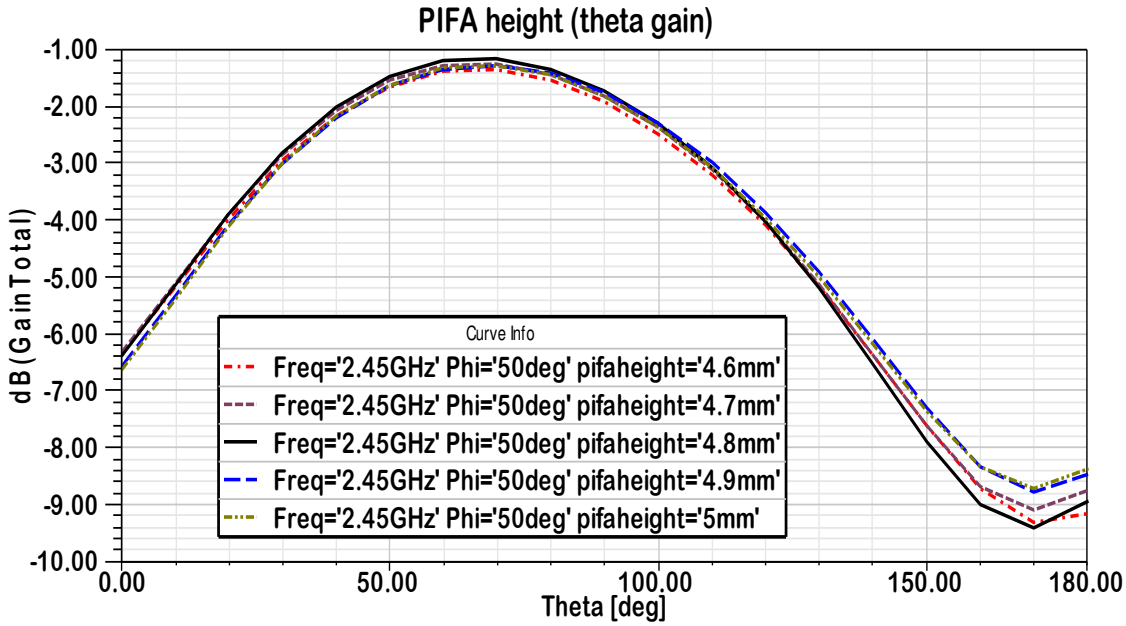

Figure 4.38 Maximum gain at theta with different values of the PIFA height.

4.1.8 PIFA Width

PIFA width parameter is another important parameter which influences the characteristics of PIFA antenna, as shown in Figure 4.40. When the width decreases the resonant frequency increases and the bandwidth improves while it slightly affects the monopole antenna. The return loss of the monopole antenna slightly changes with the decreases in PIFA width as shown in Figure 4.39.

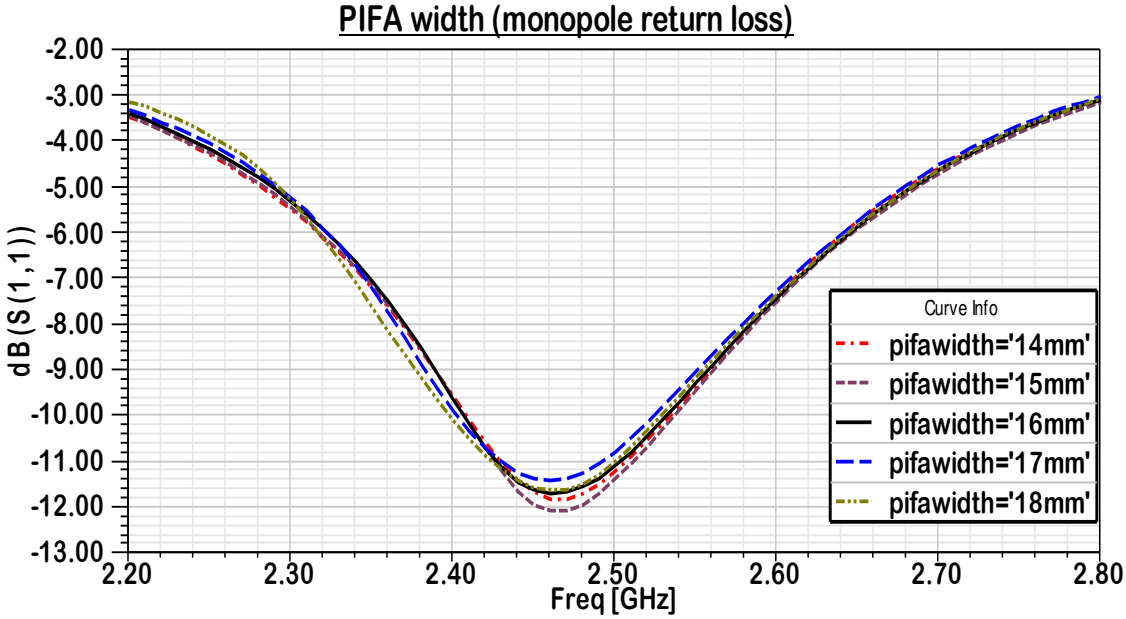

Figure 4.39 Monopole return loss with different values of the PIFA width.

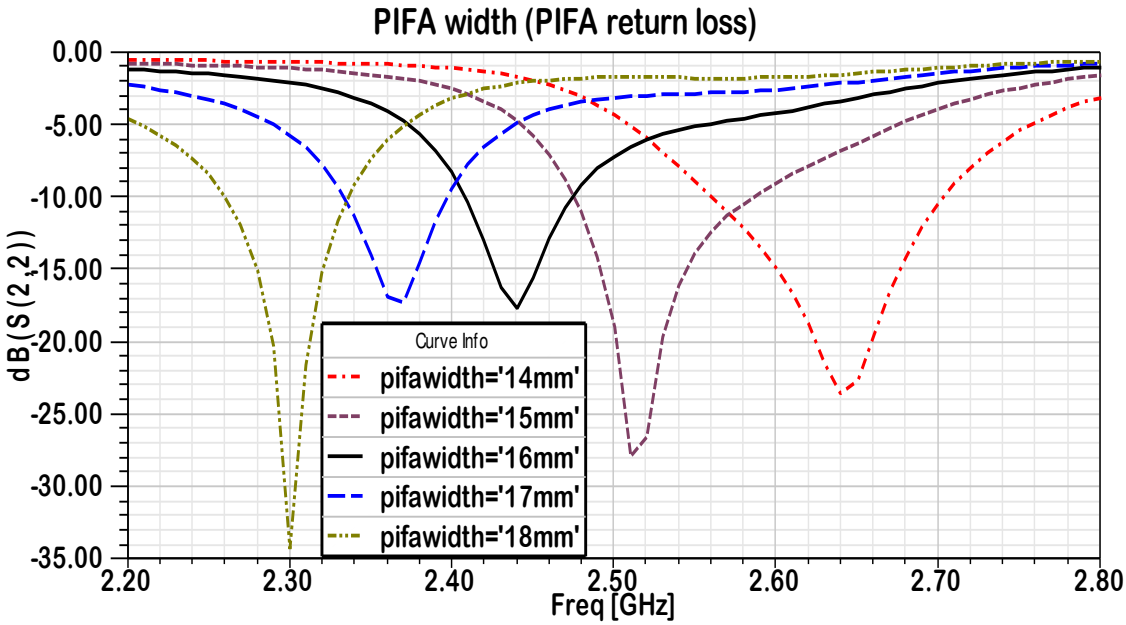

Figure 4.40 PIFA return loss with different values of the PIFA width.

PIFA width highly affects the isolation between the two antennas, as shown in Figure 4.41. The isolation improved with the decrease in PIFA width while the gain of phi and theta improved with the increase of the PIFA width as shown in Figures 4.42 and 4.43 which show slight increment in the total gain with PIFA width increment.

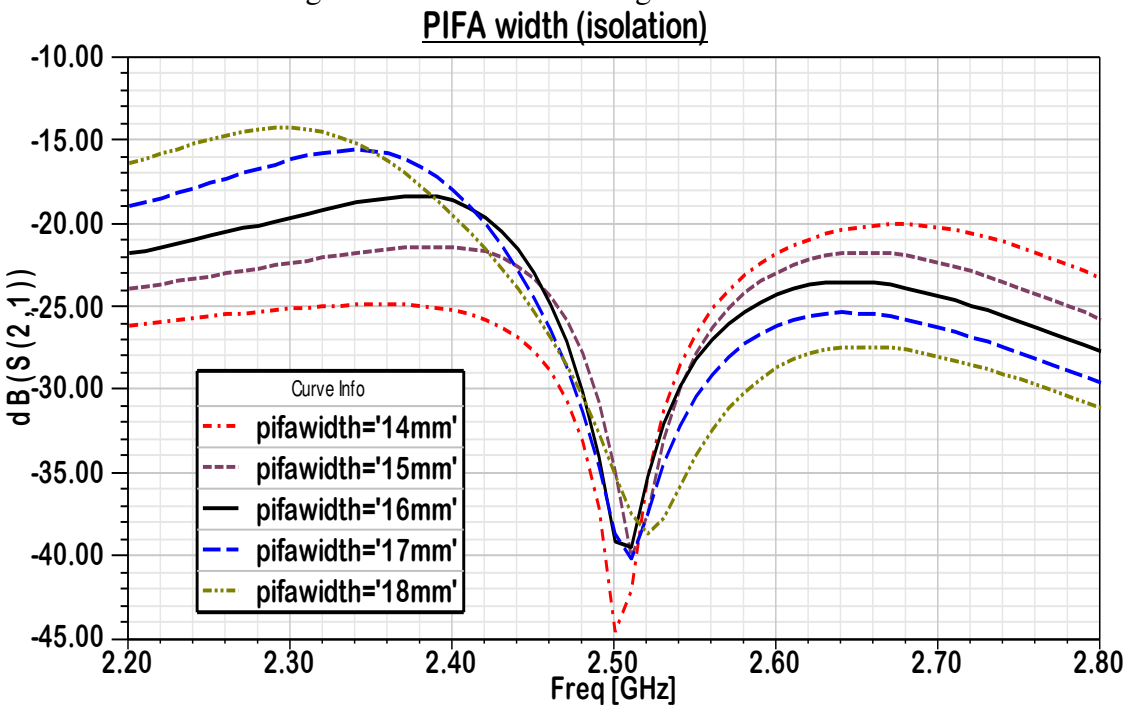

Figure 4.41 Isolation between the two antennas with different values of the PIFA width.

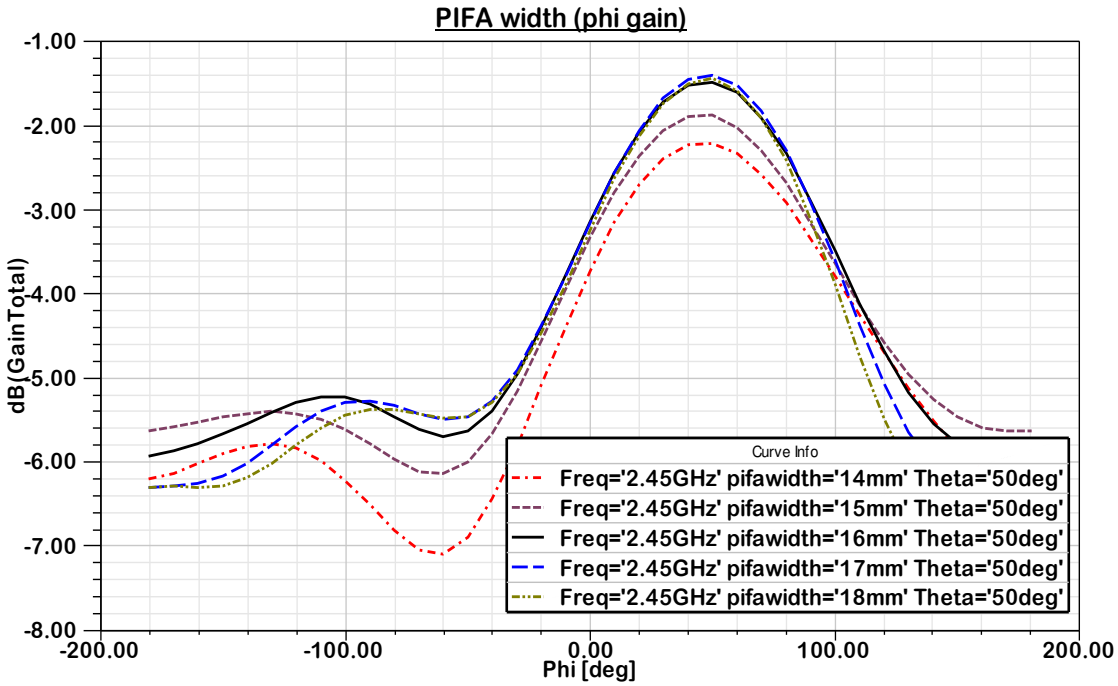

Figure 4.42 Maximum gain at phi with different values of the PIFA width.

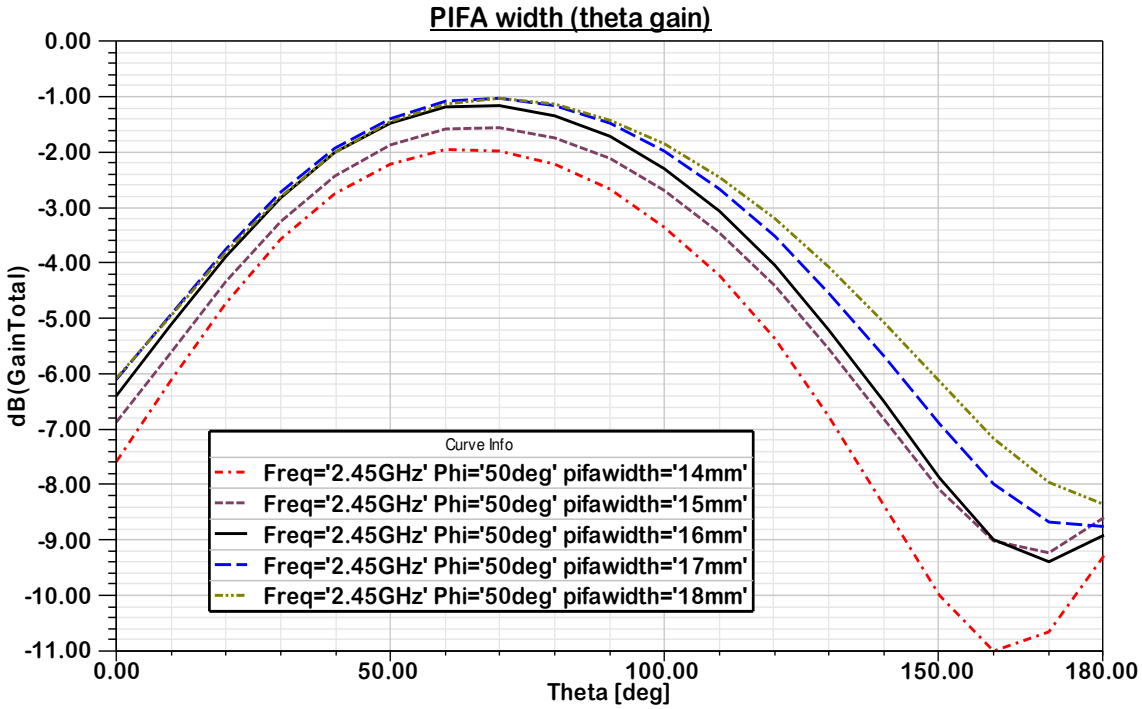

Figure 4.43 Maximum gain at theta with different values of the PIFA width.

4.1.9 PIFA Length

PIFA length has a great effect on the characteristics of PIFA antenna, and when we increase the length of PIFA, the resonant frequency, the bandwidth and the return loss decrease as shown in Figure 4.45, while the variation of PIFA length slightly reduce the return loss of the monopole antenna as shown in Figure 4.44.

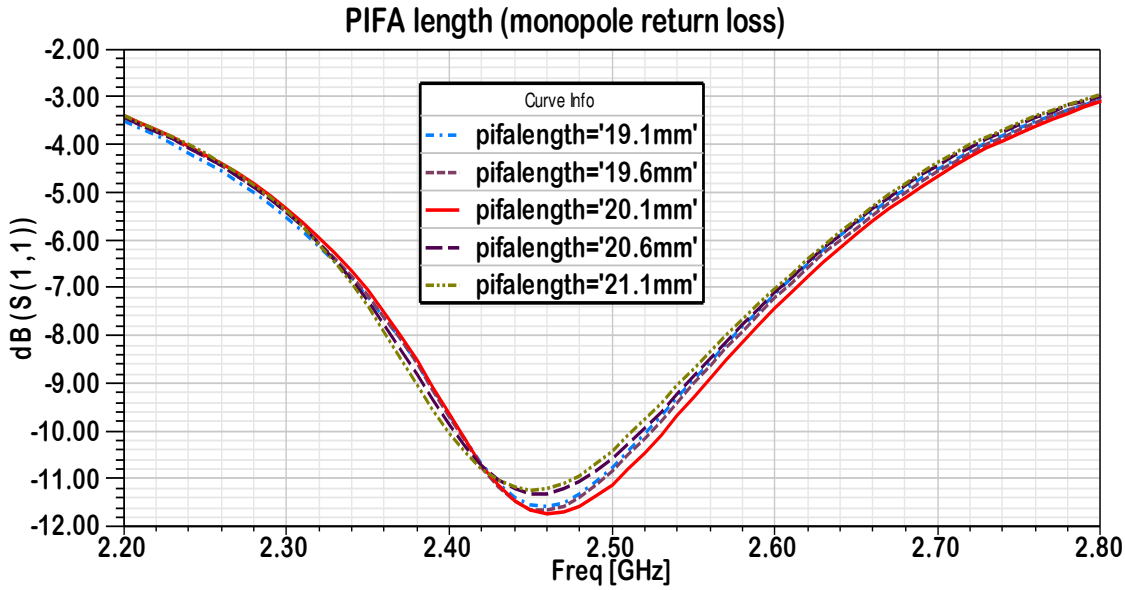

Figure 4.44 Monopole return loss with different values of the PIFA length.

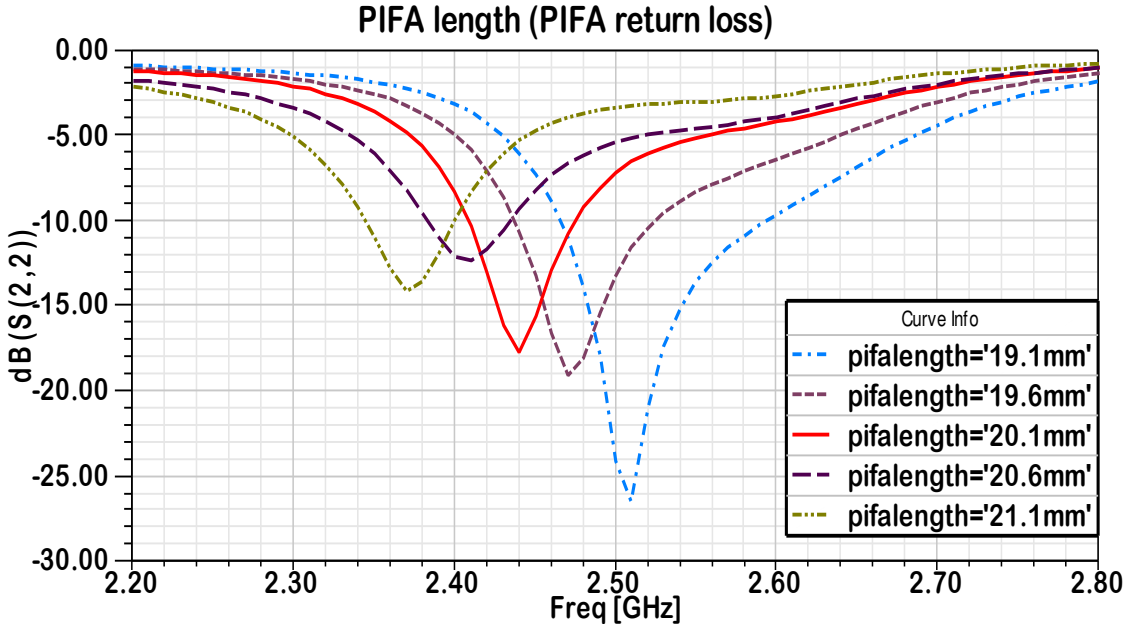

Figure 4.45 PIFA return loss with different values of the PIFA length.

Same as with PIFA width, PIFA length affects the isolation between the two antennas, as shown in Figure 4.46. The isolation improved with the decrease in PIFA length while the gain of phi and theta improved with the increase of the PIFA length as shown in Figures 4.47 and 4.48 which show a small increment in the total gain with PIFA length increment.

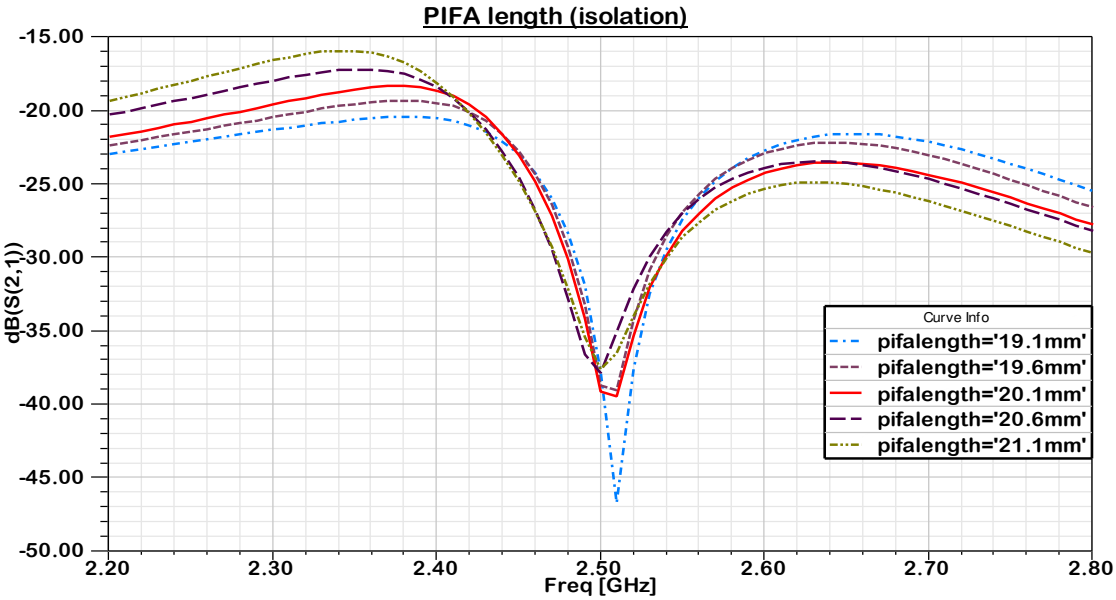

Figure 4.46 Isolation between the two antennas with different values of the PIFA length.

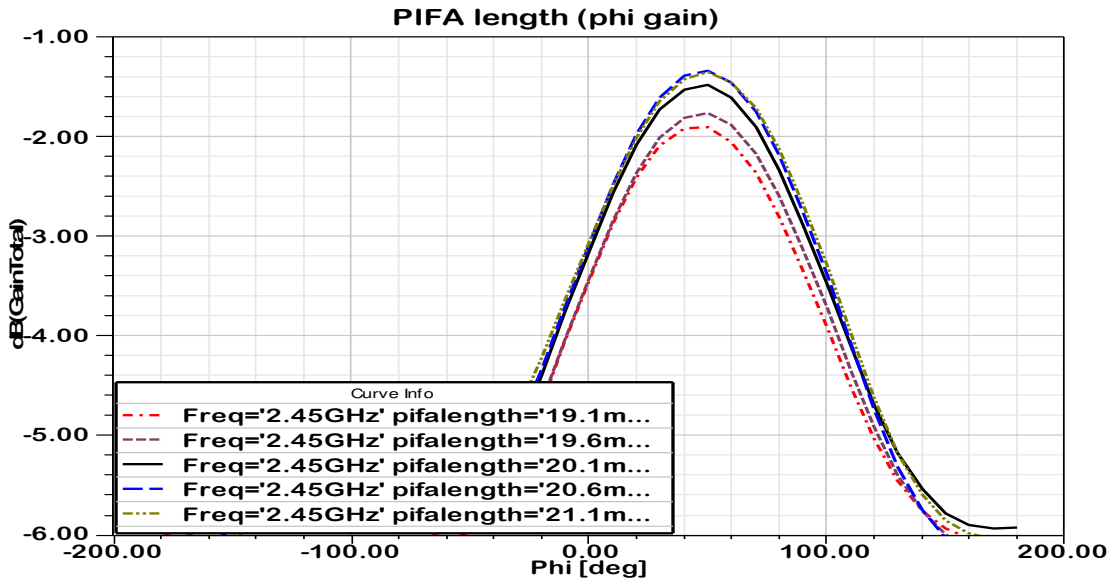

Figure 4.47 Maximum gain at phi with different values of the PIFA length.

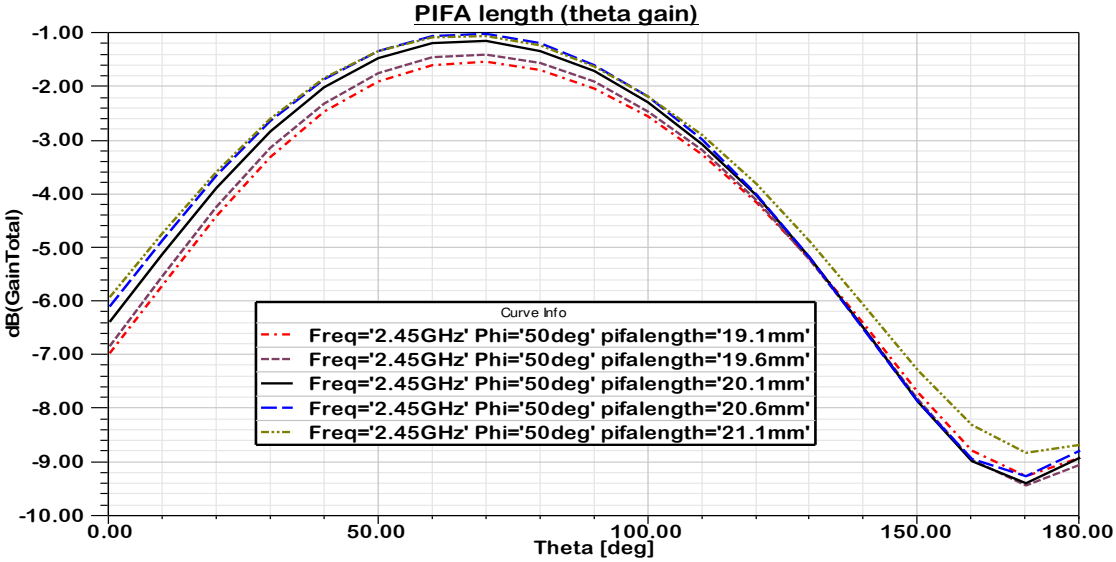

Figure 4.48 Maximum gain at theta with different values of the PIFA length.

4.2 Parasitic Elements for Monopole Antenna Enhancement

An array antenna formed of multi-elements which are essential for increasing the gain. For example Yagi-Uda antenna is widely used for television communication which operates at high frequency (HF), very high frequency (VHF) and ultra high frequency (UHF). It consists of a driven element and a number of parasitic radiators in which currents are induced by mutual coupling between the driven element and the parasitic array. The parasite elements are useful for enhancing the bandwidth impedance of the antenna [2].

Parasite elements can be either reflectors or directors. The reflector acts as an inductive element that causes the antenna to radiate more power away from it. Generally the height of reflector is 5% longer than the driven element, while the directors are capacitive elements, which direct the power radiated by the antenna in their direction. They are normally 5% shorter than the driven element. The directors support induced currents that create a wave travelling along the array.

Another method based on the idea of a Yagi-Uda array that uses one driven element with a number of parasite elements can be also applied to monopole antenna arrays, dipole antenna array and microstrip patch antenna arrays. By placing the parasite elements, the input impedance and the radiation characteristics of the antenna are modified due to the mutual coupling between the driven and parasite elements. For instance, in the monopole and patch array, the parasitic element becomes a reflector when shorted to the ground plane, and when not shorted, acts as a director [2].

In our antenna we modified the design by adding two parasite elements as a director. The resonant frequency became lower than the desired frequency then as we observed from monopole height parameter in 4.1.5 we reduced the height of the monopole antenna by 0.5 mm to tune the resonant frequency at 2.45 GHz. The height of the parasitic was 1 mm shorter than the antenna and with disk radius 4.5 mm but with same radius as the monopole antenna as shown in Figure 4.49.

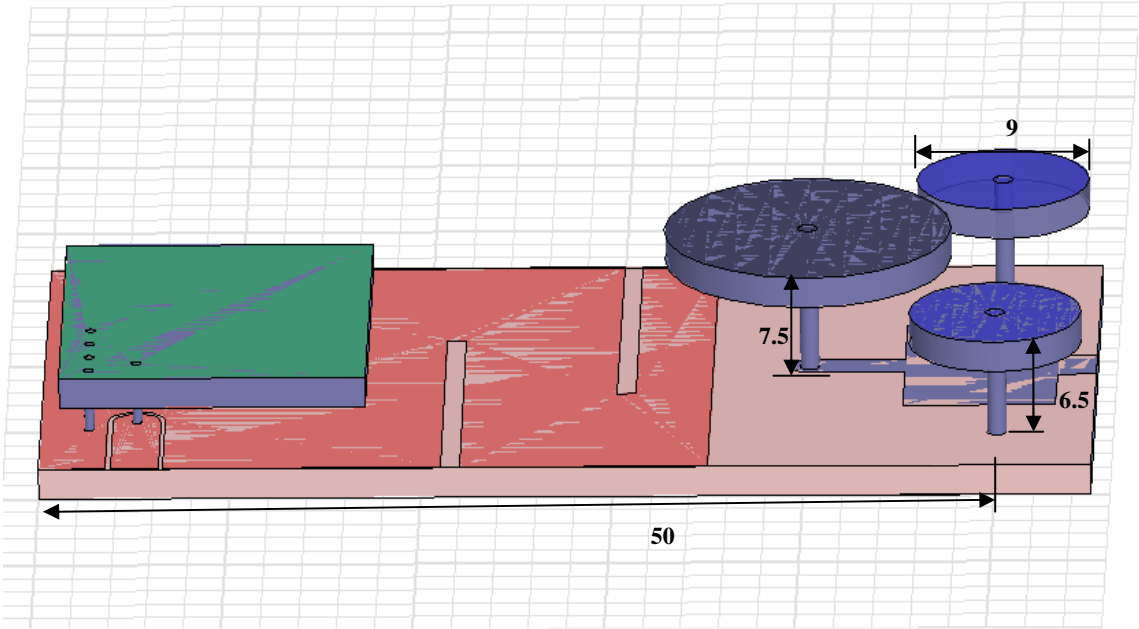

Figure 4.49 Antenna design with two parasitic elements (all dimensions are in mm).

A comprehensive parametric study has been done to optimize the location of the parasite elements (50 mm,5 mm) and (50 mm,25 mm) as well as the height and disc radius, the results in figure 4.50 show that the return loss of monopole antenna improved from -12 dB in Figure 4.2 to -15.5 dB and the fractional bandwidth from

4.9% to 6.5% which is due to the improvement in the input impedance because of the mutual coupling between the driven element and parasitic elements as shown in Figure 4.52 while the other characteristics remained the same as shown in Figures 4.50 and 4.51.

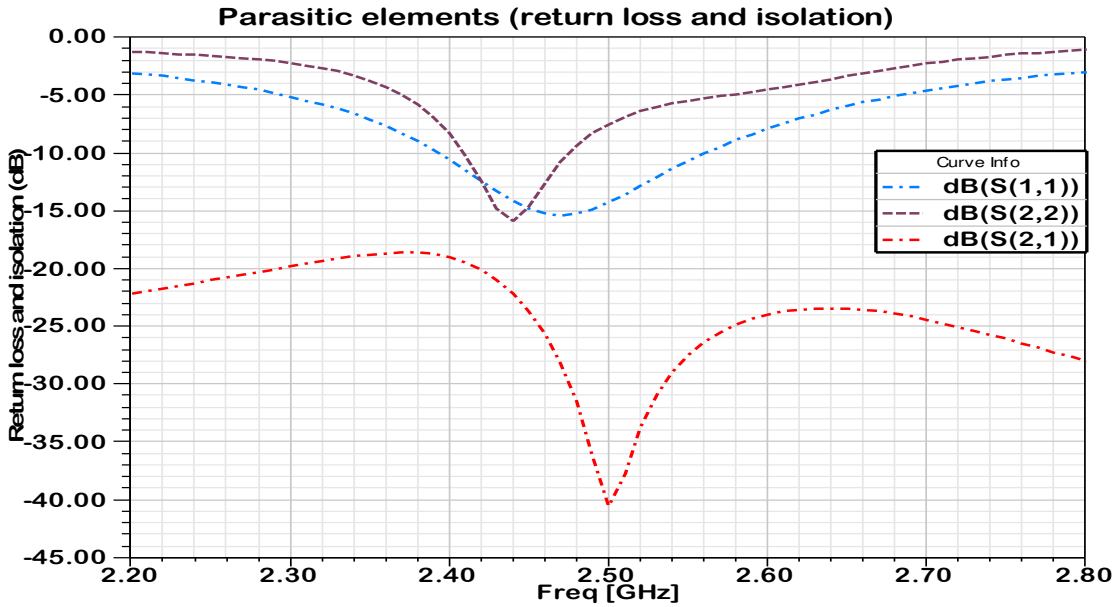

Figure 4.50 Monopole return loss S(1,1), PIFA return loss S(2,2) and isolation S(2,1) with parasitic elements.

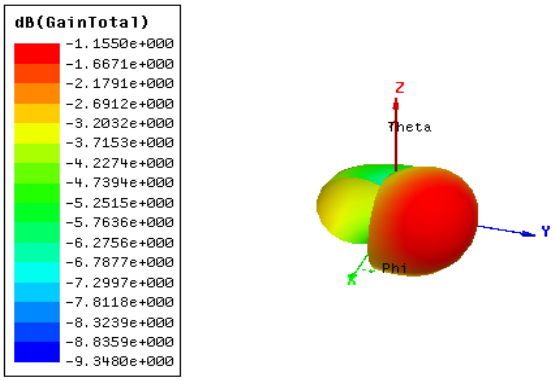

Figure 4.51 Total gain of the antennas with parasitic elements.

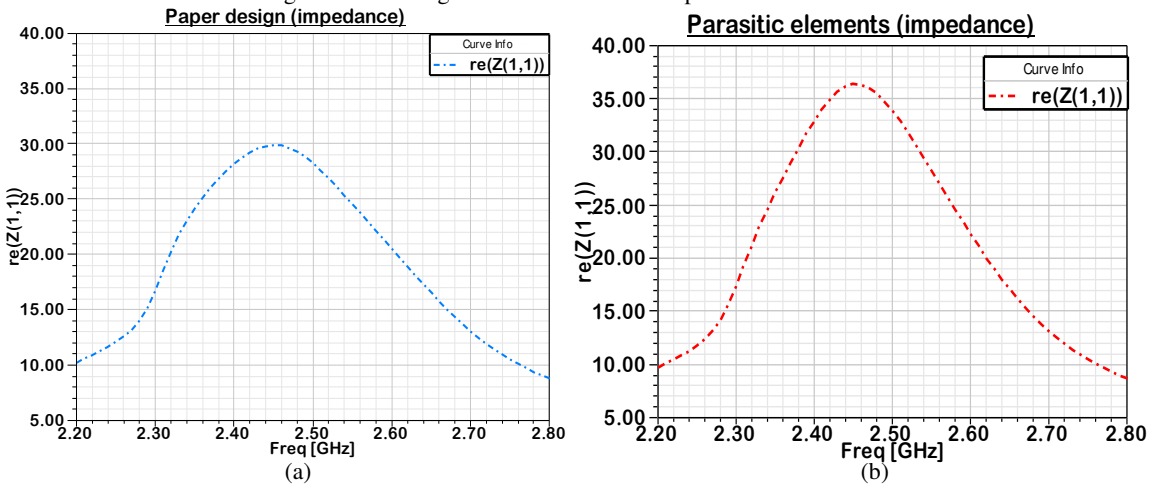

(a) (b)

Figure 4.52 Impedance of the antennas (a) paper design in [1] (b) antenna design with parasitic elements.

4.3 Folded Slots for Mutual Coupling Enhancement

In antenna arrays, it is typical to separate adjacent antenna elements by one half of a wavelength (λ/2), in order to maximize array resolution without the problem of ambiguity [3]. However, the overall size of the array structure has become a subject of current interest, following the widespread using of multiple-input multiple-output (MIMO) technology in existing and future wireless communications standards [4]. One reason for this is that the implementation of multiple antennas in compact user terminals involves challenging design tradeoffs. For example, even though techniques exist to mitigate mutual coupling and correlation among closely spaced antennas, the achievable bandwidth is reduced when compared to widely spaced antennas [5]. Nevertheless, antenna decoupling techniques can be used to facilitate a smaller antenna separation for a given set of performance requirements.

Mutual coupling is a phenomenon that distorts the behavior of radiating elements in an antenna array. Each element in an array affects every other element by radiating through the air or by propagating surface currents through the ground plane. As a result, antenna gain, beamwidth, pattern, resonance frequency, and input impedance are affected [6].

A slotted ground plane was used in [7] to reduce the mutual coupling effect in closely spaced antenna elements. The structure was measured with $0.093\lambda_o$-spaced monopole antennas, where λ_o is the free-space wavelength, and a 16-dB reduction in mutual coupling was achieved over the reference ground plane at a 2.53-GHz center frequency.

Regarding our design presented by [1] in Figure 4.1, it suffers from a small fractional bandwidth for PIFA as shown in Figure 4.2 which is about 2.6% because of the slots. When we simulate the design without slots, the monopole and PIFA characteristics improved as shown in Figures 4.53 and 4.54.

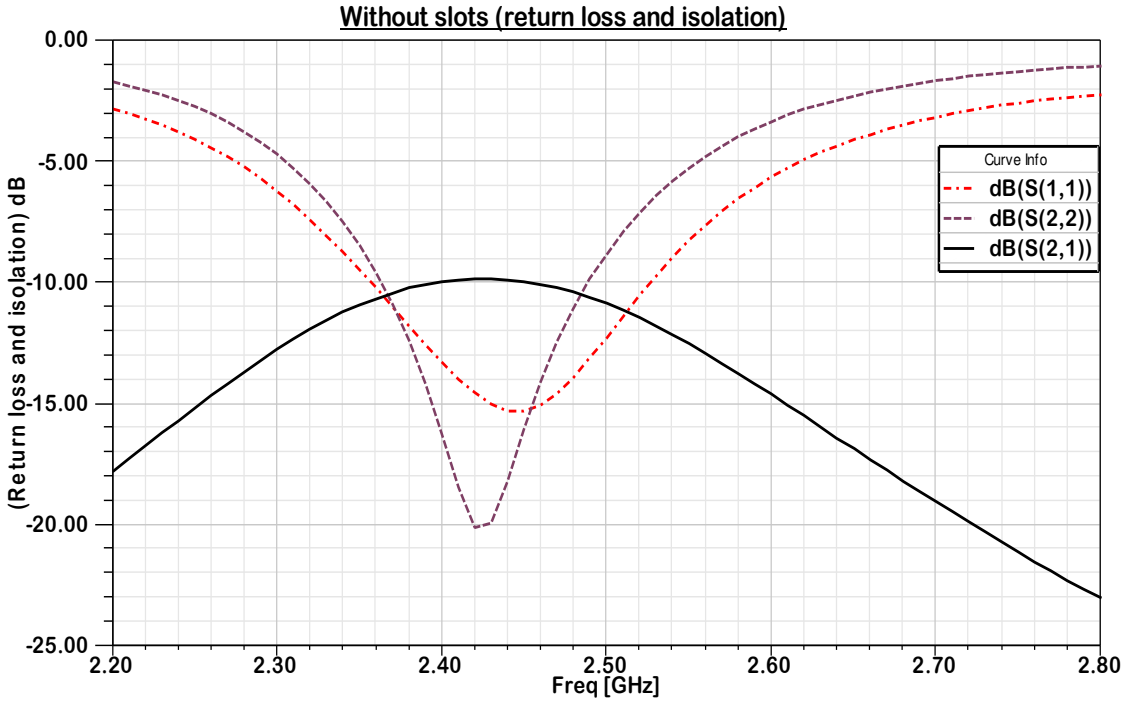

Figure 4.53 Monopole return loss S(1,1), PIFA return loss S(2,2), and isolation between them S(2,1) without slots.

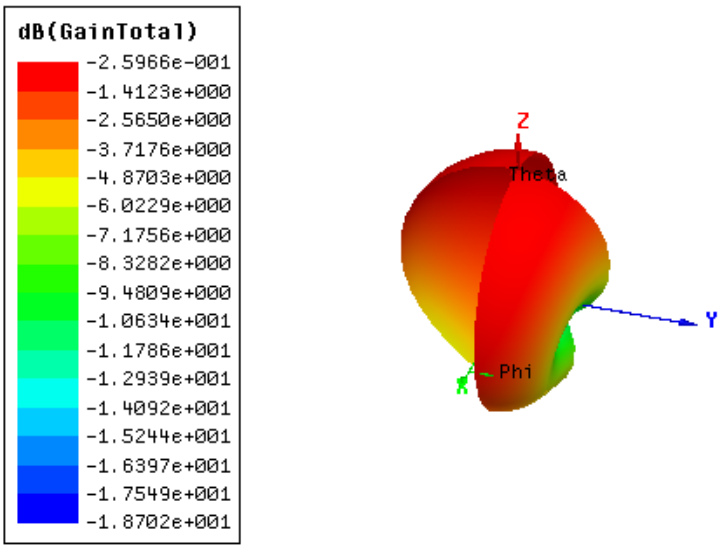

4.54 Total gain of the antenna design without slots.

From results in Figures 4.53 and 4.54, we see that the design without slots have a very bad isolation which is not acceptable but better return loss, bandwidth and gain, so we need to improve the isolation (reduce the mutual coupling) between the antennas and try to minimize the degradation in antenna characteristics.

A comprehensive study has been carried in the slots width, length, locations and gap between them, but we could not get better results than the paper [1], because we always improve one parameter on the expense of others. Therefore we started to search for other techniques for getting low mutual coupling with good antenna characteristics.

In [8] U-slot and V-slot are presented which function as bandstop filter to suppress the mutual coupling but when used instead of the two slots in the design in [1], it improved the bandwidth but reduced the gain. Another low mutual coupling technique is T-slot in [9] is used for the isolation between two PIFA antennas, but when applied to antenna in [1], it improved the gain and bandwidth but the isolation was weak and never exceeded -15 dB. Also H-slot in [10] is used to enhance the isolation between two dipole antennas at 2.45 GHz and when applied to the design in [1], it improved the gain and the bandwidth but isolation remained low.

In our design in Figure 4.55, we will describe an alternative method for isolation improvement between PIFA and monopole antennas which will suppress the current flow between the two antennas by folding the slots in [1] to reduce mutual coupling.

A parametric study has been carried in the length and width of the folded parts of the slots as shown in Figure 4.55 (b) which are identical in size. The results showed that a length of 0.9 mm and a width of 1 mm best suited our design because if we increase the folded slot length to more than 0.9 mm, it will reduce the total gain sharply. The resonant frequency shifted to lower frequency and to correct it according to the results of PIFA width parameter in section 4.1.8 we reduced the PIFA width from 16 mm to 15.85 mm. The results show that the isolation improved from -18.5 dB to -20.5 dB and the fractional bandwidth for PIFA at the resonant frequency 2.45 GHz increased from 2.6% to about 4.9% while the total gain decreased slightly from -1.15 dB to -1.49 dB as shown in Figures 4.56 and 4.57.

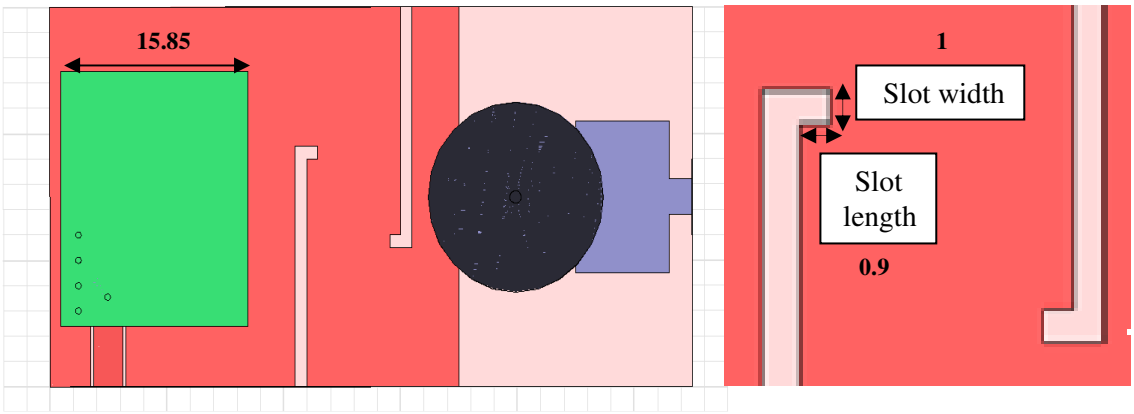

(a) all dimensions are in mm. (b) all dimensions are in mm.

Figure 4.55 (a) Antenna design with slots folded, (b) section of the antenna showing folded slots.

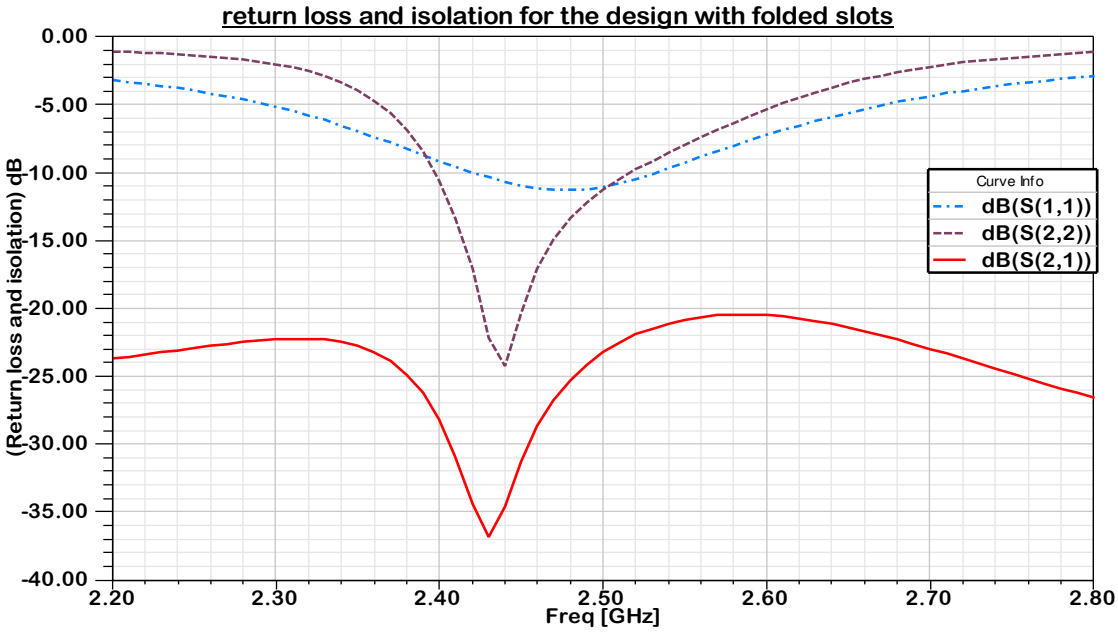

Figure 4.56 Monopole return loss S(1,1), PIFA return loss S(2,2), and isolation S(2,1) with folded slots.

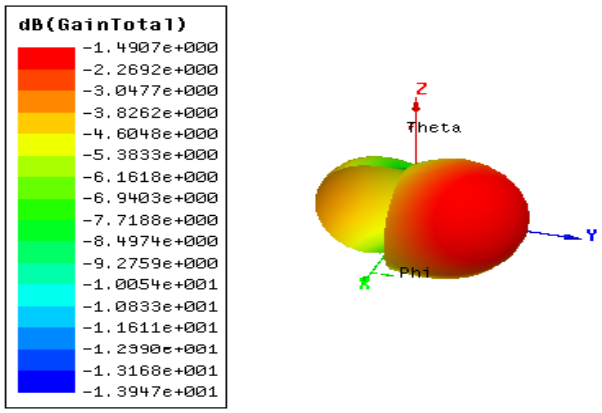

4.57 Total gain of the antenna design with folded slots.

In this section we achieved two goals by folding the two slots of the antenna design, which are the enhancement of the PIFA bandwidth from 65 to 120 MHz and improving the mutual coupling between the PIFA and monopole antennas from -18.5 to -20.5 dB which reflect on a higher data rate due to bandwidth increment and less losses due to better isolation achieved by enhancement in isolation slots.

4.4 Modified Antenna Design with Parasitic Elements and Folded Slots

So far, we have designed the antenna in [1] and a comprehensive parametric study has been carried on different parameters of the antenna design. Also we discussed each of the parameters effects on the antenna characteristics. Then, parasitic elements have been used to enhance the monopole antenna bandwidth. Furthermore, folded slots are used to reduce the mutual coupling between the monopole antenna and PIFA which lead to enhance the PIFA bandwidth.

In this section we are going to combine the modifications that have been achieved by using of the parasitic elements and folded slots and see how the two modifications together will affect each other and how they affect the characteristics of the antenna.

The antenna structure shown in Figure 4.58 has the same length and width but shorter monopole antenna height by 0.5 mm than the height in [1] which is more than 5% of the antenna height.

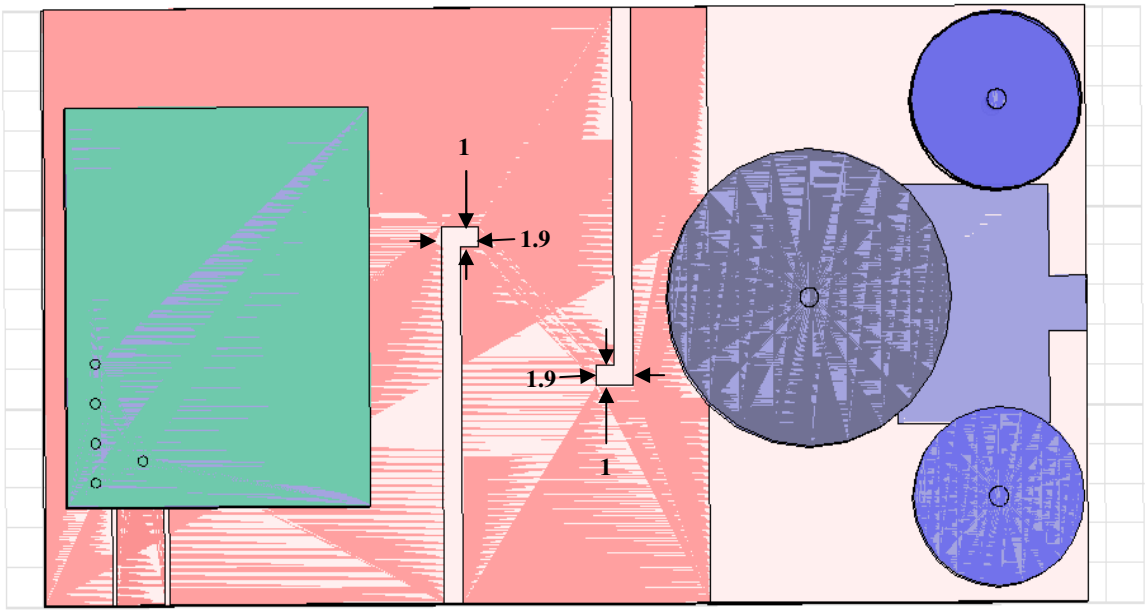

(a) all dimensions are in mm.

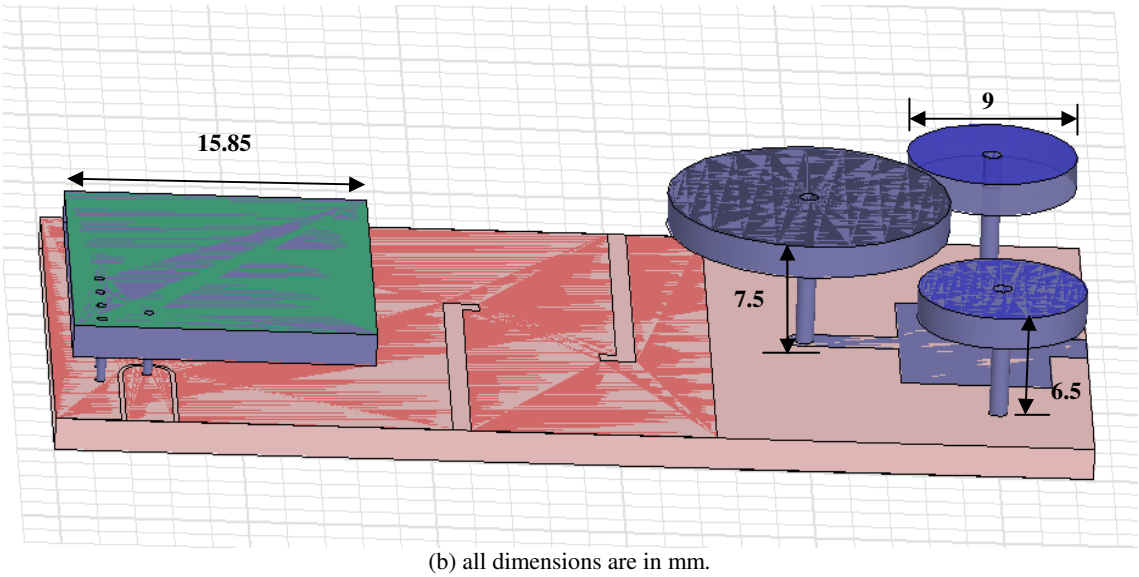

(b) all dimensions are in mm.

Figure 4.58 Modified PIFA Top Loaded Monopole Antenna with Diversity Features (a)Top view, (b)Side view.

The results of the final design shown in Figures 4.59 and 4.60 have satisfied our goals in enhancing the characteristics of the antenna compared to the design in [1] as shown in table 4.1which allow for a better signal and a higher data rate by utilizing of the wider bandwidth and higher return loss.

Parameters	The antenna modified design using parasitic elements and folded slots	The antenna design in [1]
Monopole max return loss	-15.5 dB	-12 dB
PIFA max return loss	-24 dB	-17.5 dB
Monopole 10 dB bandwidth	170 MHz	125 MHz
PIFA 10 dB bandwidth	110 MHz	65 MHz
Isolation	-21 dB	-18.5 dB
Max. gain	-1.39 dB	-1.15 dB

Table 4.1 Comparison between the antenna design in [1] and the antenna modified design.

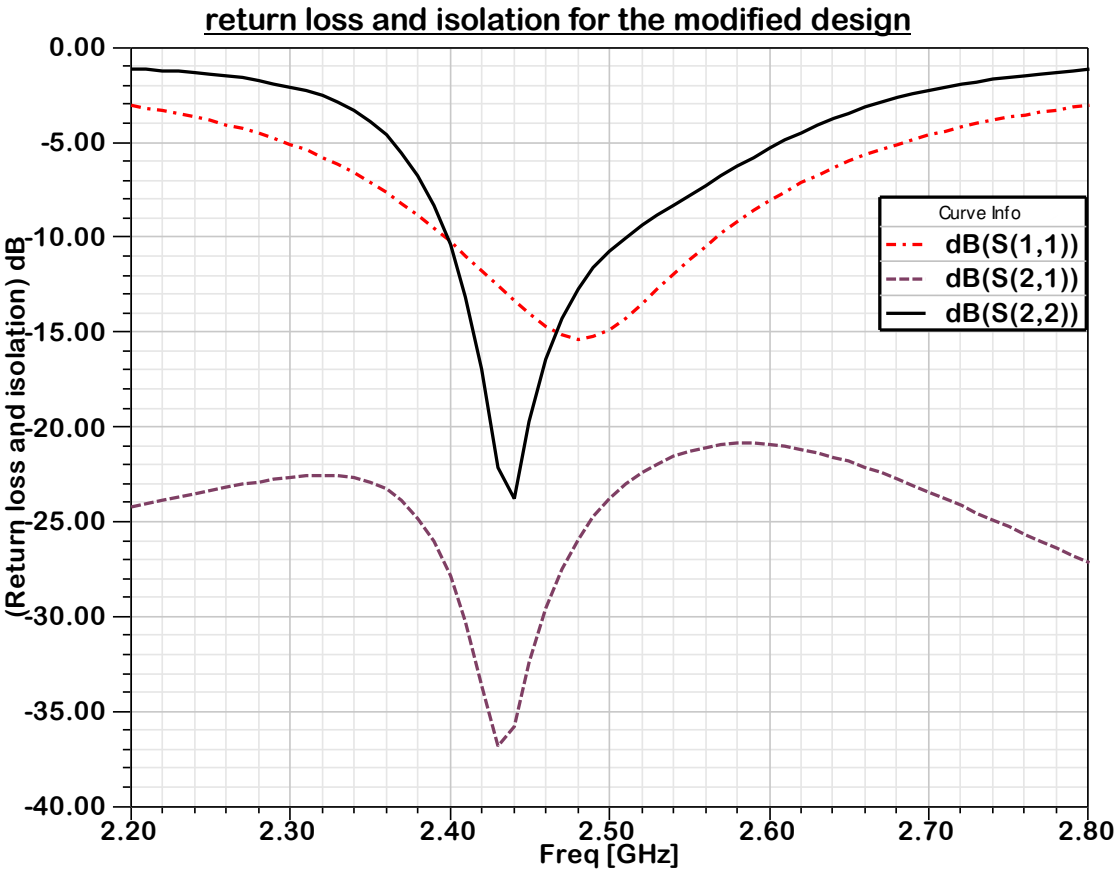

Figure 4.59 Monopole return loss S(1,1), PIFA return loss S(2,2), and isolation S(2,1) of the modified design.

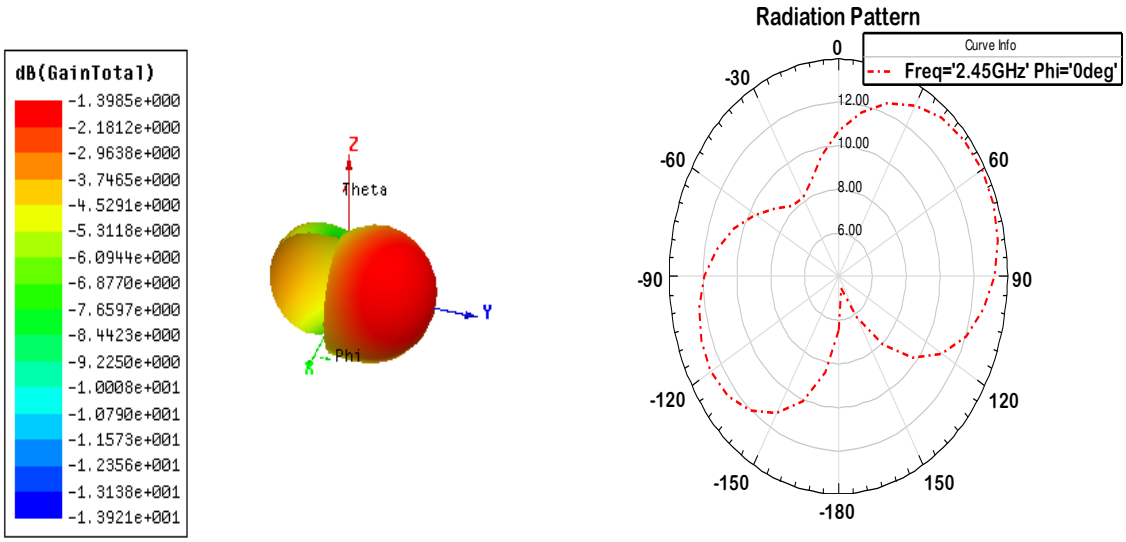

(a) (b)

4.60 (a)Total gain of the antenna modified design (b) Radiation pattern for theta at phi=0.

4.5 Human Body Effects on Antenna Characteristics

To investigate the human body effects on antenna characteristics a homogeneous dielectric cylinder with perimeter of 92 cm and length of 40 cm has been used. The electrical parameters of the tissues have been fixed to $\varepsilon_r = 50$ and $\sigma = 1.5$ s/m as in [1].

The results in Figures 4.61 and 4.62 show that monopole antenna resonant frequency shifted to a lower frequency by 50 MHz which is a direct impact of the partial ground plane of monopole antenna. The shift in resonant frequency satisfies the results in [1] even though our design keeps covering the ISM band with better return loss and isolation compared with the results of the design in [1] that are shown in Figure 4.63.

Also the resonant of PIFA antenna did not have any shift in its resonant frequency which is due to its full ground plane so it is more suitable for WBAN in order to minimize the influence of lossy human tissues on the antenna performance, therefore it is recommended.

The total gain of our design when placed on body at 3 mm distance was 2.05 dB as shown in Figure 4.62 compared with 0.31 dB of the design in [1] as shown in Figure 4.64 that is because of the parasitic elements in monopole antenna and folded slots in PIFA ground plane.

Also the isolation between PIFA and monopole antenna in our design remain better than in the paper design in [1] but it degraded from -21 dB to -18.5 dB as shown in Figure 4.61 which is due to the effects of human body on the antenna characteristics.

However, the parameters of our designed antenna are much less sensitive to the human body tissues as compared to other antennas as printed monopole and loop antennas which need to be placed at sufficient distance from human body and the frequency needs to be tuned properly.

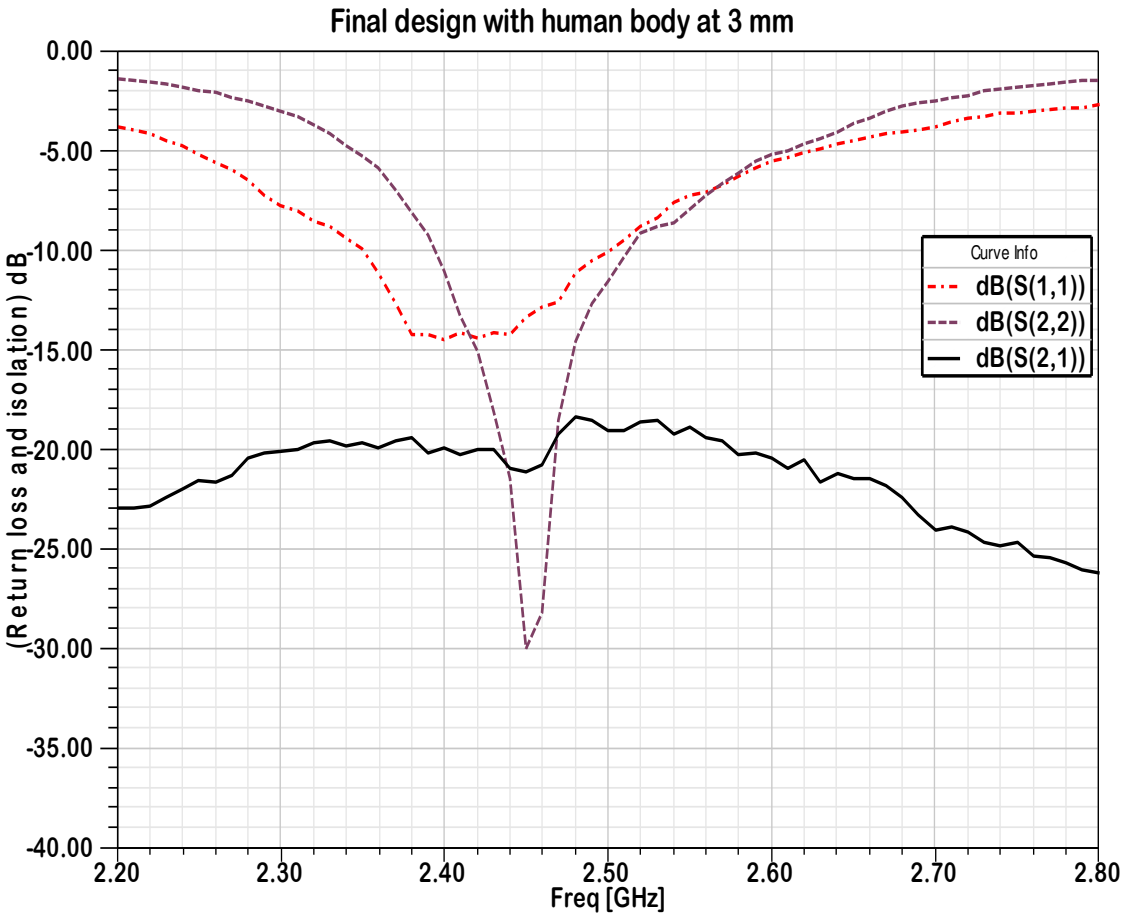

Figure 4.61 Monopole return loss S(1,1), PIFA return loss S(2,2), and isolation S(2,1) of the modified design when placed on human body at 3mm distance.

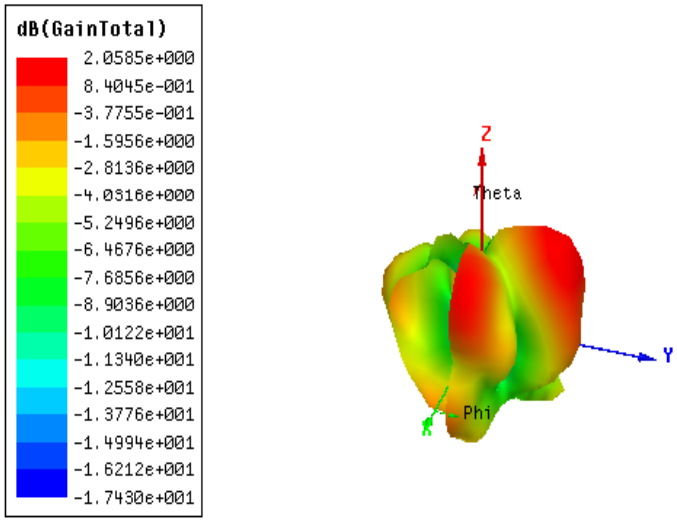

4.62 Total gain of the modified antenna when placed on human body at 3mm distance.

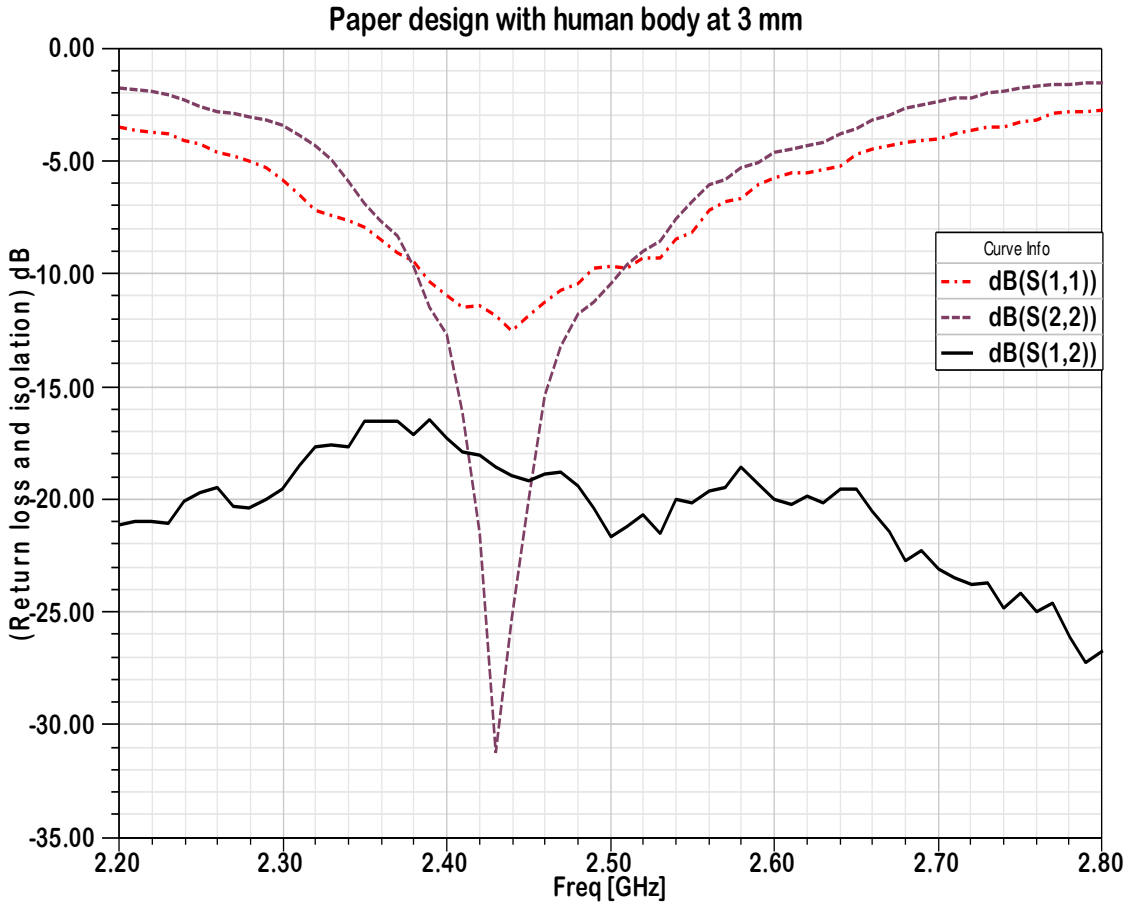

Figure 4.63 Monopole return loss S(1,1), PIFA return loss S(2,2), and isolation S(2,1) of the paper design in [1] when placed on human body at 3mm distance.

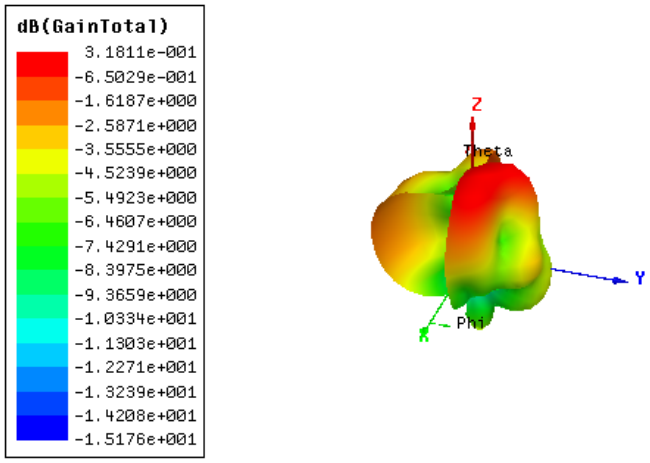

4.64 Total gain of the paper antenna in [1] when placed on human body at 3mm distance.

References

[1] T. Alves, B. Poussot, and Jean-Marc Laheurte "PIFA–Top-Loaded-Monopole Antenna With Diversity Features for WBAN Applications, " *IEEE Antennas and Wireless Propagation Letters*, Vol. 10, No. 1, pp. 693–696, July 2011.

[2] M. R. Kamarudin, O. Abdul Aziz "On-Body Antenna With Parasitic Elements" in *Recent developments in small size antenna*, pp. 113-115, 1st edition, 2008.

[3] H. Krim and M. Viberg, "Two decades of array signal processing research: The parametric approach," *IEEE Signal Process. Mag.*, vol. 13, no. 4, pp. 67–94, Jul. 1996.

[4] B.K. Lau, "Multiple antenna terminals," in *MIMO: From Theory to Implementation*, C. Oestges, A. Sibille, and A. Zanella, Eds. San Diego: Academic Press, 2011.

[5] B. K. Lau, J. B. Andersen, G. Kristensson, and A. F. Molisch, "Impact of matching network on bandwidth of compact antenna arrays," *IEEE Trans. Antennas Propag.*, Vol. 54, No. 11, pp. 3225–3238, Nov. 2006.

[6] M. Sonkki, and E. Salonen, "Low mutual coupling between monopole Antennas by using two λ/2 slots," *IEEE Antennas and Wireless Propagation Letters*, Vol. 9, No. 1, pp. 138–141, March 2010.

[7] C. Y. Chiu, C. H. Cheng, R. D. Murch, and C. R. Rowell, "Reduction of mutual coupling between closely-packed antenna elements," *IEEE Trans. Antennas Propag.*, Vol. 55, No. 6, pt. 2, pp. 1732–1738, Jun. 2007.

[8] D. J. Woo, T. K. Lee, J. W. Lee, C. S. Pyo, and W. K. Choi, "Novel U-slot and V-slot DGSs for bandstop filter with improved Q factor," IEEE Trans. Microw. Theory Tech., Vol. 54, No. 6, pp. 2840–2847, Jun. 2006.

[9] S. Zhang, B. K. Lau, Y. Tan, Z. Ying, and S. He, "Mutual coupling reduction of two PIFAs with a T-shape slot impedance transformer for MIMO mobile terminals," *IEEE Trans. Antennas Propag.*, Vol. 60, No. 3, pp.1521-1531, Mar. 2012.

[10] A. C. K. Mak, C. R. Rowell, and R. D. Murch, "Isolation enhancement between two closely packed antennas," *IEEE Trans. Antennas Propag.*, Vol. 56, No. 11, pp. 3411–3419, Nov. 2008.

Chapter 5

Conclusions

5.1 Summary

Recently, there have been many efforts made to design the WBAN antennas and to investigate the on-body radio propagation channels. In the presented work, we enhanced a diversity antenna which is proposed for reliable on-body and off-body communications intended to be applied in various applications in healthcare and sport monitoring.

A combination of a planar inverted-F antenna (PIFA) and a top loaded monopole antenna are used to satisfy the needs of WBAN environment where different natures of the received signals are present.

A parametric study was performed for different parameters in PIFA and Top Loaded Monopole Antenna in order to study the effects of each parameter on antenna performance. According to the study, the results show that there is a trade-off between performance improvement and antenna size which is an important parameter for WBAN antennas to be compact in size and comfortable. Antenna parameters have been extensively studied such as gain, isolation, and impedance bandwidth.

Also parasitic elements have been used to enhance the impedance bandwidth of the top loaded monopole antenna which proved that using two parasitic elements are suitable for the antenna that enhanced the impedance bandwidth about 45% over the antenna design without the parasitic elements and reduced the antenna height about 5% of the total height of the antenna without parasitic that make the antenna more suitable to be used on human body.

The isolation slots in the PIFA ground plane reduce the impedance bandwidth of the PIFA so a new method has been presented by folding the two slots with specific length and width could overcome the impact on impedance bandwidth as well as improving the isolation between the two antennas.

The antenna performance in the presence of the human body was investigated and compared with that of other antenna design as shown in section 4.5 which showed a better performance regarding the isolation, the impedance bandwidth and the total gain. Also the study illustrated the benefit of applying the full ground plane in minimizing the influence of lossy human tissues on antenna performance parameters. For wearable antennas, a full ground plane will be suitable in order to minimize the influence of lossy human tissues on the antenna performance, therefore it is recommended. However, if we do not want the full ground plane, the narrowband antennas need to be placed at sufficient distance away from the body and the frequency needs to be tuned properly.

The modified antenna is conformal, and it shows excellent on-body performance at ISM frequency band as well as off-body performance that is because of the enhancement which we achieved with our antenna design.

5.2 Future Work

Based on the conclusions drawn and the limitations of the work presented, the following research aspects and issues would provide potential and natural progression to the accomplished works in this thesis:

- Fabricate the modified PIFA top loaded monopole antenna for WBAN and compare its results with the simulation results.
- Use Meta-material substrate layers for PIFA to further reduce the antenna size and enhance the bandwidth and the gain.
- The modified PIFA top loaded monopole antenna can be tuned to operate in two or more bands.
- Antennas with low SAR are required, in order to minimize the electromagnetic radiation absorption by body tissue. Further work needs to be done for WBAN communications. However, it is out of the scope of my current study.
- Study of smart antenna techniques to overcome fading of on-body radio channels in WBAN communications. Due to blocked communications by the human body, the on-body radio channel experiences fading of the transmitted signal. In order to overcome this fading, smart antenna techniques will be helpful.